# NOVEL FAST ATOM BOMBARDMENT MASS SPECTROMETRIC STRATEGIES FOR POLYSACCHARIDE ANALYSIS.

Philip Richard Tiller

A thesis submitted for the Degree of Doctor of Philosophy of the University of London.

Department of Biochemistry,
Imperial College of Science, Technology and Medicine,
South Kensington,
London, SW7.

June 1989

## ABSTRACT

Novel protocols for the analysis of polysaccharides are described with their application in the structural analysis of oligosaccharides derived from Klebsiella K44 and K69 capsular polysaccharides, a nonasaccharide component of sycamore extracellular polysaccharide and core oligosaccharides from the lipopolysaccharide of Neisseria meningitidis.

The first novel protocol presented has been developed to locate the carbohydrate residue on which O-acylation occurs. The presence of such substituents has been implicated in recognition processes and in the physical properties of carbohydrates. This protocol elegantly combines simple wet chemistry with high field FAB-MS. This novel procedure has enabled the O-acetate in Klebsiella K44 to be located on the reducing terminal glucose residue, in K69 on the reducing terminal mannose residue and both O-acetates in the nonamer from sycamore extracellular polysaccharide to be located on the galactose residue within the trisaccharide branch. The O-acetates present in the core oligosaccharides from N. meningitidis LPS are located on the terminal HexNAc.

The second protocol is based upon a controlled time-course methanolysis monitored by high field FAB-MS. The aim was to sequence molecules that yield little fragmentation, and to locate branch points within oligosaccharides. This protocol has been applied to the structural analysis of lipopolysaccharide inner core structures from Neisseria meningitidis, affording data

that enabled the full sequence and all branch positions to be determined.

ACKNOWLEDGEMENTS.

I would like to acknowledge the help I have recieved from my supervisor Dr, Ann Dell, who's endless patience and enthusiasm have been a great boon.

I am grateful to the other members of the mass spectrometry group for their cheerfulness and ready wit, in particular Drs. Jane Oates and Mark Rogers, have made the last 3 years a pleasure.

The use of samples to 'experiment' on is gratefully acknowledged:-

Prof. Clinton Ballou (Glycolipid I),
Prof. Andrew Mort (Gellan gum),
Prof. Guy Dutton (K44),
Dr. Haralambous Parolis (K69),
Prof. Peter Albershiem (Xyloglucan),
Dr. Minoru Fukuda (PA1 Glycolipid),
Dr. Harry Jennings (B Streptoccocci and LPS core).

The encouragement of my family and friends has been a great support.

This work was supported by an S.E.R.C. studentship.

CONTENTS


| | Page |
|---|---|
| Abstract | 1 |
| Acknowledgements | 3 |
| Contents | 4 |
| List of Figures | 5 |
| List of Tables | 7 |
| Chapter 1 : Introduction | 11 |
| Chapter 2 : Location of O-acyl groups | 29 |
| Chapter 3 : Methanolysis/FAB-MS | 80 |
| Chapter 4 : An Examination of LPS | 122 |
| Chapter 5 : Conclusion | 191 |
| Chapter 6 : Methods | 195 |
| References | 201 |
| List of Publications | 207 |

LIST OF FIGURES.


| FIGURE | | Page |
|---|---|---|
| 2.1. | Positive ion FAB spectrum of peracetylated stachyose after deuteroacetylation. | 36 |
| 2.2. | Positive ion FAB spectrum of peracetylated maltotriose after deuteroacetylation. | 37 |
| 2.3. | Positive ion FAB spectrum of acetylated glycolipid I. | 41 |
| 2.4. | Positive ion FAB spectrum of deuteroacetylated gellan gum. | 45 |
| 2.5. | Partial FAB spectrum of deuteroacetylated gellan gum. | 49 |
| 2.6. | Positive ion FAB spectrum of native oligosaccharide from Klebsiella K44. The signals marked with a cross are those derived from the matrix. | 53 |
| 2.7. | Positive ion FAB spectrum of deuteroacetylated K44. | 54 |
| 2.8. | Molecular ion region of negative ion FAB spectrum of oligosaccharide from K69. | 58 |
| 2.9. | Positive ion FAB spectrum of deuteroacetylated K69. Signals marked with a cross are matrix derived. | 59 |
| 2.10. | Low mass end of deuteroacetyl derivative before (A) and after (B) the addition of sodium acetate. Arrows in B indicate where the signals at m/z 323 and 340 would be. | 61 |
| 2.11. | Partial positive ion FAB spectra of deuteroacetylated (A) K69 (B) de-acetylated K69 and (C) de-acetylated, de-pyruvylated K69. | 62 |
| 2.12. | Molecular ion region of negative ion FAB spectrum of the P2 repeat from K69. | 66 |
| 2.13. | Molecular ion region of deuteroacetylated P2 from K69. | 68 |
| 2.14. | Positive ion FAB spectrum of deuteroacetylated xyloglucan. | 72 |

LIST OF FIGURES CONT.


| FIGURE | | Page |
|---|---|---|
| 2.15. | Partial positive ion FAB spectra of the Xyloglucan after deuteroacetylation. The three partial spectra were recorded consecutively from the same sample. | 76 |
| 2.16. | Partial positive ion FAB spectra of the xyloglucan after deuteroacetylation, run in (A) glycerol/thioglycerol and (B) thioglycerol. | 77 |
| 3.1. | Positive ion FAB spectrum of permethylated PA1 glycolipid. | 82 |
| 3.2. | Positive ion FAB spectrum of permethylated PA1 glycolipid after 15 mins. methanolysis at 40° C. | 87 |
| 3.3. | Positive ion FAB spectrum of permethylated PA1 glycolipid after 30 mins. methanolysis at 40° C. | 88 |
| 3.4. | Positive ion FAB spectrum of permethylated K 69 P1 repeat after 5 mins. methanolysis at 60° C. | 102 |
| 3.5. | Positive ion FAB spectrum of permethylated K 69 P1 repeat after 10 mins. methanolysis at 60° C. | 103 |
| 3.6. | Positive ion FAB spectra of deuteriomethyl derivative of Xyloglucan after methanolysis for 40 mins. at 40° C. | 109 |
| 3.7. | Positive ion FAB spectra of deuteriomethyl derivative of Xyloglucan after methanolysis for 10 mins. at 60° C. | 111 |
| 3.8. | Positive ion FAB spectra of deuteriomethyl derivative of Xyloglucan after methanolysis for 20 mins. at 60° C. | 112 |
| 4.1. | Positive ion FAB spectrum of native L3-F-II (4). | 126 |
| 4.2. | Molecular ion region of permethylated L3-F-II (4). | 129 |
| 4.3. | Positive ion FAB spectrum of native L5-F-III (3). | 150 |
| 4.4. | Positive ion FAB spectrum of permethylated L5-F-II (3). | 154 |

LIST OF TABLES.


| TABLE | | Page |
|---|---|---|
| 2.1 | Summary of signals observed in the spectra of maltotriose and stachyose after acetylation and additional deuterioacetylation. | 39 |
| 2.2 | Summary of peaks in the spectrum of deuterioacetlyated glycolipid (I). | 43 |
| 2.3 | Summary of data obtained from deuterioacetyl spectrum of gellan gum from Pseudomonas eloda. | 47 |
| 2.4 | Signals observed in the native and deuterioacetyl spectra of K44 repeat. | 55 |
| 2.5 | Summary of peaks observed in the deuterioacetyl spectrum of Klebsiella K69 repeat. | 63 |
| 2.6 | Summary of peaks observed in the deuterioacetyl spectrum of the Xyloglucan nonasaccharide. | 74 |
| 3.1 | Summary of peaks observed in the spectrum of PA1 glycolipid. | 84 |
| 3.2 | Summary of new peaks observed in the spectra of permethylated PA1 glycolipid, obtained after heating at 40°C for 15 and 30 mins. | 90 |
| 3.3 | Summary of signals observed in the spectra of permethylated Streptoccoccus group B antigen from aliquots taken after 2, 5, 10, 20, 40 and 80 minutes heating at 40°C and a further 5, 10, 20 and 40 minutes at 60°C in methanolic HCl. | 93 |
| 3.4 | Summary of the possible structures each of the signals, observed in the spectra obtained throughout the course of the time course methanolysis, represents. | 94 |
| 3.5 | Summary of aliquots in which signals were observed. | 98 |
| 3.6 | Summary of the highest mass ion present in each of the methanolysis time course aliquots. | 99 |
| 3.7 | Summary of ions observed after methanolysis for 120 minutes at 40°C and for a further 10 minutes at 60°C. | 104 |

LIST OF TABLES CONT.


| TABLE | | Page |
|---|---|---|
| 3.8 | Summary of the possible structures each of the signals observed in Figures 3.4 and 3.5 may represent. | 105 |
| 3.9 | Summary of ions observed in the methanolysis/FAB-MS study of the Xyloglucan nonasaccharide. | 114 |
| 3.10 | Summary of possible structures the ions, observed during methanolysis/FAB-MS of Xyloglucan nonasaccharide, may represent. | 115 |
| 4.1 | Summary of data obtained from the negative and positive ion spectra of native L5-F-II (4). | 127 |
| 4.2 | Summary of data obtained from permethyl spectra of L3-F-II (4). | 132 |
| 4.3 | Summary of ions observed during the methanolysis time-course of L3-F-II (4). | 134 |
| 4.4 | Possible structures of ions observed in the methanolysis time-course of L3-F-II (4). | 135 |
| 4.5 | Summary of data obtained during the methanolysis time-course of L4-F-I (6). | 138 |
| 4.6 | Possible structures of ions observed in the methanolysis time-course of L4-F-I (6). | 140 |
| 4.7 | Summary of ions observed during the methanolysis of L5-F-I (5/6). | 145 |
| 4.8 | Summary of possible structures for ions observed during the methanolysis of L5-F-I (5/6). | 147 |
| 4.9 | Summary of ions observed in the positive and negative spectra of native L5-F-III (3). | 151 |
| 4.10 | Summary of ions observed in the spectrum of the deuterioacetyl derivative of L5-F-III (3). | 155 |
| 4.11 | Summary of ions observed in the methanolysis/FAB-MS study of L5-F-III (3). | 157 |

LIST OF TABLES CONT.


| TABLE | | Page |
|---|---|---|
| 4.12 | Summary of possible structures the ions observed during methanolysis/FAB-MS of L5-F-III (3). | 159 |
| 4.13 | Summary of signals observed in the negative ion spectrum of native L5-F-II (3). | 162 |
| 4.14 | Summary of signals observed in the positive ion spectrum of native L5-F-II (3). | 164 |
| 4.15 | Summary of signals observed in the positive and negative ion spectra of native L2-F-II (1). | 169 |
| 4.16 | Summary of signals observed in the deuterioacetyl and permethyl spectra of L2-F-II (1). | 171 |
| 4.17 | Summary of signals observed in the negative and positive ion spectra of L7-F-II (1). | 173 |
| 4.18 | Summary of signals observed in the negative and positive ion spectra of L9-f-I (1). | 176 |
| 4.19 | Summary of data obtained from the negative and positive ion spectra of native L3-F-I (4). | 179 |
| 4.20 | Summary of data obtained from the permethyl spectrum of L3-F-I (4). | 181 |
| 4.21 | Summary of structures found to be present in the ten LPS oligosaccharides from Neisseria meninitidis. | 187 |

## Abbreviations.

| | |
|---|---|
| Hex | Hexose |
| HexNAc | N-acetyl-hexosamine |
| HexA | Hexuronic acid |
| DeoxyHex | Deoxy-hexose |
| Pent | Pentose |
| Rha | Rhamnose |
| Hept | Heptose |
| NeuAc | N-acetyl-nuraminic acid |
| KDO | 3-deoxy-D-manno-2-Keto-Octulosonic acid |
| P-$EtNH_2$ | Phosphoethanolamine |
| Ac | Acetate |
| Pyr | Pyruvate |
| G | Glycerol |

# CHAPTER 1 : INTRODUCTION

## 1:1. INTRODUCTION.

Polysaccharides, oligosaccharides and glycoconjugates are present on the surface of all cells, and as such mediate recognition processes, act as receptors and are involved in cell-cell and host-pathogen interactions. These interactions are based upon the structure of particular carbohydrate moieties. Thus to examine and understand such processes it necessarily requires knowledge as to the composition and structure of putative receptor molecules.

Cell-surface carbohydrate structures present as part of glycoproteins, or as glycolipids have been shown to play an important role in many cellular interactions with "exogenous ligands"[1]. For example glycolipids play a major role as differentiation markers during histogenesis[2] and as markers relating to cell maturity[3]. Carbohydrates are also good candidates for markers relating to some disease states and carbohydrate structures on glycoproteins have been found to be significantly different between normal and cancerous cells, with leukemic polylactosaminoglycans being shorter, more highly sialylated and carrying less fucosyl residues than is normally the case[4,5,6].

In plants carbohydrates do not merely fill a passive non-interactive role, but carry structural features that are involved in the mediation or regulation of plant - pathogen interactions and plant growth and development[7,8]. For example the type of residue present

in cell wall fragments seems to define the bonding properties of the carbohydrate in reactions with protein receptors[9]. Extracellular carbohydrates play a role, not merely as a matrix to bind cells together, but also in the defense of the plant, for example polysaccharide exudates such as gellan gum[10].

Bacteria, like plants, utilise extracellular polysaccharides as a protective layer. The capsular polysaccharide secreted by many bacteria fulfills a defensive role[11], particularly in the case of pathogenic species. In Baccillus streptococci type III strains the capsule is itself almost non-immunogenic because the saccharide chains are terminated with sialic acid residues[12], and are recognised by the immune system as being of host origin, and this has been found to be the case with other species[13]. The capsule, though, is permeable to complement factors, allowing them to bind to sub-capsular components, without itself being a site for binding. The capsule then acts as a physical barrier to leucocyte receptors, thus the leucocytes do not come into contact with the bound complement components and complement induced phagocytosis is inhibited. In human disease the presence or absence of a particular carbohydrate component on the cell surface of a bacteria can determine its pathogenicity. For example, all known strains of Neiserria meningitidis that cause meningitis lack the O-specific polysaccharide chain in their lipopolysaccharide, and it is only the R-type strains that are pathogenic[14] (see introduction to chapter 4).

The effectivness with which capsular polysaccharide mimics host carbohydrate structures affects dramatically the treatment of disease. Meningococci species from both sero groups A and C have proved to be susceptible to treatment by vaccination using isolated capsular polysaccharides from organisms of these sero groups as vaccines. In the case of sero group B strains, the capsular polysaccharide is cross-reactive with polysialosyl glycoproteins in foetal and infant brain tissue, preventing their use as vaccines[13].

Relatively minor structural differences in carbohydrate groups can have a profound effect on the properties of a molecule. For example the presence or absence of O-acetyl groups can alter the immunogenicity of a carbohydrate[14a,15,16]. It is therefore of prime importance to accurately and reliably determine all aspects of carbohydrate structure before a full understanding of cell-cell interactions can be reached.

Defining the structure of a carbohydrate is a complex operation due to the great variation in structures found. The complete structural analysis of a carbohydrate is demanding and some components still prove very difficult to analyse, for example alkylphosphoesters and acyl groups. Methods for the analysis of such moieties do exist but are often difficult to execute, and may afford ambiguous data.

This thesis addresses two key areas of structural analysis, and introduces new strategies for defining complex carbohydrate structures. The structures defined by these methods will facilitate the study of structure-

function relationships and will further our understanding of the biological significance of carbohydrates.

## 1:2. HISTORICAL BACKGROUND.

To define completely the structure of a saccharide it is necessary to determine the monosaccharide units present, the ring type of each constituent, the hydroxyl groups involved in each glycosidic linkage the configuration ($\alpha$- or $\beta$-) of the glycosidic bonds, the sequence of the sugar residues and the presence, location and linkage of non-carbohydrate substituents.

In the first studies on bacterial polysaccharides they were hydrolysed by acid, then paper chromatographic[17] and colourimetric[18,19,20] methods were used to separate the monosaccharides and define their composition. Unfortunately single sugars exhibited similar chromatographic profiles which complicated interpretation of the data. The advent of g.l.c[21] in 1958 enhanced greatly the analysis of monosaccharides though g.l.c. requires derivatisation of the sugars to make them volatile enough. The first derivative used was the per-O-methyl[22], but because of difficulties in obtaining fully methylated sugars the favoured derivatives became the per-O-trimethylsilyl [23] or the acetyl. [22]

In 1964 Hakomori[25] developed a new procedure to methylate saccharides in good yields routinely. This method employs a methylsulphinyl carbanion to "extract" the hydroxide protons followed by reaction with methyl iodide forming the methyl ether; and has been applied to carbohydrates of many diferent types.[26,27]

Routine reliable methylation was the stimulus for the development of methylation analysis. This is more informative than an examination of the hydrolysate as data relating to linkage is obtained. The intact carbohydrate is methylated then hydrolysed yielding partially methylated monosaccharides. The acid hydrolysis conditions are altered depending on the data desired. Hexosyl and aminohexosyl sugars are released using sulphuric acid (0.5N) in acetic acid (95%)[28] though these conditions destroy neuraminic acids. Neuraminic acids are obtained using methanolysis (anhydrous HCl 0.5M in methanol at 80 C for 18hr).[29] The products of these degradations are then reduced and acetylated yielding partially methylated alditol acetates which are analysed by gc-ms.[30] The glc and ms data are compared with known standards, thus isomers, with the same substitution patterns can be distinguished, by the combination of their retention times and mass spectra. This classical approach enables linkages to be determined and therefore which residues are branched while a quantitative analysis of the monosaccharides may be obtained from the glc data[31], but no information is obtained relating to the sequence of the molecule under examination.

The Smith degradation was a further development in oligosaccharide analysis and involves the use of periodate, which specifically reacts with vicinal hydroxyl groups. The hemiacetals obtained are subsequently reduced with borohydride forming a polyalcohol. Hydrolysis, which occurs more readily where the glycosidic ring has been

cleaved, is then performed and the products of hydrolysis analysed. The Smith degredation when applied in combination with hydrolysis affords linkage information and data relating to adjacent residues, therefore enabling sequences to be determined.

One problem with the derivatives and hydrolyses used in carbohydrate analysis is that labile groups are frequently lost. The degradation of neuraminic acid under hydrolytic conditions has been mentioned. Other, non-carbohydrate, groups frequently present as substituents are similarly lost, a prime example being that of O-acetates. De Belder and Norman[32] introduced a chemical procedure for determining the location O-linked acyl groups. Their strategy and its limitations are discussed in Chapter 2.

Many polysaccharides, particularly those of bacterial origin, consist of a single oligosaccharide repeated many times to form the polymer. In the analysis of such polysaccharides an effective approach is to partially degrade the polymer, by the use of chemical hydrolyses, thus yielding oligosaccharides, typically less than 2000 dalton,[30] which can then be analysed to determine the structure. This approach has some disadvantages though, the hydrolyses occur randomly at a number of glycosidic linkages, thus forming a mixture of oligosaccharide components. In addition chemical hydrolysis may remove labile sustituent groups, thus the oligosaccharide obtained in such a manner would not be truly representative of the native polysaccharide.

An alternative method of obtaining the repeat unit of

a polysaccharide is to subject the polymer to enzymic degradation. Enzymes capable of hydrolysing bacterial polysaccharides were first isolated by Dubos and Avery in 1931.[33] The use of endoglucanases, so named since they hydrolyse glycosidic bonds within the main body of a glucan, to assist in structural analysis was first demonstrated by Sutherland[34] and they are still used today. These enzymes are obtained from bacteriophage infected cultures of bacteria. It has proved difficult to isolate a preparation exhibiting a single enzyme activity, so the oligosaccharides afforded by endoglucanase digestion are often the result of both lyase and hydrolase activity.

In 1956 Adams and Park[35] postulated the use of bacteriophage enzymes to depolymerise bacterial polysaccharides. The first bacteriophages, which utilise depolymerising enzymes, were isolated in 1962 by Eklund and Wyss[36], and the use of bacteriophage enzymes in structural studies is an important technique today.[37] This approach utilises the hydrolytic enzymes that the virus uses to penetrate the bacterial cell wall surface , to depolymerise specific polysaccharides. Such cleavage affords a repeat unit (P1) or a simple multiple of the repeat, (P2, P3 etc.) with all substituent groups present; as they are apparently unaffected by the enzyme. Examining such oligosaccharides means that only a few experiments need to be performed on the native polymer, such as molecular weight determination, usually by sedimentation rate and composition analysis.

Another approach taken to study bacterial surface structures is to utilise mutant strains of bacteria. These mutants, designated "R-type", because they develop rough surfaced colonies when cultured, incompletely synthesise their lipopolysaccharide (LPS) antigens, providing a source of oligosaccharides that are normally "hidden" at the core of the LPS.[38,39]

## 1:3. MODERN ANALYTICAL METHODS.

The application of sophisticated instrumentation to the analysis of carbohydrates has greatly speeded-up analysis time and allowed more reliable conclusions to be reached. Two techniques in particular have had a great impact in this area; nuclear magnetic resonance spectroscopy (n.m.r.) and mass spectrometry (M.S.).

### 1:3.1 N.M.R.

Both proton and $^{13}C$ n.m.r. have proven themselves to be suited to the analysis of carbohydrates. The development of superconducting magnets has allowed complex molecules to be examined, since the increased magnetic field affords increased resolution. The application of proton n.m.r. to sequencing of carbohydrates is based upon resonances, referred to as structural reporter groups[40,41], that define the primary structure, for example, anomeric protons and the aminosugar N-acetyl methyl protons. $^{13}C$ n.m.r. complements proton n.m.r., even though it is less sensitive, because it provides data on the carbon "backbone" of the molecule under examination. The development of 2-dimensional (2-D) n.m.r. enabled more complex molecules to be examined and sequenced as it

provides more detailed data defining adjacent residues. In addition to information on the primary structure, 2-D n.m.r. is able to provide detailed information as to the 3-dimensional arrangement of a molecule. For example, a nuclear overhauser effect (NOE) experiment will afford data as to which groups or nuclei are adjacent spatially. In studies on polysaccharide structure n.m.r. has been utilised in examination of both native molecules and phage or chemically cleaved repeats. When compared, it has been found that the spectra obtained from the native polysaccharide is, effectively, a less resolved duplicate of that derived from the repeat[42].

N.m.r. has proven to be an effective complement to classical carbohydrate techniques, in that it provides linkage and conformational data on the molecule in its intact form rather than as an hydrolysate. Additionally, n.m.r. has been used to locate O-acyl groups, though this has proven difficult when the sample is a mixture or contains a natural variation in the level of acylation. Also n.m.r. has difficulty in differentiating signals derived from some residues. Some of the chemical shifts derived from fucose are very similar to those of galactose and some shifts observed due to xylose are close to those due to glucose. For this reason n.m.r. analysis of carbohydrates is most effective when guided by, at least, composition analysis data, if not other techniques as well.

1:3.2 Mass spectrometry

The application of electron impact (E.I.) mass spectrometric techniques in carbohydrate analysis was

pioneered by Kochetkov and Chizhov in 1966[43] with their paper outlining the fragmentation pathways of derivatised oligosaccharides. This was a landmark in the field of carbohydrate analysis. With the conjoint use of good chromatographic techniques in g.l.c., complete derivatisation using the Hakomori permethylation and mass spectrometry a revolution in structural investigations occurred[44]. Comprehensive reviews have been published outlining these developments[44,45,22,]. The application of mass spectrometry to carbohydrate analysis was initially used in conjunction with g.l.c. (GC-MS) allowing separation and identification to be carried out in one experiment, and this combination is still a widely used technique today. But, g.l.c. is unable to successfully separate oligosaccharides of more than ten residues, in fact, larger molecules may not pass through a g.l.c. column. So m.s. was applied to these larger molecules, using direct insertion techniques. Electron impact (E.I.) mass spectrometry initially was the ionisation method used, which requires the sample to be volatile. Volatility was not a problem in itself, but the derivatives used to afford a volatile product, often resulted in an increase in mass beyond the range of the mass spectrometers then available. Another problem observed in data obtained from EI experiments is that the signal intensity is rapidly lost with an increase in mass, which may make the identification of the molecular ion problematic. For this reason chemical ionisation (C.I.) was utilised, since under C.I. conditions the sample is ionised indirectly by

the reagent gas so less fragmentation occurs and more of the ion current is contained in the pseudomolecular ion.

In 1977 the development of the high field magnet[46,47], which increased the mass range of spectrometers to 3,000 dalton, allowed the analysis of much larger molecules than was previously possible. The use of E.I. m.s. in studies on high mass carbohydrates followed[48,49,50] and E.I. is still used today, though the loss of signal intensity at higher mass is still a concern. For this reason some researchers turned to Field Desorption (F.D.) as a method to obtain molecular ion information[51] even though it is technically very difficult.

In 1981 the new ionisation method, fast atom bombardment (FAB), was developed[52]. This technique has subsequently revolutionised carbohydrate mass spectrometry, particularly when applied in conjunction with high field magnet technology. FAB-MS is a method whereby a sample dissolved in a viscous liquid, known as the matrix, on a metal target, is bombarded with a beam of accelerated atoms. This results in the transfer of energy from the atom beam to the molecules at the surface of the matrix, affording ions, both positive and negative, which are sputtered out of the matrix. These ions are then analysed in the normal manner.

The advantage of FAB-MS, over some mass spectrometric techniques, is that, like C.I. it is a soft ionisation technique and provides both fragmentation and molecular ion data, with a significant proportion of the ion current contained in the molecular ion. Additionally it's only

requirement is that the sample be presented dissolved in a viscous liquid, typically glycerol or thioglycerol.

This has meant that a vast range of molecules has proved to be amenable to FAB-MS, indeed FAB-MS is almost universally applicable. The advantages to using FAB, rather than E.I. or C.I., are most clearly shown in the analysis of large biomolecules and for this reason FAB was quickly applied in such areas. The application of FAB-MS to the analysis of carbohydrates has been reviewed recently[53] detailing the massive contribution FAB-MS has made to the field.

A variety of structural information is afforded by a FAB mass spectrum. If the molecule under examination is within the mass range of the instrument then pseudomolecular ion species are observed. These are ions in which the sample molecule, as a result of adduction or abstraction of a charged species, forms an ion. The most frequently observed adducts are $H^+$, $NH_4^+$, $Na^+$ and $K^+$ in the positive ion selection mode and $Cl^-$ in the negative ion mode. In negative ion spectra the most frequently observed pseudomolecular ion is that resulting from the abstraction of a proton, affording $[M-H]^-$ species.

Pseudomolecular ions define the composition of the species under examination, including both the type and number of sugar residues and the presence of any substituents, such as acyl groups, though the presence of isomers cannot be determined in a FAB-MS experiment.

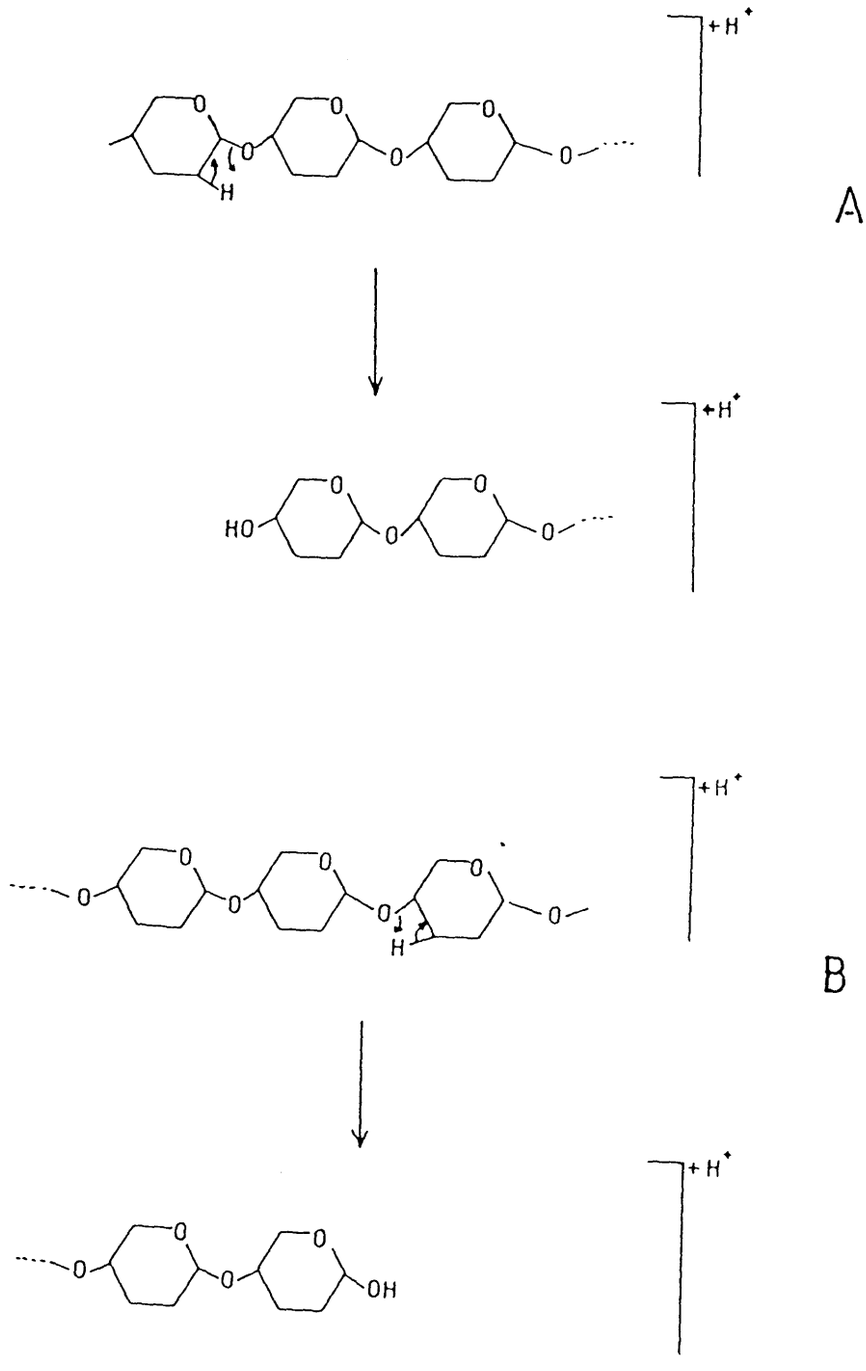
Since positive molecular ions are formed as a result of adduction it is possible to enhance the abundance of

pseudomolecular ions by adding a cation to the matrix. This is often performed using mild aqueous acid (to provide $H^+$) or an ammonium salt (providing $NH_4^+$). The same effect is achieved in the negative ion mode by addition of chloride ($Cl^-$) or a thiocyanate salt.

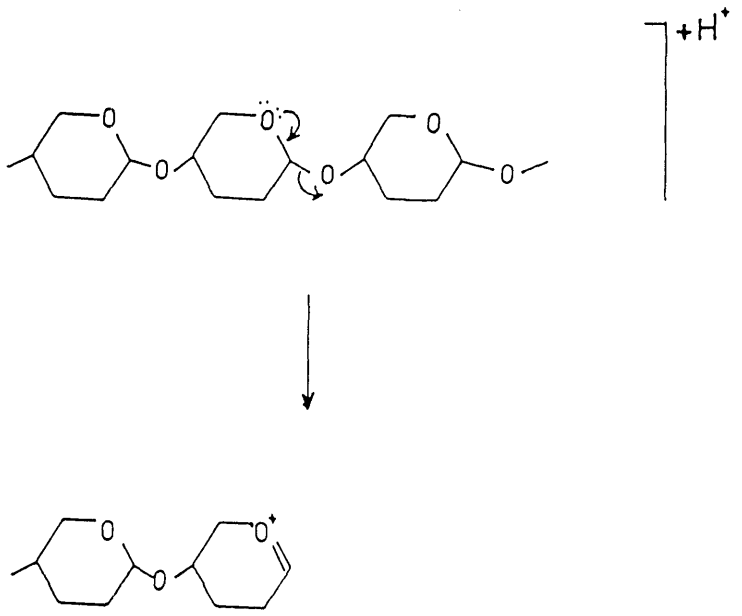
In the first spectra obtained from native molecules it was observed that some of the fragmentation data afforded was ambiguous; it was not possible to determine whether the fragment ions were derived from the reducing or non-reducing end of the molecule. This is because the fragmentation pathways illustrated in Scheme 1.1. are indistinguishable.

In the case of $\beta$-cleavage the charge is retained on the reducing end of the molecule, (Scheme 1.1a) whereas the reverse is true in the case of glycosidic cleavage with hydrogen transfer (Scheme 1.1B). Additionally double cleavages can occur providing further ambiguity. These ambiguities are eliminated with the use of derivatisation as this has the advantage of directing the fragmentation observed and effectively "labels" the terminal residues. In the case of peracetylated and permethylated derivatives the major fragment ions observed are consistent with glycosidic cleavage with the charge being retained on the non-reducing end (see Scheme 1.2.).

This species is referred to as the 'A-type' ion because it is the counterpart of the $A_1$-type fragment ion described by Kochetkov and Chizhov[43]. One particular form of A-type ion is predominantly observed in the spectra of molecules containing amino sugars. It appears that fragmentation occurs preferentially at the

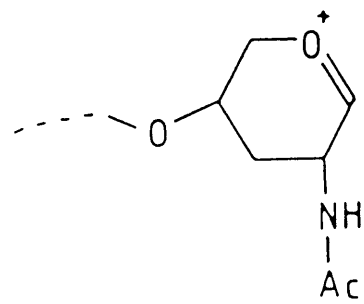



Scheme 1.1. Two possible fragmentation pathways that occur in native samples, (A) $\beta$-cleavage, (B) glycosidic cleavage with hydrogen transfer.




Scheme 1.2. Fragmentation pathway resulting in A-type ion formation in derivatised molecules.

aminoglycosidic linkage[53] affording the ion illustrated in structure (I). The presence of the nitrogen atom probably stabilises the positive charge. $\beta$-cleavage fragment ions are still observed in the spectra of such derivatives, but as minor components.




Structure (I)

In addition to directing fragmentation and eliminating the ambiguities associated with native samples, derivatisation, in particular peracetylation and permethylation, results in an increase in sensitivity. The most plausible explanation for this phenomenon is that the act of derivatisation eliminates many of the hydrogen bonds that otherwise would form between the sample and matrix, resulting in an increased propensity to ionise and desorb from the matrix.

In the analysis of bacterial polysaccharides, FAB-MS has been used to assign the sugar type (i.e. hexosyl, pentosyl), substituent groups, and to define the sequence. In fact, the structure of mycobacterial methylglucose polysaccharide MGP, one of the first polysaccharides to be

analysed by FAB-MS, was revised as a result of the spectrum obtained, which indicated that the molecule contained two extra residues[54]. Many other studies on bacterial polysaccharides have demonstrated the applicability of FAB-MS to such problems[55,56,57,58].

N.m.r. and MS have proven to be complementary techniques, with M.S providing the sequence and composition data that is used to guide subsequent n.m.r. analysis (see chapter 2.3.4.), and n.m.r. affording linkage and 3-dimensional information. Although n.m.r. is less able to distinguish mixtures and is less sensitive than MS it is a non-destructive method, whereas MS has proved itself capable of mixture analysis at high sensitivity[59]. The combination of n.m.r., mass spectrometry and bacteriophage cleavage has been demonstrated clearly by Dutton[60,42].

At the start of the work reported in this thesis, FAB-MS was able to provide composition data, particularly from native samples, including the presence and number of non-carbohydrate substituents. Permethyl and peracetyl derivatives were being exploited to direct fragmentation via predictable pathways to facilitate sequencing. The application of FAB-MS to carbohydrate structure analysis had resulted in some notable breakthroughs. For example the detailed structure of the haptenic form of the Enterobacteriacea common antigen, was finally delineated using FAB-MS coupled with derivatisation and hydrolysis[61]. Despite these successes a number of problems remained to be solved. For example, sequence data was sometimes incomplete if the fragmentation was too

strongly directed by aminosugar residues and the loss of labile groups upon derivatisation was a major disadvantage.

The work persued in the course of this research was aimed at developing mass spectrometric protocols to enable full sequence determination particularly of molecules containing more than one branch and to locate the residue within the sequence of a saccharide that contains labile substituents.

The new FAB strategies reported in this thesis were incorporated into structural analyses of Klebsiella K69 and K44 capsular polysaccharides, sycamore extracellular polysaccharide and oligosaccharides from the group specific lipopolysaccharide from Neisseria meningitidis.

## Chapter 2 : Location of O-acyl groups.

### 2:1. Introduction.

O-acylation has been found to be widespread in bacterial polysaccharides with a number of different acyl groups present, though acetates are the most common substituent.

The presence of O-acetate in a bacterial polysaccharide was first reported by Avery and Goebell[14] from their studies on Pneumococcus type I capsule. The presence of O-acetate was found to be necessary to account for all the serological properties of Pneomuccocus type I. O-pyruvyl groups were first reported as substituents in Xanthamonas campestris[62] and hydroxybutanoate as a substituent in Rhizobium leguminosum. Many other acyl groups have been recognised as being present in bacterial polysaccharides including glyceryl,[63] isobutyl, propionyl and octanoyl.[59]

The purpose of such groups is not fully understood [64,65]. It has been suggested that O-acetyl groups are involved in biosythesis, as a protecting group to prevent further modification [66,67]. In addition O-acetyl groups have been shown to affect viscosity, solubility and immunogenicity[14,15,16], and to affect secondary and tertiary structure, preventing the formation of gels[68]. One study has shown that the O-acetyl group is essential to the formation of the meningococcal group I group-specific determinant[69].

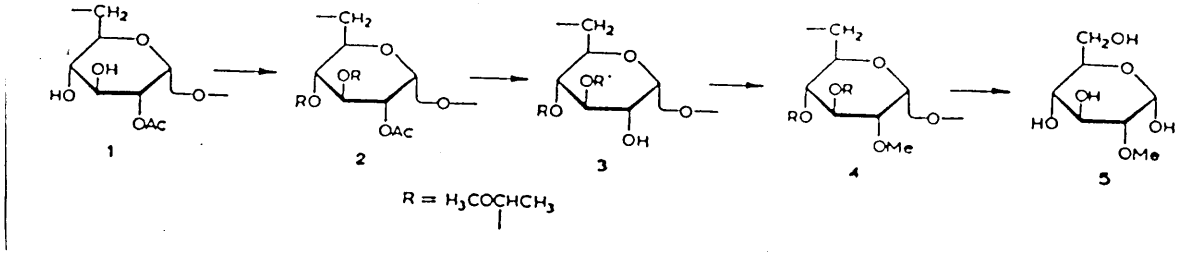
## 2:2. Methods for the location of O-acyl groups.

### 2:2.1 Chemical location of O-acyl groups.

Our knowledge of the role of O-acyl groups has been limited by the ability of workers to recognise and locate such substituents. As analytical methods have improved the body of knowledge concerning acylation has increased.

Hestrin[70] developed a method to quantitate the number of acetates present in a molecule, but this gave no indication of the site of O-acylation and until 1968, with the introduction of the methyl vinyl ether procedure of De Belder and Norman[32], there was no effective method of identifying and locating such groups.

The methyl vinyl ether method was a major advance and involves the free hydroxyl groups in the molecule under examination being protected by reaction with methyl vinyl ether in anhydrous methyl sulphoxide, using p-toluensulphonic acid as a catalyst (see scheme 2.1 **1**). The product is then deacetylated **2** to remove the natural acetates and methylated **3**.




Scheme 2.1

Originally De Belder and Norman used N,N-dimethylformamide with methyl iodide and silver oxide to methylate the free hydroxyl groups[32], though today the

Hakomori[25] permethylation is used; this removes all acetates, replacing them with methyl ethers, leaving the vinyl ethers intact **4**. The partially methylated vinyl ether product is then hydrolysed in acid which generates monosaccharides in which the methyl vinyl ethers have been lost, leaving free hydroxyls in their place and a methyl group where the O-acetate was originally located. A reduction is then carried out followed by an acetylation, producing partially methylated alditol acetates, which are then analysed by g.l.c. and the linkages present in the original O-acetylated material determined by the presence of the O-methyl ethers.

Although the methyl vinyl ether method has been successfully applied in structural analyses[42,71,72,73], the technique involves several chemical manipulations that can result in incomplete derivatisation, making interpretation of the results difficult[74,75].

2:2.2 Location of O-acyl groups using N.M.R.

The location of O-acetate groups by n.m.r. is achieved by the use of $^{1}H$ n.m.r. to observe the O-acetyl methyl protons with $^{13}C$ n.m.r. to define the carbon which is substituted. These experiments are often performed on both the native and de-O-acetylated molecule to unambiguously define the location assignment[42,76]. N.m.r. does have some difficulties in examining O-acetyl substitution. A common technique used to chemically shift solvent derived signals out of the anomeric region is to heat the sample; unfortunately O-acetates often migrate

under such conditions. Additionally the analysis of mixtures that are heterogenous with respect to acetate location and abundance is problematic. The most effective use of n.m.r. seems to be in the analysis of single components or simple mixtures.

This chapter describes the development of a novel FAB-MS protocol[77] to locate O-linked acyl groups and shows the method's application to solving structural problems.

## 2:3. Model experiments.

### 2:3.1. Strategy.

An underivatised sample affords data that can be ambiguous due to the several possible fragmentation pathways that occur (see introduction). Because β - cleavages may occur either side of the glycosidic bond double cleavage reactions are impossible to identify, making fragmentation data unreliable. Additionally native samples are very sensitive to the presence of impurities affording less abundant ions because they desorb less readily from the matrix. This is due to the electrostatic interactions between the carbohydrate hydroxyl groups and the polar moieties of the matrix. Derivatisation excludes or reduces such electrostatic interaction, thus enhancing desorption from the matrix and therefore ion formation/transmission. Additionally derivatisation removes the ambiguities associated with the fragmentation of native samples and also directs such fragmentation in a predictable manner.

Therefore, to exploit the FAB-MS properties of derivatives, to assist in the examination of O-acylated saccharides, it was necessary to develop a derivatisation procedure that affords a stable product which fragments in a reproducible and predictable manner and that also leaves the O-acyl groups intact.

In exploratory derivatisation experiments it was observed that the acyl groups were reasonably stable at low pH. Therefore the acidic peracetylation reaction[78], which has been successfully utilised as a method of

obtaining stable derivatives that fragment predictably and reproducibly, was modified to form the basis of this methodology. The approach taken was to carry out an acetylation[78] using trifluoroacetic anhydride (TFAA)/deuteroacetic acid, which forms the perdeuteroacetyl derivative on all free hydroxyls.

2.3.2.1. Stability of O-acyl groups under the perdeuteroacetylation conditions.

For a derivatisation procedure to be useful it is essential that it leaves all naturally occurring O-acyl groups intact. A series of model experiments were carried out to confirm that such groups are indeed stable to the conditions used during the acidic peracetylation.

Maltotriose and stachyose were peracetylated using TFAA/acetic acid. A FAB spectrum of peracetylated maltotriose gave molecular ions at m/z 967, 984 and 907 consistent with $[M+H]^+$, $[M+NH_4]^+$ and the oxonium molecular ion respectively. A-type [79] fragment ions were observed at m/z 331 and 619 consistent with the compositions Hex and $Hex_2$ respectively. The spectrum of peracetylated stachyose afforded molecular ions at m/z 1255 and 1272 consistent with $[M+H]^+$ and $[M+NH_4]^+$. No oxonium molecular ion was observed since stachyose is a non-reducing sugar. A-type fragment ions were observed at m/z 331, 619 and 907 consistent with Hex, $Hex_2$ and $Hex_3$.

The peracetylated maltotriose and stachyose were then subjected to the acetylation reagent in which acetic acid was replaced by deuteroacetic acid . If an acetyl group

was substituted by a deuteroacetyl moiety in the product, this would be indicated by a mass shift within the spectrum of 3 a.m.u. (the mass difference between acetyl and deuteroacetyl).

The FAB spectrum (Fig. 2.1) of stachyose after perdeuteroacetylation gave the same signals as those observed previously (m/z 331, 619, 907, 1255 and 1272) with no signals observed 3 a.m.u. higher which would have indicated the substitution of an acetate by a deuteroacetate. This confirmed that O-acetates were indeed stable to the acidic conditions of the deuteroacetylation reagent.

After perdeuteroacetylation maltotriose (Fig. 2.2) afforded a FAB spectrum in which the fragment ions were exactly those observed previously after peracetylation, namely m/z 331 and 619. The molecular ion region of the spectrum contained two new signals at m/z 970 and 987 in addition to those expected , and previously observed, at m/z 907, 967 and 984. These data are summarised in TABLE 2.1. The new signals (970 and 987) were 50% as intense as those at m/z 967 and 984, indicating that 30% of the molecules have one acetyl substituted by a deuteroacetate. No signal was observed at m/z 910, indicating that the replacement of an acetyl by a deuteroacetyl had not occurred in the oxonium molecular ion. This indicated that the substitution, as evidenced by m/z 970 and 987, occurred in the reducing terminal hexosyl residue on the reducing hydroxyl. Stachyose, a non-reducing sugar, does not incorporate deuteroacetate under the same experimental

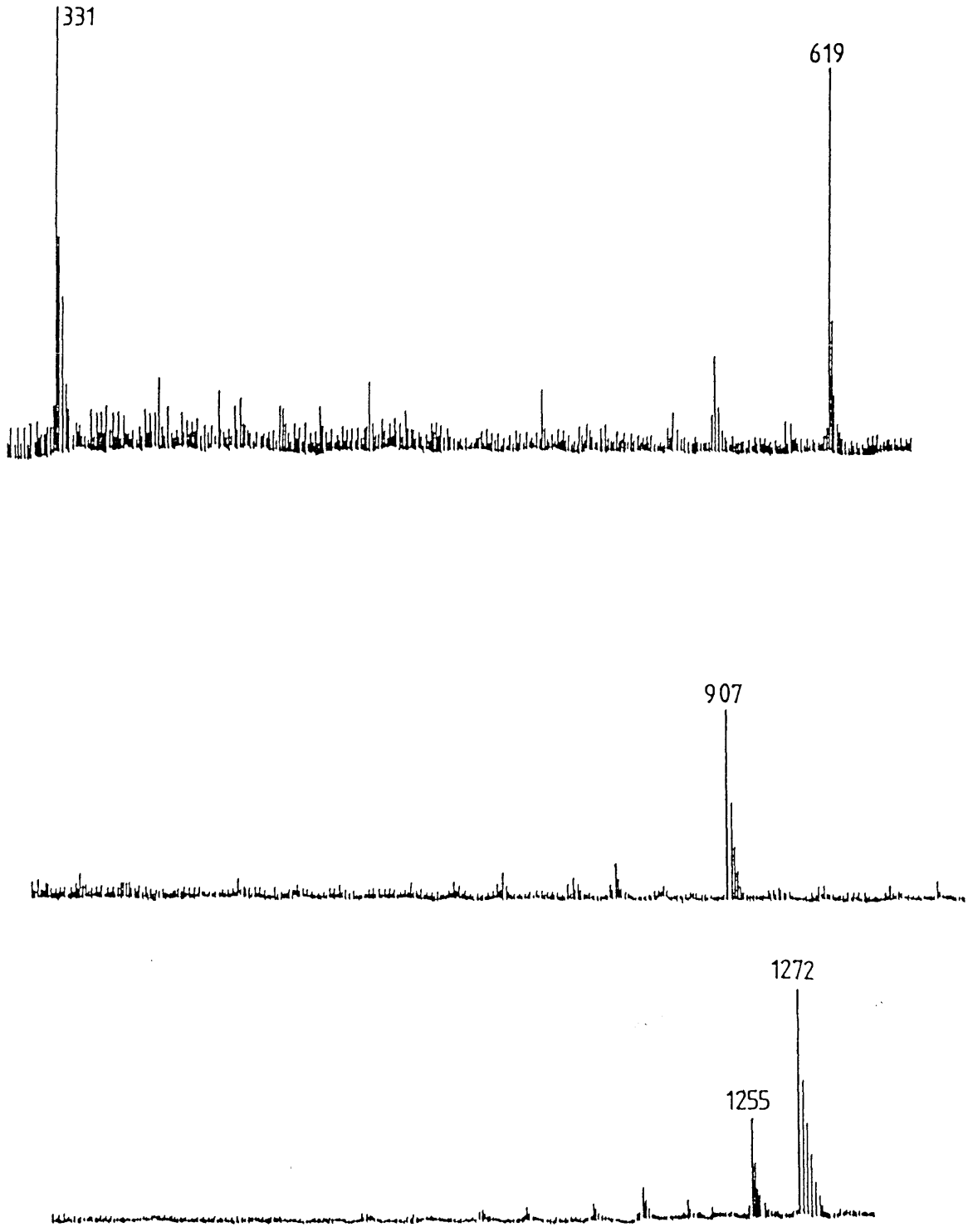



Figure 2.1. Positive ion FAB spectrum of peracetylated stachyose after deuteroacetylation.

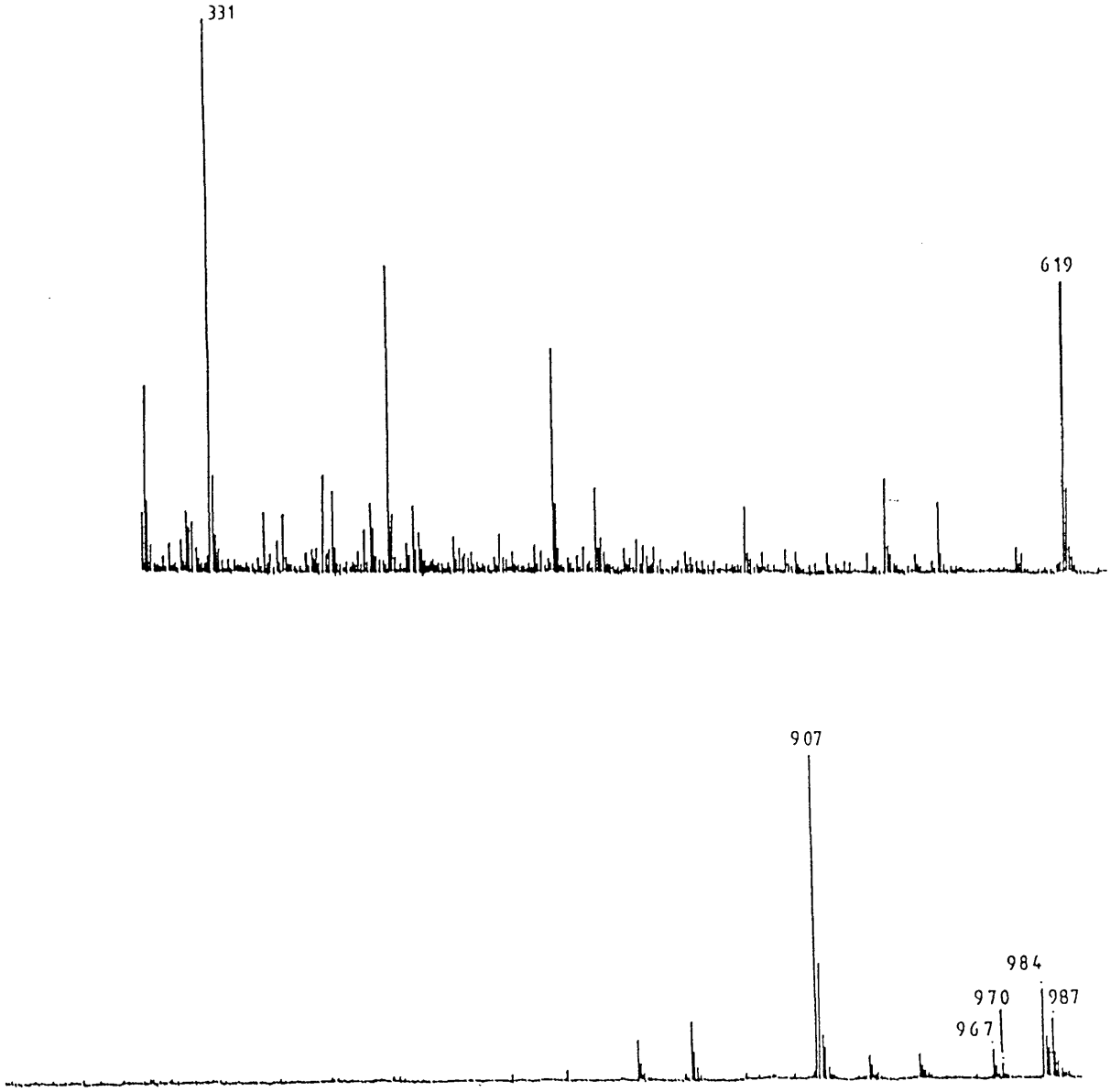



Figure 2.2. Positive ion FAB spectrum of peracetylated maltotriose after deuteroacetylation.

conditions. This corroborated the suggestion that the reducing hydroxyl was the group whose acetyl substituent was labile. In studies carried out on replacement reactions occurring in carbohydrates in the presence of acetic anhydride it has been shown that it is the reducing hydroxyl that is suceptible to substitution[80].

The fact that the reducing hydroxyl is not stable to the acidic derivatisation conditions used in this protocol is relatively unimportant in structural studies carried out on oligosaccharides derived from bacterial polysaccharides, and in fact from oligosaccharides derived from any glycoconjugates. This is because the hydroxyl on position 1 normally participates in the formation of the glycosidic bond. It is therefore unavailable for modification by substituents, such as acetate, in its native state.

### 2:3.2.2 Stability of O-acetyl groups under severe conditions.

The stability of the O-acetyl group under rigorous conditions was determined by subjecting peracetylated maltotriose and stachyose to the perdeuteroacetylation conditions for 30 min and 60 min. The FAB spectra afforded were identical to those obtained after a 10 min reaction.

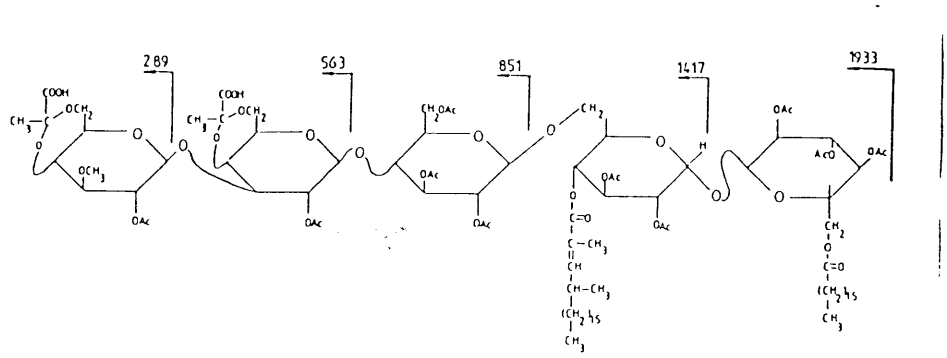
The conclusions reached from these experiments are that O-acetates are resistant to substitution under the deuteroacetylation conditions normally used and also under more severe conditions.

**TABLE 2.1.** Summary of signals observed in the spectra of Maltotriose and Stachyose after acetylation and additional deuterioacetylation.

| STACHYOSE | | | |
|---|---|---|---|
| ACETYLATED | | DEUTERIOACETYLATED | |
| ION | COMPOSITION | ION | COMPOSITION |
| 1272 $[M+NH_4]^+$ | $Hex_4$ | 1272 $[M+NH_4]^+$ | $Hex_4$ |
| 1255 $[M+H]^+$ | " | 1255 $[M+H]^+$ | " |
| 907 A-Type | $Hex_3$ | 907 A-Type | $Hex_3$ |
| 619 " | $Hex_2$ | 619 " | $Hex_2$ |
| 331 " | $Hex_1$ | 331 " | $Hex_1$ |
| MALTOTRIOSE | | | |
| ACETYLATED | | DEUTERIOACETYLATED | |
| ION | COMPOSITION | ION | COMPOSITION |
| 984 $[M+NH_4]^+$ | $Hex_3$ | 987 $[M+NH_4]^+$ | $Hex_3$* |
| 967 $[M+H]^+$ | " | 984 $[M+NH_4]^+$ | $Hex_3$ |
| 907 A-Type | " | 970 $[M+H]^+$ | $Hex_3$* |
| 619 " | $Hex_2$ | 967 $[M+H]^+$ | $Hex_3$ |
| 331 " | $Hex_1$ | 907 A-type | $Hex_3$ |
| | | 619 " | $Hex_2$ |
| | | 331 " | $Hex_1$ |

2:3.2.3. Stability of other O-acyl groups.

The glycolipid (I), of known structure was used as a model compound to determine the stability of O-acyl




(I)

groups other than acetate. This molecule contains two long chain fatty acid moieties and also two pyruvyl O-acetal groups. The pyruvyl groups do not present as much of a challenge to the classical carbohydrate chemist as do O-acyl groups[81], in the determination of their location. This is because they are stable to the Hakomori methylation, and can therefore be analysed by methylation analysis. This molecule was chosen since it would be an example of the application of this new MS protocol to the analysis of O-linked substituents in general.

The sample was peracetylated, (since there were no acetyl groups present the deuterium labelling procedure was not neccessary) and the FAB mass spectrum of the product obtained (Fig. 2.3). The signals observed in the spectrum are listed in TABLE 2.2. The spectrum afforded molecular ions, as expected, at m/z 1933, 1950 and 1955 consistent with $[M+H]^+$, $[M+NH_4]^+$ and $[M+Na]^+$ of composition $Hex_5$ with two O-acetal pyruvyl and two long

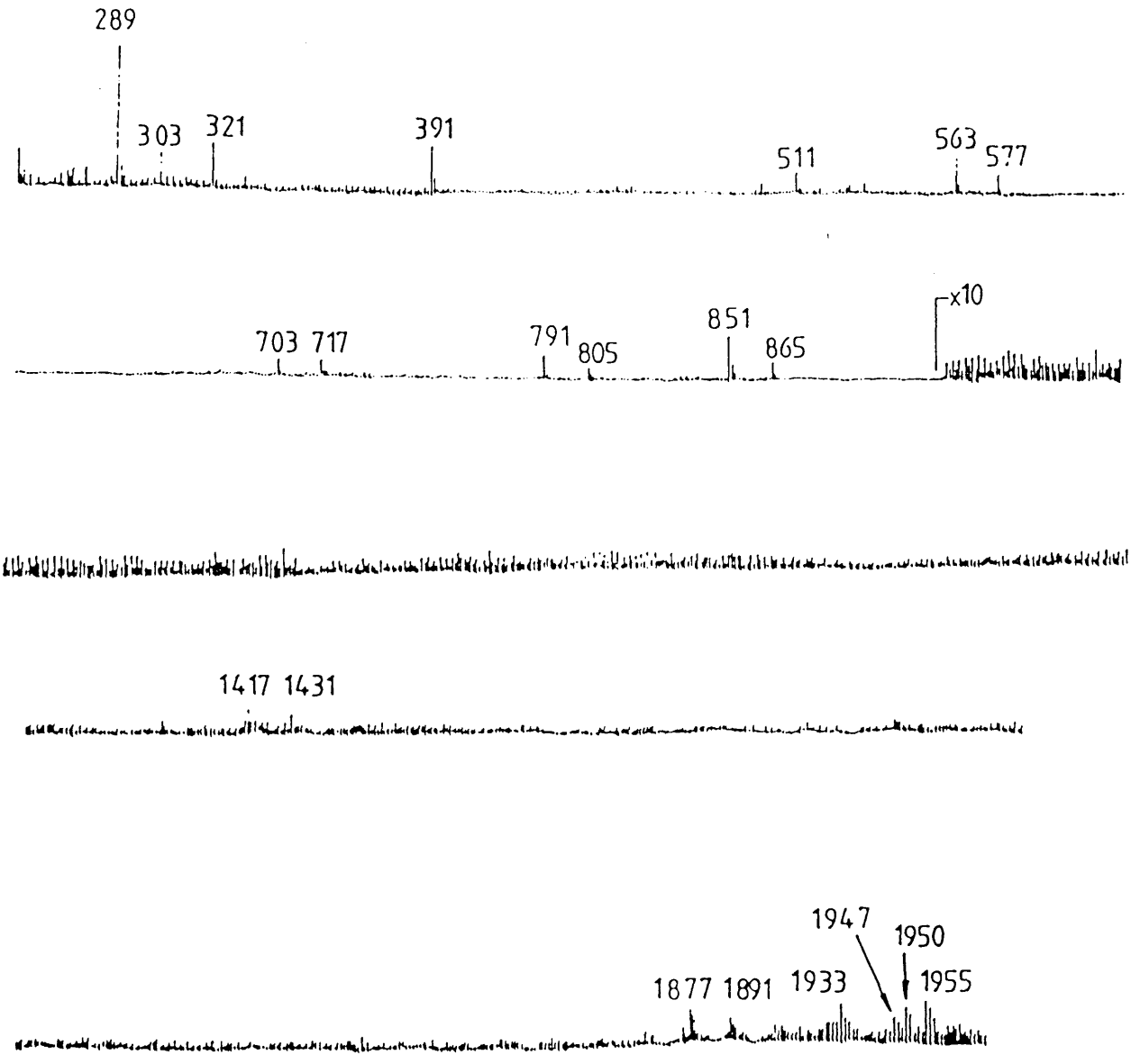



Figure 2.3. Positive ion FAB spectrum of acetylated glycolipid I.

chain fatty acid groups. The signals at m/z 1877 and 1891 are $[M+H]^+$ molecular ions generated by a component with the same sugar composition as glycolipid I but with differing fatty acyl chains. The mass difference between the two sets of molecular ions is 56 a.m.u. equivalent to there being 4 less carbons in the acyl chains. The minor signal observed at m/z 1947 is from a molecule in which a pyruvyl group has been replaced with two acetates. A-type fragment ions were observed at m/z 289, 563, 851 and 1417, fully consistent with the structure of this molecule. The signals at m/z 791 and 805 are due to the elimination of acetic acid from m/z 851 and 865 respectively. The signals at m/z 303, 577, 865 and 1431 are derived from a minor component which has had a single pyruvyl group replaced by two acetyl groups. These minor signals remain constant throughout the spectrum and therefore indicates that the terminal pyruvyl is the labile substituent. No signals were observed at m/z 1403, 1613 or 1723 which would be present if one (1723 or 1613) or both of the long chain acyl groups had been substituted by acetate. From this experiment it was concluded that fatty acyl groups are stable to the derivatisation procedure and in addition that O-acetal groups are sufficiently stable to allow unambiguous analysis. In subsequent work, substitution of pyruvyl groups, under the derivatisation conditions, has not been observed (see section 2.3.3.).

**TABLE 2.2.** Summary of peaks observed in the spectrum of deuterioacetylated glycolipid (I).

| MOLECULAR IONS | | COMPOSITIONS |
|---|---|---|
| 1955 | $[M+Na]^+$ | glycolipid I |
| 1950 | $[M+NH_4]^+$ | glycolipid I |
| 1933 | $[M+H]^+$ | glycolipid I |
| 1947 | $[M+H]^+$ | glycolipid I with only 1 pyr |
| 1891 | $[M+H]^+$ | glycolipid with different acyl |
| 1877 | $[M+H]^+$ | moieties. |
| FRAGMENT IONS | | COMPOSIITONS |
| 1431 | | $MeHex_1Hex_3Pyr_1$ + lipid |
| 1417 | | $MeHex_1Hex_3Pyr_2$ + lipid |
| 865 | | $MeHex_1Hex_2Pyr_1$ |
| 851 | | $MeHex_1Hex_2Pyr_2$ |
| 805 | | 865 minus AcOH |
| 791 | | 859 minus AcOH |
| 577 | | $MeHex_1Hex_1Pyr_1$ |
| 563 | | $MeHex_1Hex_1Pyr_2$ |
| 303 | | MeHex |
| 289 | | $MeHex_1Pyr$ |

2:3.3. Analysis of mixtures.

A sample comprising mixtures of oligosaccharides, obtained by liquid HF hydrolysis of gellan gum, the extracellular polysaccharide produced by Pseudomonas eloda, was used to assess whether the data obtained from deuteroacetylation experiments would allow unambiguous assignment of O-acyl groups on a mixture of molecules.

Previous observations [82] indicated that it would not be possible to determine the relative amounts of each component in the sample from a FAB spectrum of the native material. The aim of this experiment was to examine the effectiveness of the deuteroacetylation procedure in determining the location and abundance of O-acylation in a mixture of components.

This sample was subjected to perdeuteroacetylation and the positive ion FAB mass spectrum recorded, generating a complex series of signals (Fig. 2.4.). These signals are in complete agreement with the assigments made previously[82] except that no fluorine containing species are present; the fluorine being labile to the acidic deuteroacetylation conditions. The loss of the fluorine is of benefit since this results in simplified spectra. The pairs of signals observed at m/z 983/986, 1116/1119, 1216/1219/1222, 1352/1355 and 1485/1488 are $[M+H]^+$ molecular ions of composition $Hex_2HexA_1Ac_1$ / $Hex_2HexA_1$, $Hex_2HexA_1G_1Ac_1$ / $Hex_2HexA_1G_1$, $Hex_2HexA_1Rha_1Ac_2$ / $Hex_2HexA_1Rha_1Ac_1$ / $Hex_2HexA_1Rha_1$, $Hex_2HexA_1Rha_1G_1Ac_1$ / $Hex_2HexA_1Rha_1G_1$ and $Hex_2HexA_1Rha_1G_2Ac_1$ / $Hex_2HexA_1Rha_1G_2$ respectively.

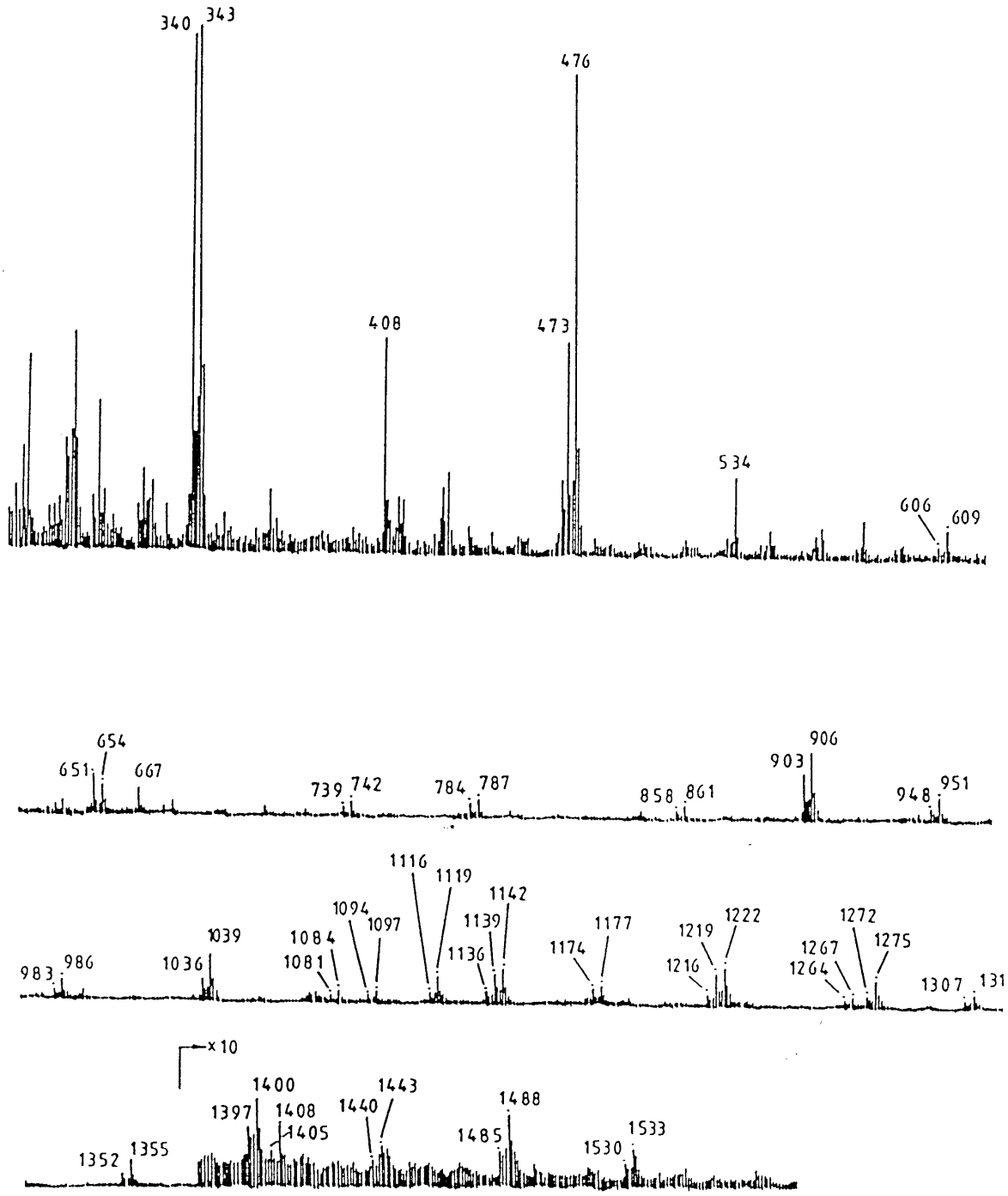



Figure 2.4. Positive ion FAB spectrum of deuteroacetylated gellan gum.

The signals at m/z 903/906, 1036/1039, 1136/1139/1142, 1272/1275 and 1405/1408 are oxonium molecular ions corresponding to the compositions above. Paired A-type fragment ions were observed at m/z 739/742, 606/609, 473/476 and 340/343 of composition $Hex_1HexA_1G_1Ac_1$ / $Hex_1HexA_1G_1$, $Hex_1HexA_1Ac_1$ / $Hex_1HexA_1$, $Hex_1G_1Ac_1$ / $Hex_1G_1$ and $Hex_1Ac_1$ / $Hex_1$ respectively. The ions observed are listed with the corresponding compositions in TABLE 2.3.

The spectrum in figure 2.4. shows the relative intensities of signals relating to components of a particular sugar composition with differing degrees of O-acetylation, making it possible to determine the level of O-acetylation on different components in the sample. The level of acetylation in the different components of this sample, expressed as a percentage of that particular component, is listed in TABLE 2.3 in the column '% Ac'. These data clearly show that four of the five components (according to the sugar composition) have very similar, if not the same, level of acetylation. Approximately 30% of the components of compositions $Hex_2HexA_1$, $Hex_2HexA_1G_1$, $Hex_2HexA_1Rha_1G_1$ and $Hex_2HexA_1Rha_1G_2$ are naturally O-acetylated. Whereas the component with the sugar composition $Hex_2HexA_1Rha_1$ carries two acetates in 18% of cases one acetate in 40% of cases and no acetates in 42% of cases. It is possible to state that the second O-acetate present in the molecule generating the signal at m/z 1216 is not located on the non-reducing terminal hexose. This conclusion is reached because there is no signal at m/z 337 ($Hex_1Ac_2$) which would be that expected

**TABLE 2.3.** Summary of data obtained from deuterioacetyl spectrum of gellan gum from Pseudomonas elodea.

| Molecular ions $[M+NH_4]^+$ | Oxonium ions | Compositions | % Ac | mixed-anhydride | |
|---|---|---|---|---|---|
| | | | | $[M+NH_4]^+$ | A-type |
| 983 | 903 | $Hex_2HexA_1Ac_1$ | 28 | 1028 | 948 |
| 986 | 906 | $Hex_2HexA_1$ | 72 | 1031 | 951 |
| 1116 | 1036 | $Hex_2HexA_1G_1Ac_1$ | 29 | 1161 | 1081 |
| 1119 | 1039 | $Hex_2HexA_1G_1$ | 71 | 1164 | 1084 |
| 1216 | 1136 | $Hex_2HexA_1Rha_1Ac_2$ | 18 | 1261 | 1181 |
| 1219 | 1139 | $Hex_2HexA_1Rha_1Ac_1$ | 40 | 1264 | 1184 |
| 1222 | 1142 | $Hex_2HexA_1Rha_1$ | 42 | 1267 | 1187 |
| 1352 | 1272 | $Hex_2HexA_1Rha_1G_1Ac_1$ | 33 | 1397 | 1317 |
| 1355 | 1275 | $Hex_2HexA_1Rha_1G_1$ | 67 | 1400 | 1320 |
| 1485 | 1405 | $Hex_2HexA_1Rha_1G_2Ac_1$ | 32 | 1531 | |
| 1488 | 1408 | $Hex_2HexA_1Rha_1G_2$ | 68 | 1533 | |
| | 739 | $Hex_1HexA_1G_1Ac_1$ | | | 784 |
| | 742 | $Hex_1HexA_1G_1$ | | | 787 |
| | 606 | $Hex_1HexA_1Ac_1$ | | | 651 |
| | 609 | $Hex_1HexA_1$ | | | 654 |
| | 473 | $Hex_1G_1Ac_1$ | | | |
| | 476 | $Hex_1G_1$ | | | |
| | 340 | $Hex_1Ac_1$ | | | |
| | 343 | $Hex_1$ | | | |

for a doubly acetylated terminal hexose. Further, since no doubly acetylated A-type ions are observed with the compositions Hex, $Hex_1HexA$ and $Hex_2HexA$, the data indicates that the second acetate is located on the reducing terminal rhamnose. It was observed that several of the components exhibited one degree of 'over deuteroacetylation' due to the formation of the mixed anhydride with the hexuronic acid carboxylic hydroxyl group In the case of some signals this is most clearly observed as signals 45 a.m.u. higher than those for the A-type ions, and not so clearly as ions 45 a.m.u. higher than the molecular ions. These signals are also listed in TABLE 2.3 in the column 'mixed-anhydride'. In Fig. 2.4 the signals at m/z 651/654, 784/787 and 948/951 correspond to mixed anhydrides of the same composition as the components at m/z 606/609, 739/742 and 903/906 respectively.

In figure 2.5 a section of the spectrum is reproduced to show more clearly these minor signals. The signals observed at m/z 1028/1031, 1161/1164, 1261/1264/1267, 1397/1400 and 1530/1533 are the mixed anhydrides corresponding to the same composition as the components at m/z 983/986, 1116/1119, 1216/1219/1222, 1352/1355 and 1485/1488 respectively. A-type ion signals for the mixed anhydrides corresponding to the signals at m/z 1036/1039, 1136/1139/1142 and 1272/1275 were observed at m/z 1081/1084, 1181/1184/1187 and 1317/1320. No signals were observed at m/z 1450/1453 corresponding to the mixed anhydride of the component generating the signals at m/z 1405/1408. This may be because the signal intensity is not

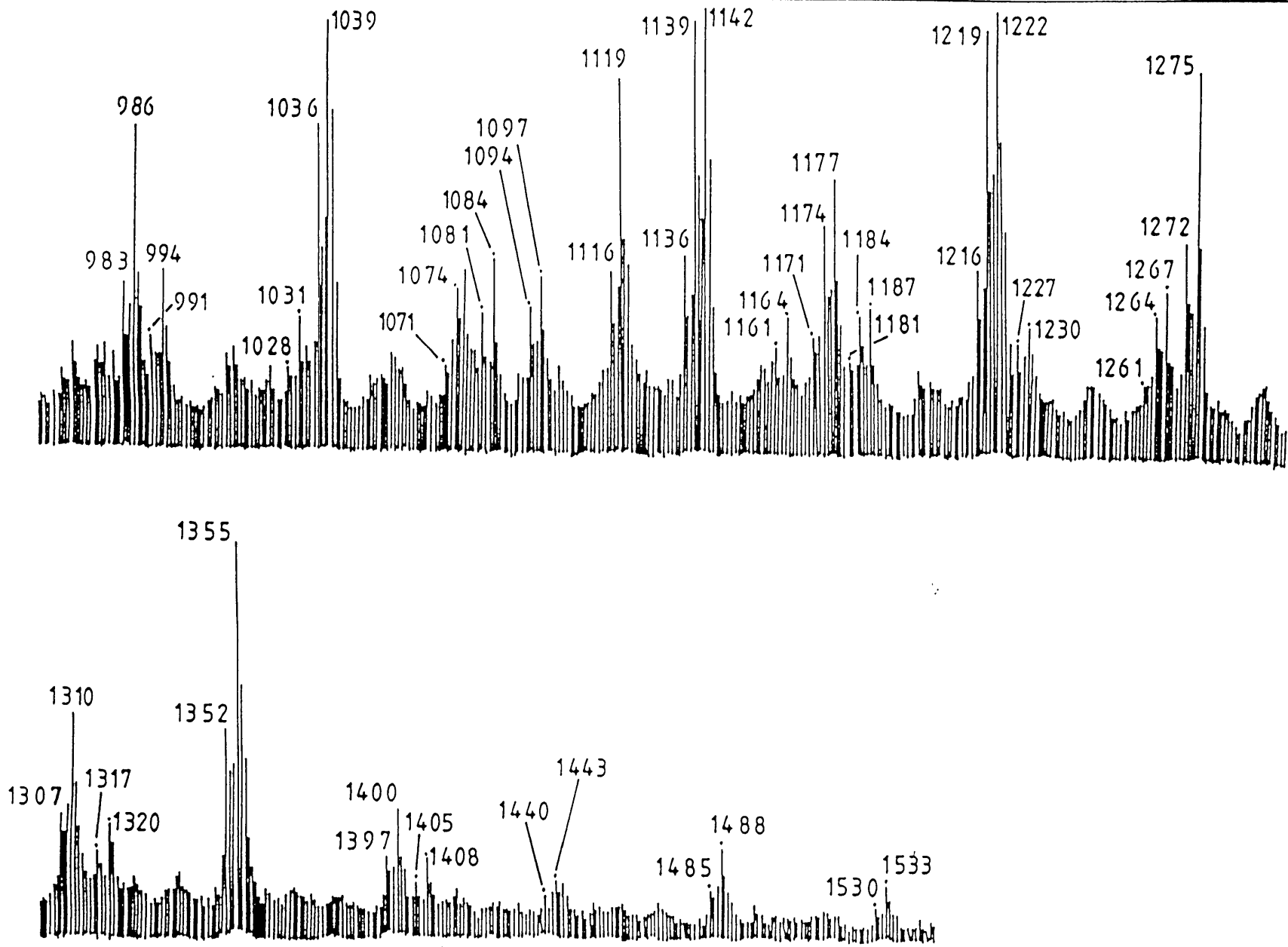



Figure 2.5. Partial FAB spectrum of deuteroacetylated gellan gum.

sufficient for the signals to be recognised above the background.

Additionally signals were observed due to one degree of under-deuteroacetylation at m/z 858/861 (in Fig. 2.4), 991/994, 1071/1074, 1091/1094/1097, 1171/1174/1177, 1227/1230, 1307/1310 and 1440/1443 which correspond to the same sugar compositions as the signals observed at m/z 903/906 (Fig. 2.4), 1036/1039, 1116/1119/, 1136/1139/1142, 1216/1219/1222, 1272/1275, 1352/1355 and 1485/1488 respectively. No signals for under-deuteroacetylated components corresponding to the A-type ions at m/z 1405/1408 were observed, this may again be due to the background signals obscuring them.

This experiment has clearly shown the effectiveness of the deuteroacetylation procedure in the analysis of samples containing mixtures of components, where there is a variation in the level of O-acetylation on the different components.

2:4. Summary.

These experiments have shown that naturally occurring O-acyl groups are left intact and are not substituted by deuteroacetyl moieties under the deuteroacetylation conditions used. This protocol requires a FAB spectrum of the perdeuteroacetyl product to be acquired and the sequence of the oligosaccharide determined from the fragment ions afforded in the spectrum. The sequence data obtained indicates the residue(s) on which acyl group(s) are naturally occurring.

The deuterioacetyl derivative thus fulfills all the prerequisits for its application to O-acyl location:-

i) it is stable

ii) it directs fragmentation predictably and reproducibly

iii) it is a sensitive technique, requiring 0.5 - 1 ug of sample per analysis

iv) it leaves the O-acyl groups intact

## 2:5. Applications of the deuteroacetylation procedure.

### 2.5.1. Klebsiella K44 Polysaccharide.

The first test of this new procedure in a situation where the sample structure was not known at the time of the analysis, was the location of the residue that is O-acetylated in a pentasaccharide obtained by bacteriophage enzyme action on the capsular polysaccharide from Klebsiella K44. The oligosaccharide was supplied by Dr. G.G.S. Dutton, who has successfully utilised classical carbohydrate chemical and NMR techniques in an examination of bacterial surface capsular structures[37,42,60,83].

The positive FAB spectrum (Fig. 2.6) of the native, reduced material was obtained, which afforded molecular ions at m/z 855, 872, 877 and 893, consistent with $[M+H]^+$, $[M+NH_4]^+$, $[M+Na]^+$ and $[M+K]^+$ of composition $HexA_1Hex_1DeoxyHex_2Hexitol_1$ with one acetyl group. No sequence information was obtained from this spectrum. Therefore the perdeuteroacetyl derivative of this sample was prepared to obtain sequence and O-acylation data. The FAB spectrum of the perdeuteroacetylated sample is shown in Fig. 2.7. The molecular ion signals observed at m/z 1485, 1502 and 1507 are consistent with $[M+H]^+$, $[M+NH_4]^+$ and $[M+Na]^+$ of composition $HexA_1Hex_1DeoxyHex_2Hexitol_1$ with one acetyl and 18 deuteroacetyl groups. If there had been no O-acetyl group in the molecule the molecular ion signals would have been 3 a.m.u. higher at m/z 1488, 1505 and 1510. The signals at m/z 312, 548, 784 and 1081 are deuteroacetylated A-type fragment ions of composition

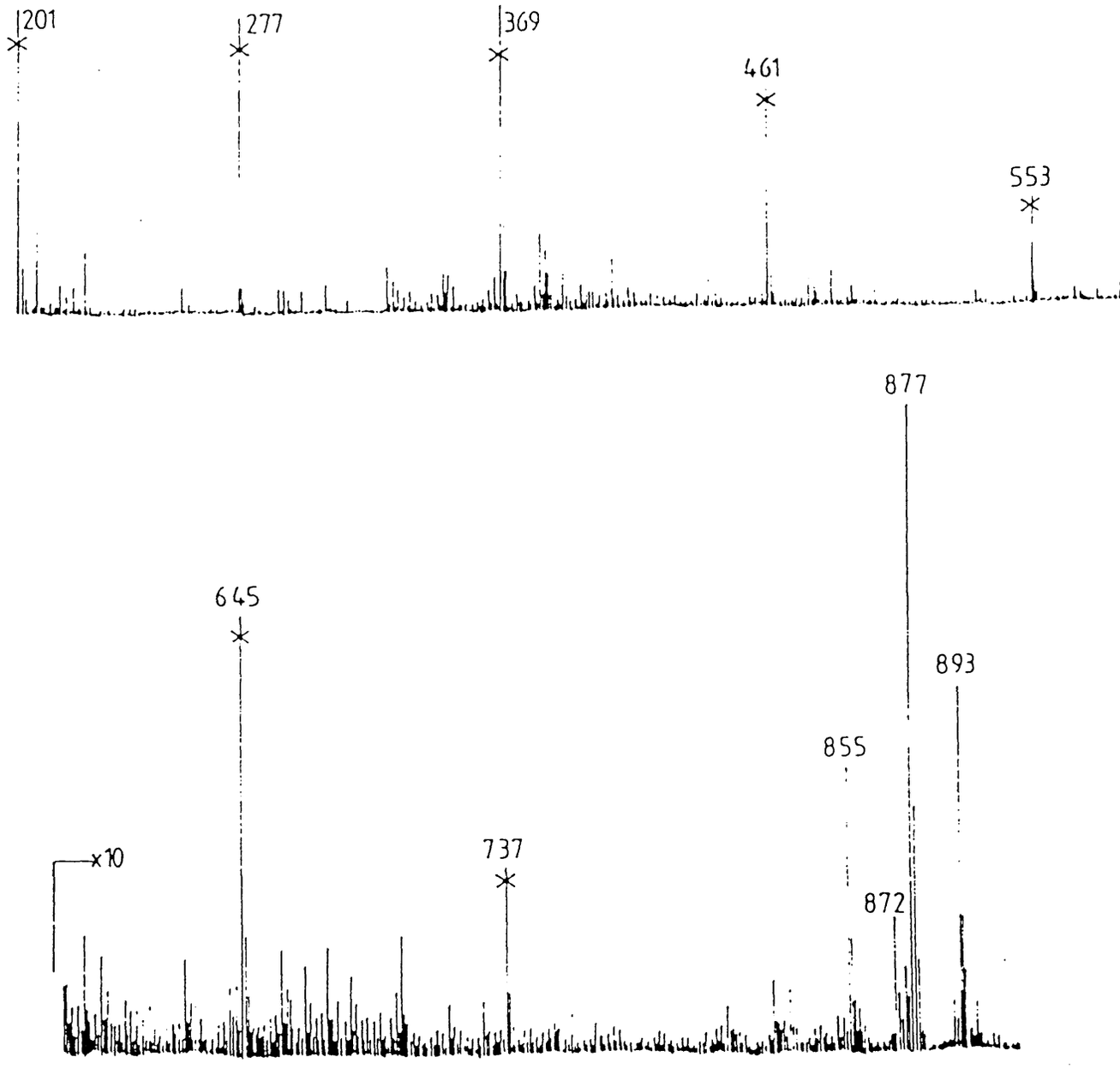



Figure 2.6. Positive ion FAB spectrum of native oligosacchari from Klebsiella K44. The signals marked with a cross are those derived from the matrix.

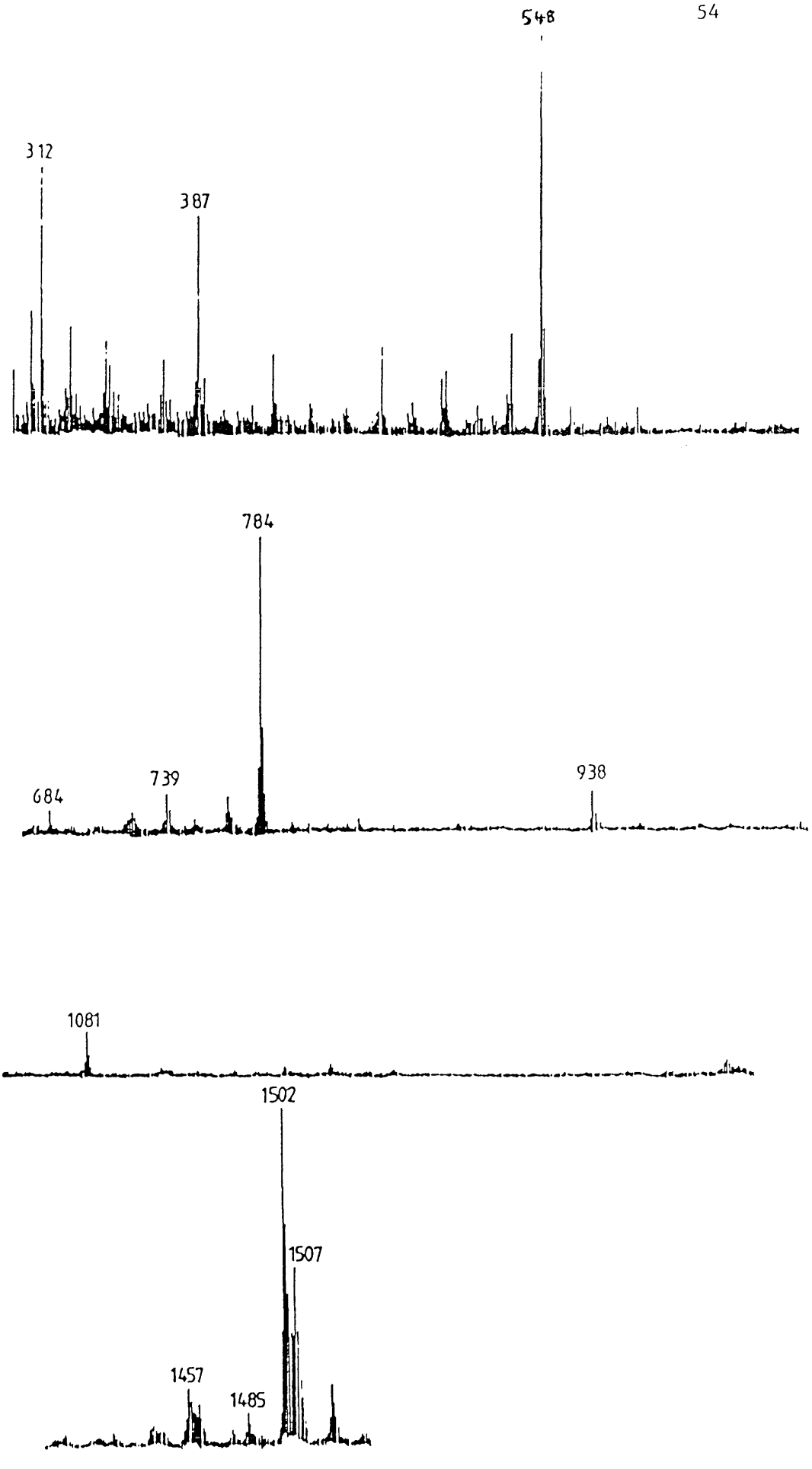
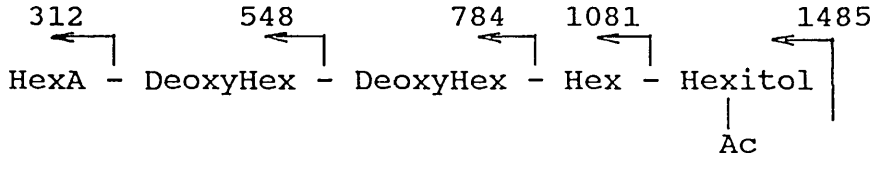



Figure 2.7. Positive ion FAB spectrum of deuteroacetylated K44.

**TABLE 2.4.** Signals observed in the native and deuterioacetyl spectra of K44 repeat.

| NATIVE | | | |
|---|---|---|---|
| | ION | COMPOSITION | |
| 893 | $[M+K]^+$ | $HexA_1Hex_2DeoxyHex_2Ac_1(R)$ | |
| 877 | $[M+Na]^+$ | " | |
| 872 | $[M+NH_4]^+$ | " | |
| 855 | $[M+H]^+$ | " | |
| **DEUTERIOACETYL** | | | |
| | ION | COMPOSITION | |
| 1507 | $[M+Na]^+$ | $HexA_1Hex_2DeoxyHex_2(R)$ | with 1 acetyl |
| 1502 | $[M+NH_4]^+$ | " | and 18 |
| 1485 | $[M+H]^+$ | " | deuterioacetyl |
| | | | moieities. |
| 1081 | | $HexA_1DeoxyHex_2Hex_1$ | fully |
| 784 | | $HexA_1DeoxyHex_2$ | deuterioacetylated |
| 548 | | $HexA_1DeoxyHex_1$ | " |
| 312 | | HexA | " |

HexA, $HexA_1DeoxyHex_1$, $HexA_1DeoxyHex_2$ and $HexA_1DeoxyHex_2Hex_1$. These data are summarised in TABLE 2.4. Since none of these fragment ions contains an acetyl group, while the mass increment from m/z 1081 to the molecular ion at m/z 1485 is 3 a.m.u. less than that expected for a fully deuteroacetylated residue, the conclusion reached is that the natural O-acetate is located on the reducing terminal hexitol residue. The data obtained in this experiment support the following structural assignment (II).




(II)

This conclusion is in agreement with the structure that was obtained by Dutton and Karunaratne [42] using a combination of classical chemical and NMR techniques.

GlcA 1--2**Rha**1--3**Rha**1--3**Glc**1--4**Glc**-OH
|6
OAc

2.5.2. Klebsiella K69.

A pentasaccharide supplied by Dr. H. Parolis, which was obtained from the capsular polysaccharide of Klebsiella K69 by bacteriophage action was examined by FAB-MS.

The negative ion FAB mass spectrum of the native material was obtained (Fig. 2.8). Molecular ion signals present at m/z 911 and 953 correspond to the compositions, $Hex_4HexA_1Pyr_1$ and $Hex_4HexA_1Pyr_1Ac_1$ respectively. The relative intensities of these signals may not reflect the relative concentrations since it is known that acylation will facilitate ionisation / desorption [78]. In order to obtain further information on the amount of O-acetylation, the location of the O-acetylated residue and the sequence, the deuteroacetyl derivative was prepared.

The positive ion FAB mass spectrum of the deuteroacetylated product (Fig. 2.9) contained signals listed in TABLE 2.5. at m/z 1557/1560 and 1477/1480 for $[M+NH_4]^+$ and oxonium molecular ions of composition $Hex_4HexA_1Pyr_1Ac_1$ and $Hex_4HexA_1Pyr_1$ respectively. The relative intensities of the ions indicates that the sample contains approximately 30% natural mono-O-acetylation. A-type fragment ions were observed at m/z 1183, 1180, 872, 343, 340 and 323 consistent with the compositions $Hex_3HexA_1Pyr_1$, $Hex_3HexA_1Pyr_1Ac_1$, $Hex_3Pyr_1$-OH (due to elimination of terminal Hexuronic acid), $Hex_1$, $Hex_1Ac_1$ or $Hex_1Pyr_1NH_3$ and $Hex_1Pyr_1$.

The signal observed at m/z 1180 is very much less intense with respect to m/z 1183 than either m/z 1477 with respect to m/z 1480 or m/z 1557 with respect to m/z 1560.

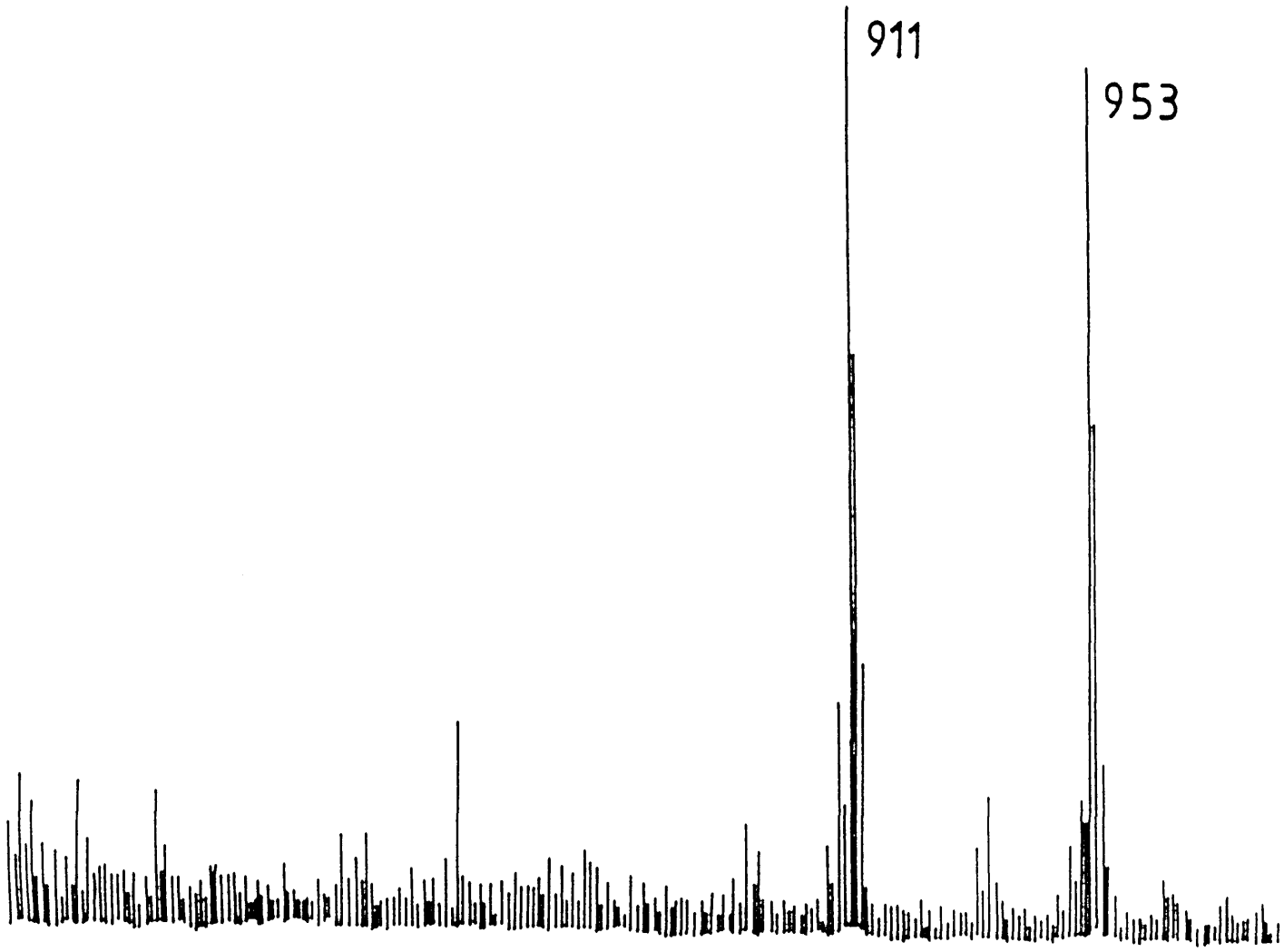



Figure 2.8. Molecular ion region of negative ion FAB spectrum of the native oligosaccharide from K69.

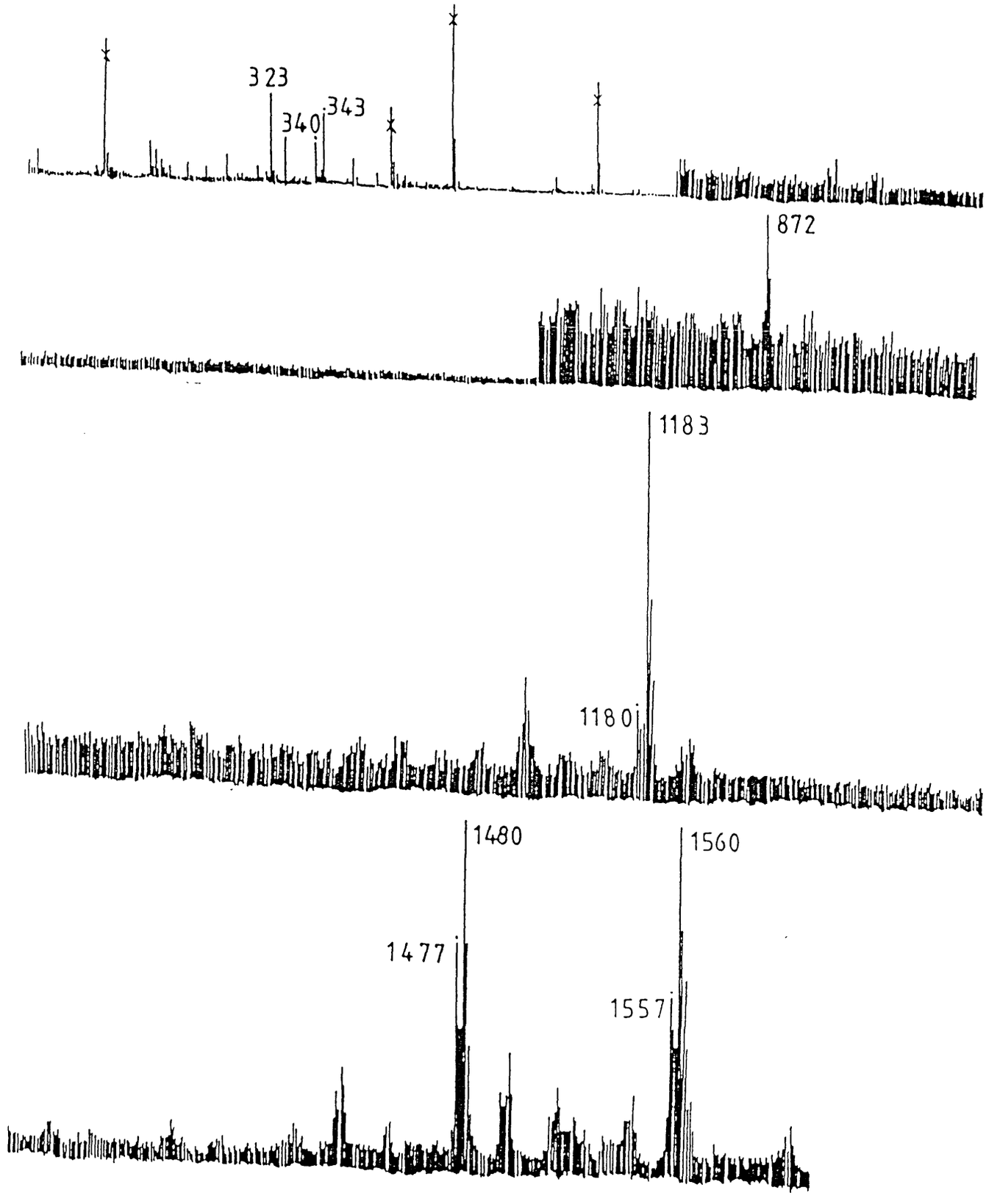



Figure 2.9. Positive ion FAB spectrum of deuteroacetylated K69. Signals marked with a cross are matrix derived.

This indicates that the majority of natural O-acetylation is located on the reducing terminal hexosyl residue. Signals which are in potential conflict with this conclusion were observed in the low mass region of the spectrum, where the signal at m/z 340 can be attributed to the A-type ion of composition $Hex_1Ac_1$, suggesting the presence of O-acetate on the non-reducing terminal hexose residue. Alternatively, m/z 340 could be due to the A-type ion arising from the ammonium salt of $Hex_1Pyr_1$. The latter was found to be the case when sodium dosing experiments were performed. Sodium acetate was added to the matrix and then spectra of the deuteroacetylated sample were obtained. It was observed (Fig. 2.10) that the signal at m/z 340 was almost totally absent from the spectrum. In addition the signal at m/z 323 ($Hex_1Pyr_1$) was absent also, indicating that sodiation of the sample had altered the fragmentation pattern such that pyruvylated hexose did not form the A-type ion. Since the signal at m/z 343 (Hex) is still observed in the absence of the signal at m.z 340, this is evidence that there was no natural O-acetylation located on the non-reducing terminal hexose.

In addition to the sodium dosing experiments, other experiments were carried out to confirm the location of the acetate (Fig. 2.11). Figure 2.11a shows partial spectra of the deuteroacetylated and native material. The signals in the negative ion spectrum of the native material at m/z 953 and 911 correspond to the $[M-H]^-$ molecular ions of compositions $Hex_4HexA_1Pyr_1Ac_1$ and $Hex_4HexA_1Pyr_1$. The A-type ions in the deuteroacetyl

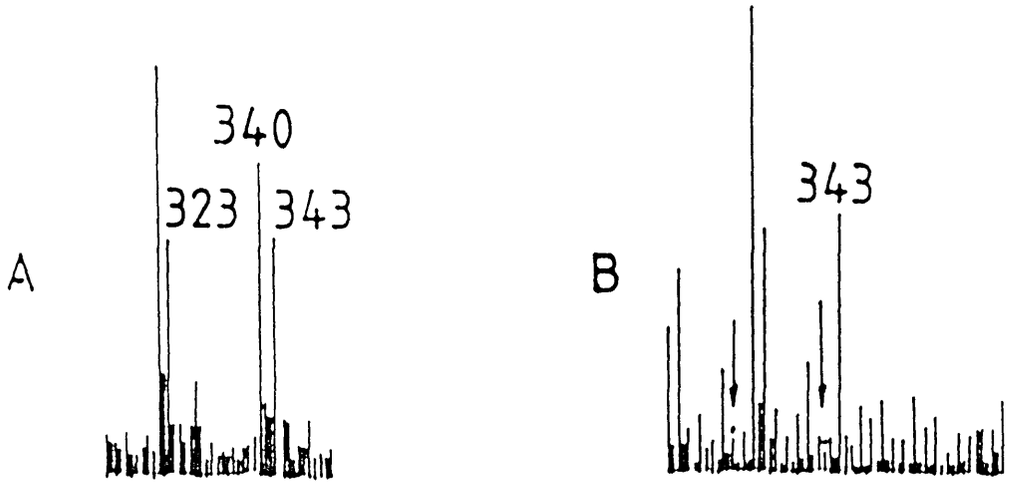



Figure 2.10. Low mass end of deuteroacetyl derivative before (A) and after (B) the addition of sodium acetate. Arrows in B indicate where the signals at m/z 323 and 340 would be.

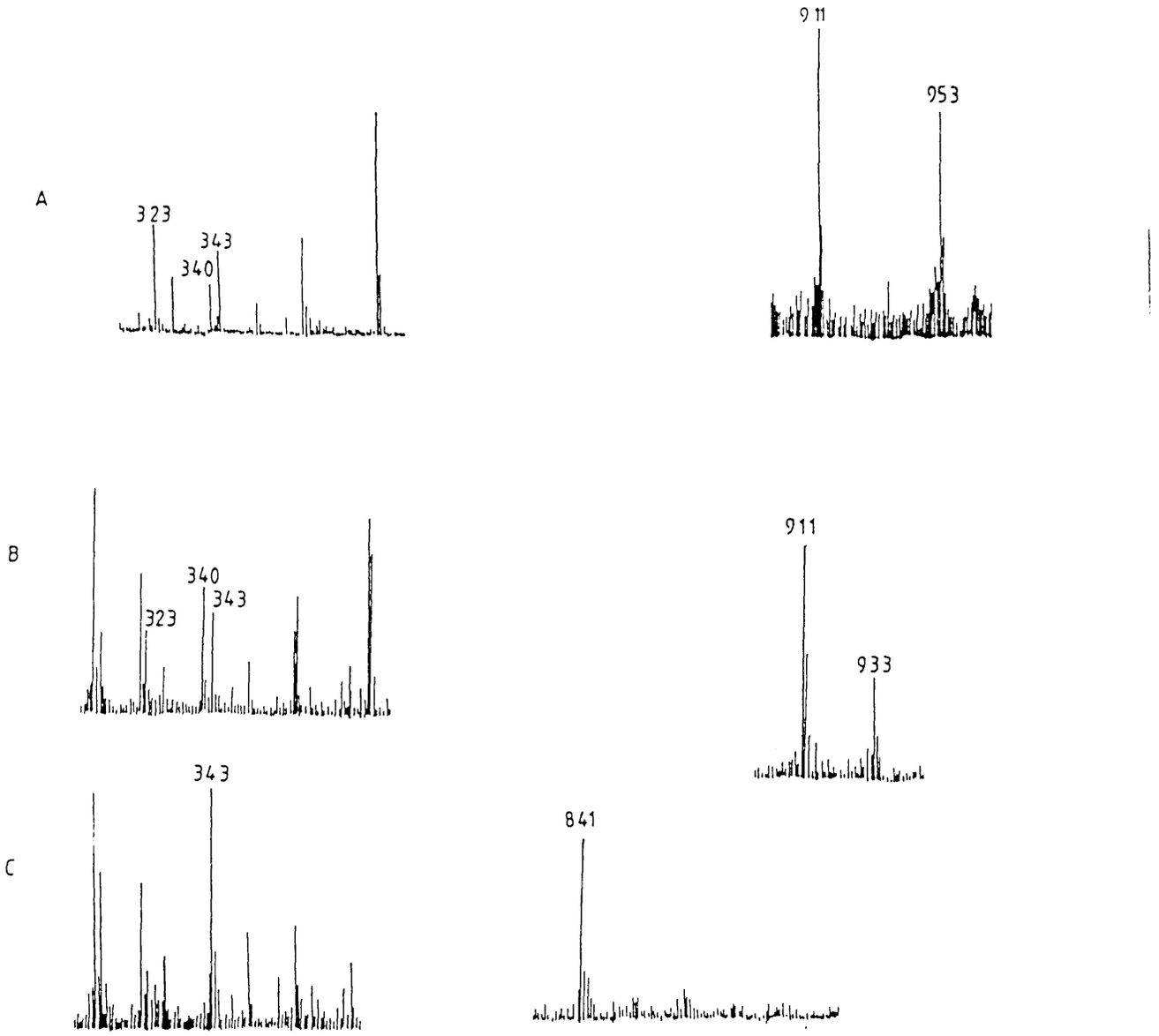



Figure 2.11. Partial positive ion FAB spectra of deuteroacetylated (A) K69 (B) de-acetylated K69 and (C) de-acetylated, de-pyruvylated K69.

**TABLE 2.5.** Summary of peaks observed in the deuterioacetyl spectrum of Klebsiella K69 repeat.

| MOLECULAR IONS | COMPOSITIONS |
|---|---|
| 1557/1560 $[M+NH_4]^+$ | $Hex_4HexA_1Pyr_1Ac_{0/1}$ |
| 1477/1480 A-type | " |
| **FRAGMENT IONS** | **COMPOSITIONS** |
| 1183 | $Hex_3HexA_1Pyr_1$ |
| 1180 | $Hex_3HexA_1Pyr_1Ac_1$ |
| 872 | $Hex_3Pyr_1$-OH (elimination of HexA) |
| 343 | $Hex_1$ |
| 340 | $Hex_1Ac_1$ or $Hex_1Pyr_1NH_3$ |
| 323 | $Hex_1Pyr_1$ |

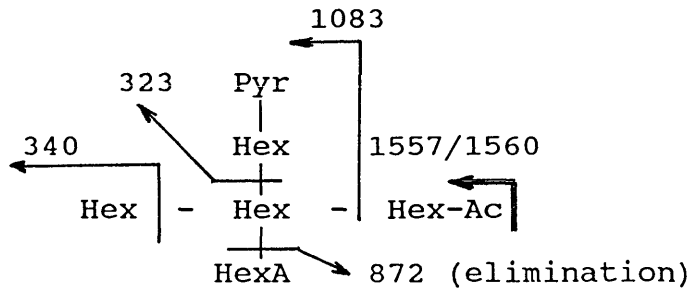
spectrum at m/z 343, 340 and 323 correspond to the compositions $Hex_1$, $Hex_1Ac_1$ or $Hex_1Pyr_1NH_3$ and $Hex_1Pyr_1$.

Figure 2.11b shows the spectrum of the de-acetylated material. The signals at m/z 933 and 911, in the negative ion spectrum of the native material, correspond to $[M+Na-H]^-$ and $[M-H]^-$ of composition $Hex_4HexA_1Pyr_1$. No signal was observed at m/z 953 for the acetylated material. The low mass A-type fragment ions in the deuteroacetyl spectrum at m/z 343, 340 and 323 correspond to the compositions $Hex_1$, $Hex_1Ac_1$ or $Hex_1Pyr_1NH_3$, and $Hex_1Pyr_1$. The signal at m/z 340 could not be due to the presence of $Hex_1Ac_1$ since there was no acetate in the sample (as evidenced by the fact that there was no signal at m/z 953 in the native spectrum). Therefore the signal at m/z 340 must be generated by $Hex_1Pyr_1NH_3$.

Figure 2.11c is of partial spectra of the negative ion native and deuteroacetyl derivative of the de-acetylated, de-pyruvylated material. The signal at m/z 841 in the spectrum of the native material corresponds to the $[M-H]^-$ molecular ion of composition $Hex_4HexA_1$. There were no signals observed at either m/z 911 or 953 ($Hex_4HexA_1Pyr_1$ and $Hex_4HexA_1Pyr_1Ac_1$). In the deuteroacetyl spectrum the only signal observed was m/z 343 of composition $Hex_1$. Both m/z 340 and 323 were absent, as expected, since neither acetate or pyruvate was present in the sample. Thus the apparent conflict in the assignment of the location of the O-acetate, is explained. As previously stated the O-acetate is located on the reducing

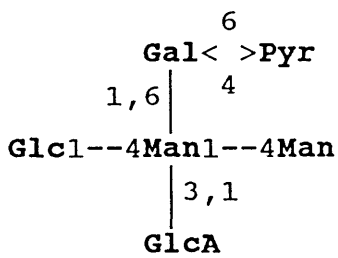
terminal hexose residue.

The mass spectrometric data described above allowed the basic structure of Klebsiella K69 repeat (P1) to be determined (III).




(III)

The data described above in conjunction with n.m.r. and methylation analysis data have resulted in the complete structure of the Klebsiella K69 capsular polysaccharide P1 repeat being determined(IV)[84].




(IV)

The n.m.r. experiments afforded results that could be interpreted to indicate that the acetate was located on every third repeat in a uniform manner. In order to confirm this speculation the P2 double repeat was analysed by FAB-MS. The molecular ion region of the negative ion spectrum obtained from the native material is reproduced in Fig 2.12. $[M-H]^-$ molecular ions are observed at m/z 1805, 1847 and 1889 of composition $Hex_8HexA_2Pyr_2$, $Hex_8HexA_2Pyr_2Ac_1$ and $Hex_8HexA_2Pyr_2Ac_2$. This spectrum

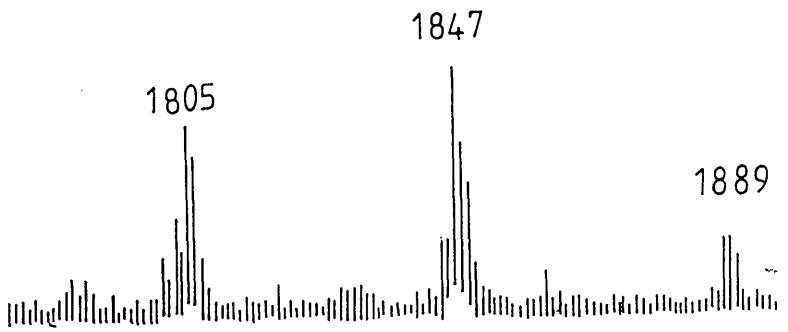



Figure 2.12. Molecular ion region of negative ion FAB spectrum of the P2 repeat from K 69.

indicates that a significant amount of the sample is monoacetylated and that some diacetylated species are present. In order to enable a quantitative assessment of the level of acetylation and to determine the residue location of such acetylation, the deuterioacetyl derivative was obtained.

The molecular ion region of the perdeuterioacetylated P2 is shown in Figure 2.13. $[M+NH_4]^+$ molecular ions are observed at m/z 2994 and 2991 consistent with the compositions $Hex_8HexA_2Pyr_2$ and $Hex_8HexA_2Pyr_2Ac_1$. The signals observed at m/z 2949 and 2946 are oxonium ions derived from the species giving rise to the signals at m/z 2994 and 2991 respectively. The relative intensity of the molecular ion signals indicates that the level of natural O-acetylation is approximately 40%, thus contradicting the suggested conclusion based on the n.m.r. data.

The perdeuterioacetylated P2 repeat gave rise to A-type ions at m/z 1777 ($Hex_5HexA_1Pyr_1$), 1774 ($Hex_5HexA_1Pyr_1Ac_1$), 1480 ($Hex_4HexA_1Pyr_1$), 1477 ($Hex_4HexA_1Pyr_1Ac_1$), 1183 ($Hex_3HexA_1Pyr_1$), 1180 ($Hex_3HexA_1Pyr_1Ac_1$), 343 ($Hex_1$), 340 ($Hex_1Ac_1$) or ($Hex_1Pyr_1NH_3$) and 323 ($Hex_1Pyr_1$).

The relative intensities of the signals were used to assess the proportion of each ionic species that contains natural O-acetylation. These data for P2 are contrasted with similar data obtained from the deuterioacetyl spectrum of K69 P1 (Fig. 2.9), in order to quantify the difference in acetylation levels and pattern within the 2 samples. The two molecular ion doublets at m/z 1557/1560 and 2991/2994 indicate that in P2 the overall level of

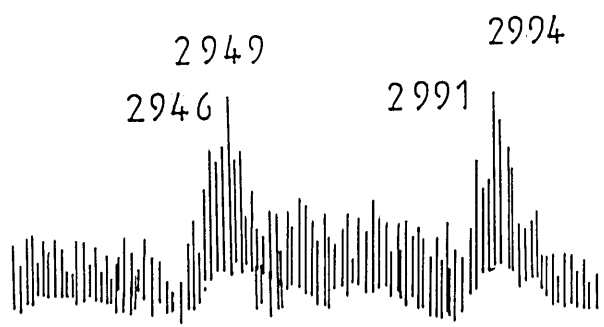



Figure 2.13. Molecular ion region of deuteroacetylated P2 repeat from K 69.

natural acetylation is higher, 40% rather than 30% in P1. It is a change in the level of acetylation, as evidenced by the ratio of signals for non and mono-acetylated species, that pinpoints sites of acetylation. In P1 the level of acetylation changes between (m/z 1180/1183 and 1477/1480) from 0% to 30% indicating that the reducing terminal residue is the only site for acetylation. In P2 the level of acetylation changes between m/z 1774/1777 and 2946/2949 from 35% to 40%, indicating that the reducing terminal hexose is not the only site for acetylation.

Sodium dosing experiments were performed, as in the analysis of P1, to determine the origin of the signal at m/z 340. The results of those experiments indicated that the signal at m/z 340 is not completely due to the $Hex_1Pyr_1NH_3$ salt. This suggested that the P2 repeat contains some acetylation on the non-reducing hexose. To confirm the validity of this conclusion the propionyl derivative was prepared and a FAB spectrum recorded. The ions observed at m/z 323, 340 and 343 in the perdeuterioacetyl derivative were seen to have shifted in mass to m/z 345, 373 and 387 respectively. Again indicating the presence of non-reducing terminal $Hex_1Ac_1$. To further confirm this observation, diazomethane esterification was carried-out on the deuterioacetylated sample. This reagent will esterify the carboxylic hydroxyls, thus preventing them from forming ammonium adducts. The ion previously observed at m/z 323 was shifted in mass to m/z 337 as expected, indicating that methyl esterification has occurred. An ion at m/z 340 was still observed indicating that the non-reducing terminal

residue is acetylated.

From these experiments it was concluded that, unlike the P1 repeat, the P2 repeat has some O-acetate located on the non-reducing terminal hexose. Since both P1 and P2 are derived from the same polysaccharide this suggests that the presence of the acetyl group affects the phage digestion.

2.5.3. Xyloglucan.

Xyloglucan is the name given to a group of polysaccharides present in the walls of higher plants. They consist of a 4-linked glucose backbone that is greatly branched, with each branch initiated by a xylose residue. The length and composition of these branches varies between species and tissues.[85] Experiments have suggested that a nonasaccharide component of the xyloglucan is involved in the control of stem elongation.[7,8] Specifically, the enhancement of pea stem growth effected by 2,4-D is inhibited by low concentrations of the nonasaccharide isolate from sycamore extracellular polysaccharide.

FAB-MS analysis of the active xyloglucan fractions showed that they contained mono and di-acetylated components. It is not clear whether the acetate(s) are required for biological activity. The purpose of the work described below was the assignment of the residue or residues that contain O-acetyl substituents.

The xyloglucan examined herein was isolated from sycamore extracellular polysaccharide by the action of a $\beta$-1,4-endoglucanase from Trichoderma viride[85] and was subjected to perdeuteroacetylation and a FAB mass spectrum recorded (Fig. 2.14). Ions were observed at m/z 2490/2493 2507/ 2510 and 2427/2430 for $[M+H]^+$, $[M+NH_4]^+$ and oxonium molecular ions respectively, of composition $DeoxyHex_1Pent_3Hex_5$ with either one or two acetates. The signals at m/z 2382/2385 were consistent with under deuteroacetylation on the component giving rise to the signals at m/z 2427/2430. The signal intensities indicate

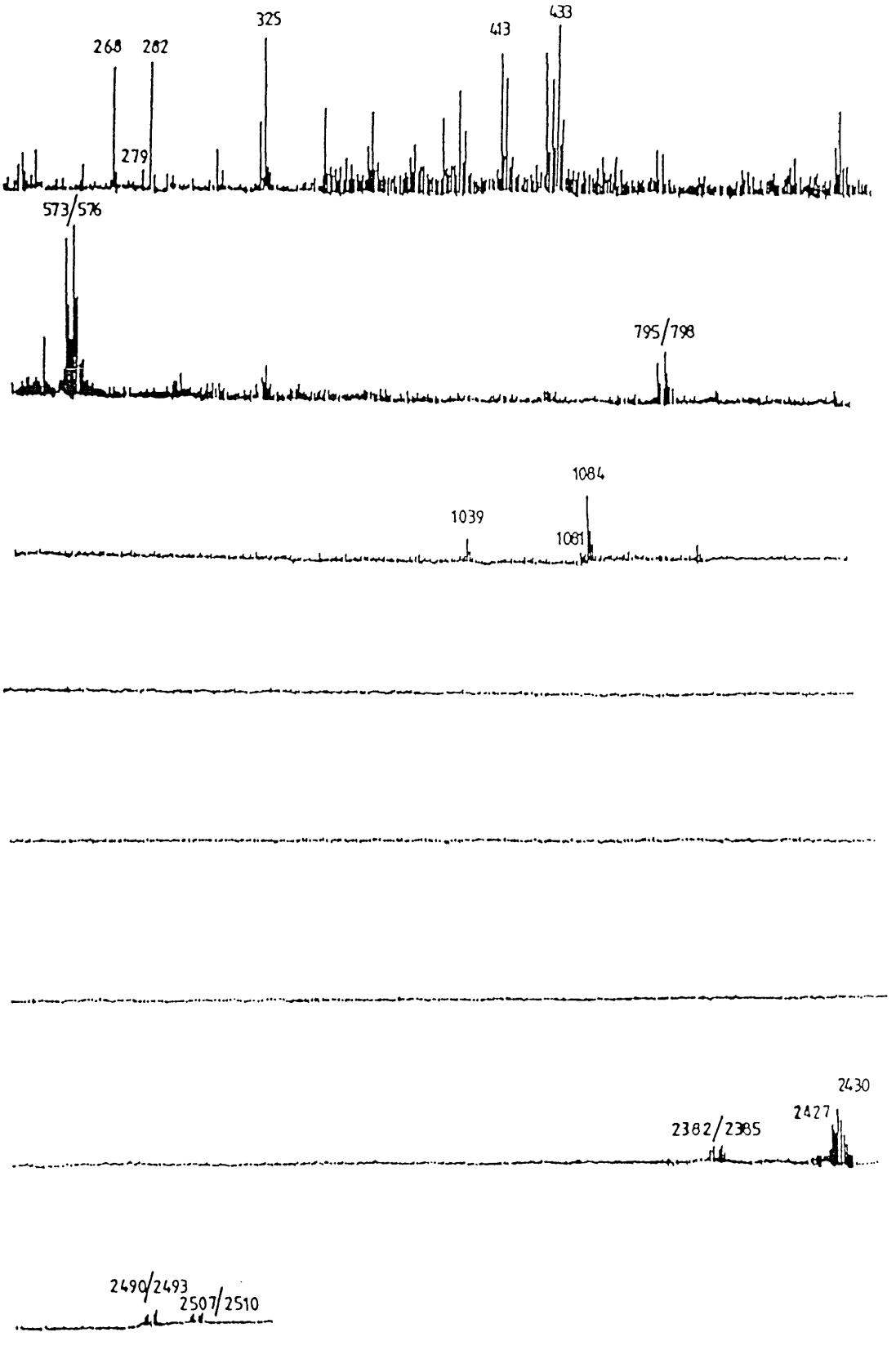
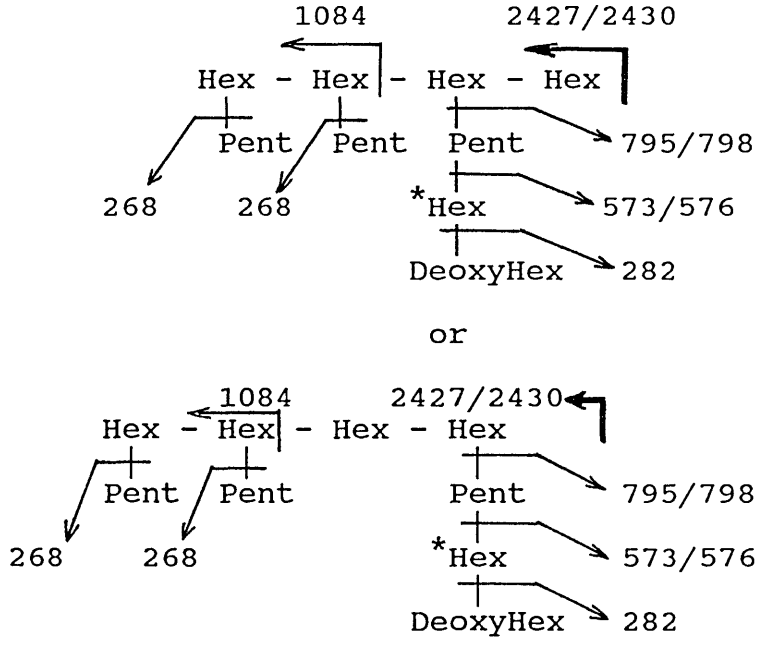



Figure 2.14. Positive ion FAB spectrum of deuteroacetylated xyloglucan.

that the ratio of mono to di-O-acetylated species is 1.3 : 1.0. Additionally A-type fragment ions were observed at m/z 268, 282, 573/576, 795/798, 1039 and 1084, consistent with the compositions Pent, DeoxyHex, $DeoxyHex_1Hex_1Ac_{1/2}$, $DeoxyHex_1Hex_1Pent_1Ac_{1/2}$, $Pent_2Hex_2$ under deuteroacetylated and $Pent_2Hex_2$. These data are listed in TABLE 2.8 and allow either of the two structures (V) to be proposed.




(V)

A signal at m/z 279 consistent with the composition $DeoxyHex_1Ac$ was also observed. Since an impurity that changes in abundance with time contributes to this signal, futher experiments were carried out to determine what level of monoacetylated deoxyhexose was present in the sample.

**TABLE 2.6.** Summary of peaks observed in the deuterioacetyl spectrum of the Xyloglucan nonasaccharide.

| MOLECULAR IONS | COMPOSITIONS |
|---|---|
| 2507/2510 $[M+NH_4]^+$ | $DeoxyHex_1Pent_3Hex_5Ac_{1/2}$ |
| 2490/2493 $[M+H]^+$ | " |
| 2427/2430 A-type | " |
| 2382/2385 A-type | " minus deuterio AcOH |
| **FRAGMENT IONS** | **COMPOSITIONS** |
| 1084 | $Pent_2Hex_2$ |
| 1039 | $Pent_2Hex_2$ minus deuterio AcOH |
| 795/798 | $DeoxyHex_1Hex_1Pent_1Ac_{1/2}$ |
| 573/576 | $DeoxyHex_1Hex_1Ac_{1/2}$ |
| 282 | $DeoxyHex_1$ |
| 268 | $Pent_1$ |

After three consecutive scans (Fig. 2.15) the signal at m/z 279, which in the first scan was 26% of the intensity of the deoxyhexose signal (m/z 282), becomes 107% of the intensity of m/z 282. Therefore the highest possible level of monoacetylated deoxyhexose present is 20% This is an overestimate as the signal is contributed to by an impurity. In figure 2.16 the change in intensity of the signal at m/z 279 with respect to the signal at m/z 282 is observed in two different matrices (glycerol/thioglycerol ; thioglycerol). The ratio of m/z 279 : 282 increases when in thioglycerol only, whereas the ratio of di to mono-acetylation as evidenced by m/z 573 : 576 stays constant. From this it can be deduced that less than 1/5 of the deoxyhexose is naturally monoacetylated and may, indeed, be totally free of acetyl. The ratio of mono to di-acetylation in the deuteroacetyl derivative was examined using the signals at m/z 573/576 (1.25 : 1) and m/z 795/798 (1.2 : 1) to determine whether the pentosyl residue in the branch was acetylated. The ratios were very similar indicating no change in the level of acetylation further up the branch. From this it was concluded that in more than 80% of the sample, if not all, both sites of acetylation are located on the hexose residue within the branch labelled with * in structure (V). Structure (VI) was defined as a result of further analysis (Chapter 3.3.)

The minor signal observed at m/z 1081 of composition $Pent_2Hex_2Ac_1$ indicates that a minor amount of acetyl is present on the $Pent_2Hex_2$ moiety. Since no signals were observed at m/z 265 ($Pent_1Ac$) this minor acetylation must be located on one of the two "backbone" hexosyl residues.

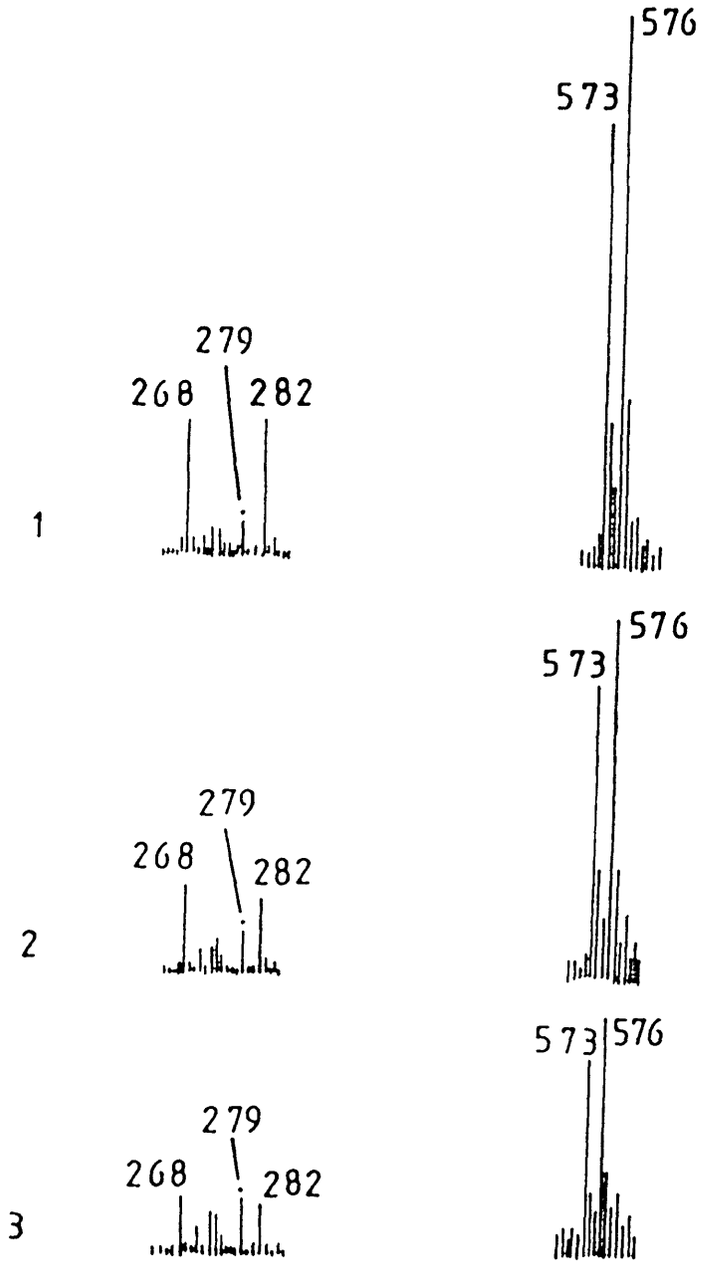



Figure 2.15. Partial positive ion FAB spectra of the Xyloglucan after deuteroacetylation. The three partial spectra were recorded consecutively from the same sample.

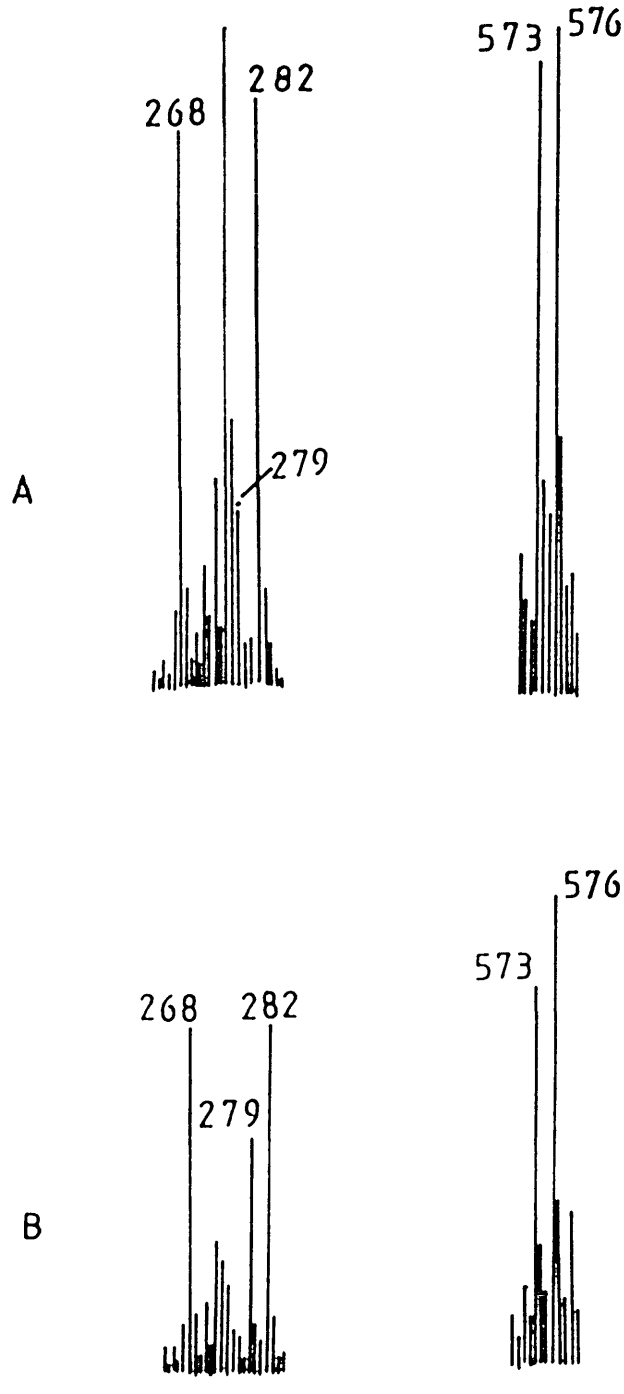
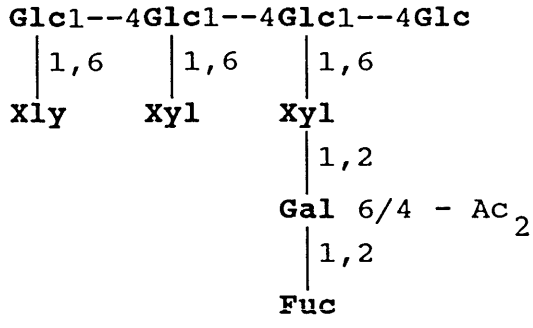



Figure 2.16. Partial positive ion FAB spectra of the xyloglucan after deuteroacetylation, run in A glycerol/thioglycerol and B thioglycerol.




(VI)

Because of the similarities in the chemical shifts of protons on the fucosyl and galactosyl residues, n.m.r. data obtained by Professor Albershiem, was unable to determine the location of the O-acetates. Using the FAB-MS data to guide interpretation it was possible to conclude that :-

1) the O-acetates are linked at positions 6 and 4 of the galactosyl residue
2) the relative abundance of mono and di-o-acetylated species are as indicated by the FAB-MS data
3) the 6 and 4 positions of the galactosyl residue are O-acetylated in 55-60% and 20-25% of molecules respectively

Further FAB-MS analysis of this sample was carried-out to determine which of the two possible structures in (V) is correct and in conjunction with the n.m.r. data a complete structural assignment was made (see Chapter 3 section 3.2).

## 2:6. Conclusion.

The facility with which the deuterioacetyl protocol affords structural data has been described above. This methodology provides composition and sequence data and enables the residue location of O-acyl moieties within the sequence of an oligosaccharide to be determined. It is possible to establish the level of O-acylation on each residue, allowing an assessment of the variation in acylation patterns throughout a molecule. The data obtained can provide guidance for subsequent n.m.r. experiments and in conjunction with n.m.r. and classical carbohydrate techniques enables a complete structural analysis to be performed.

## Chapter 3 : Methanolysis/FAB-MS.

### 3:1. Introduction.

FAB-MS has been used to sequence derivatised carbohydrates with great success, since the use of derivatives have solved the problems of ambiguity associated with native samples. Derivatives have afforded simplified spectra by directing fragmentation in a well defined and reproducible manner (see chapter 1). The selective fragmentation that is observed in spectra of aminosugars can present difficulties. In aminosugar containing oligosaccharides the fragmentation can almost exlusively occur at the aminosugar glycosidic bond, resulting in incomplete sequence information.

This chapter addresses the problem of full sequence assignment and the location of branch positions within oligosaccharides.

## 3:2. Development of Methanolysis/FAB-MS.

### 3:2.1. The First Use of Methanolysis/FAB-MS.

In a study of the glycolipids from human embryonal carcinoma cell line PA1 a novel glycolipid was isolated[86]. The spectrum of the permethylated product (Fig. 3.1) afforded molecular ions at m/z 2159 and 2187 corresponding to $NeuAc_2HexNAcHex_3Cer_{16:0}$ and $NeuAc_2HexNAcHex_3Cer_{18:0}$ respectively. The ion observed at m/z 2145 is the ion corresponding to m/z 2159 which contains one degree of under methylation. Additionally a minor monosialylated component afforded a molecular ion at m/z 1798 consistent with the composition $NeuAc_1Hex_3HexNAc_1Cer_{16:0}$.

Fragment ions were observed at m/z 1921, 1562, 1390, 1186, 1029, 825, 811, 793, 548, 376 and 344 consistent with the compositions M-acyl (2159-238 and 2187-266), $NeuAc_2Hex_3HexNAc$-MeOH, $NeuA_2HexNAc_1Hex_2$, $NeuAc_2Hex_1HexNAc_1$ $NeuAc_1Hex_2HexNAc_1$, $NeuAc_1Hex_1HexNAc_1$, $NeuAc_1Hex_1HexNAc_1$-OH, $NeuAc_1Hex_1HexNAc_1$-MeOH, $NeuAc_1Hex_1$-MeOH, $NeuAc_1$ and NeuAc-MeOH respectively. The signal at m/z 811 is rationalised as a $\beta$-cleavage product of $NeuAc_2Hex_1HexNAc_1$ (1186) giving rise to monohydroxylated $NeuAc_1Hex_1HexNAc_1$. The signals at m/z 1562, 793, 548 and 344 are consistent with the loss of methanol from NeuAc, a phenomenon that has been observed in the past to be associated with sialic acid residues. These data are summarised in TABLE 3.1. Because the fragmentation was strongly directed to the HexNAc residue it was not possible to determine the full sequence of this glycolipid. The data this spectrum

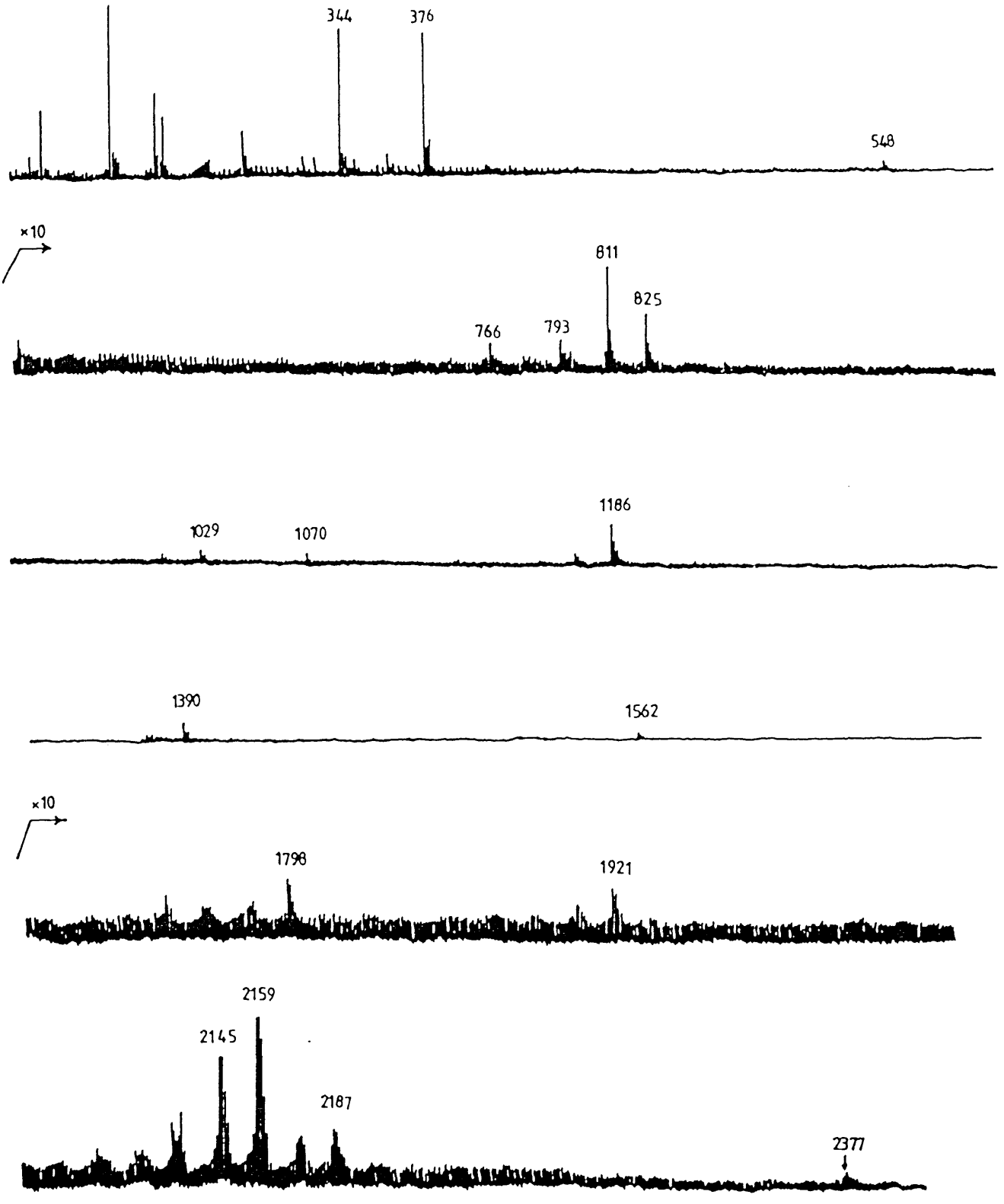
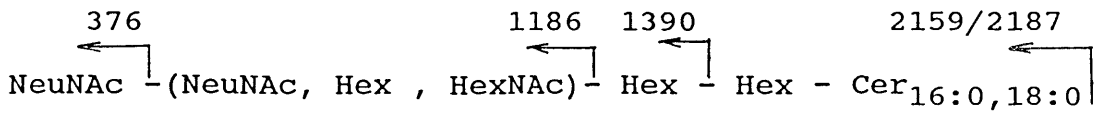



Figure 3.1. Positive ion FAB spectrum of permethylated PA1 glycolipid.

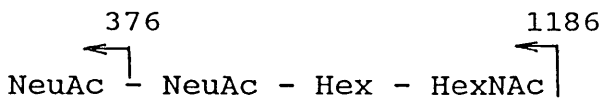
afforded allowed the partial sequence (VI) to be rationalised.



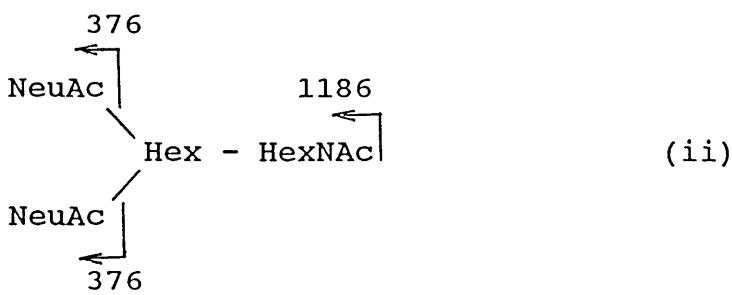

(VI)

The data obtained are consistent with the two sialic acid residues being either linked at different sites or present as NeuAc -> NeuAc -> as previously observed in related glycoproteins from the same cell line[86].

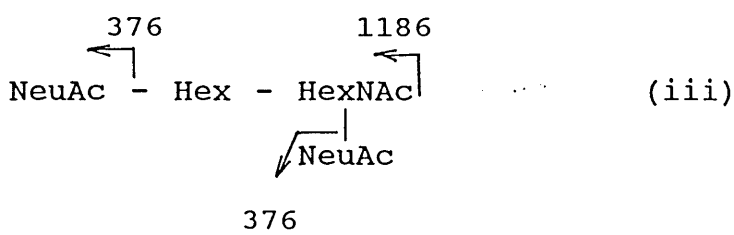
The data obtained thus far, is consistent with three possible structures (i),(ii) and (iii) based on the signals at m/z 376 (NeNAc) and 1186 ($NeuAc_2Hex_1HExNAc_1$).




(i)




(ii)




(iii)

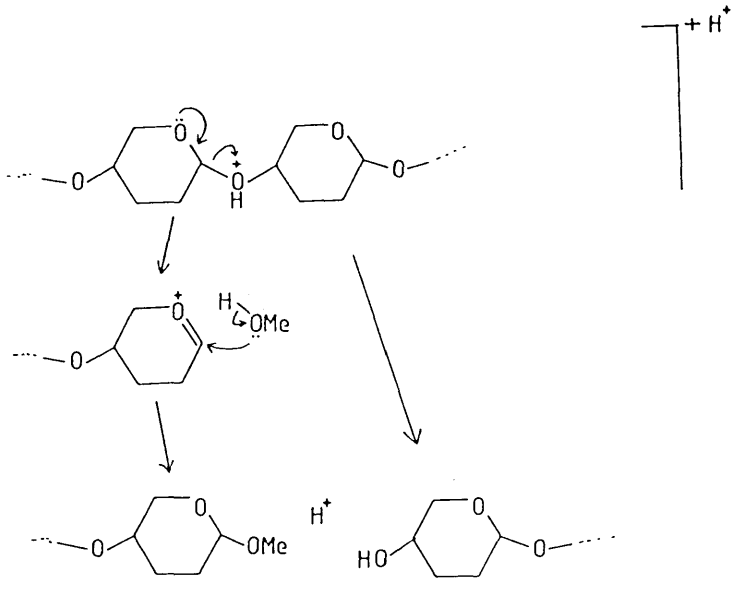
Because of the presence of the minor component at m/z 1798 methylation analysis would have afforded ambiguous data. Therefore to exploit the mixture analysis

**TABLE 3.1.** Summary of peaks observed in the spectrum of PA1 glycolipid. (see Fig. 3.1).

| MOLECULAR IONS | | COMPOSITION |
|---|---|---|
| 2187 | $[M+H]^+$ | $NeuNAc_2Hex_3HexNAc_1Cer_{18:0}$ |
| 2159 | " | $NeuNAc_2Hex_3HexNAc_1Cer_{16:0}$ |
| 2145 | " | $NeuNAc_2Hex_3HexNAc_1Cer_{16:0}$ minus $d_3Me$ |
| 1798 | " | $NeuNAc_1Hex_3HexNAc_1Cer_{16:0}$ |
| FRAGMENT IONS | | COMPOSITION |
| 1921 | | M-acyl (2159-238 and 2187-266) |
| 1562 | | $NeuNAc_2Hex_3HexNAc_1$ - MeOH |
| 1390 | | $NeuNAc_2Hex_2HexNAc_1$ |
| 1186 | | $NeuNAc_2Hex_1HexNAc_1$ |
| 1029 | | $NeuNAc_1Hex_2HexNAc_1$ |
| 825 | | $NeuNAc_1Hex_1HexNAc_1$ |
| 811 | | HO-$NeuNAc_1Hex_1HexNAc_1$ |
| 793 | | $NeuNAc_1Hex_1HexNAc_1$ - MeOH |
| 548 | | $NeuNAc_1Hex_1$ - MeOH |
| 376 | | $NeuNAc_1$ |
| 344 | | $NeuNAc_1$ - MeOH |

properties[59] of FAB-MS, hydrolytic experiments were carried-out on the permethylated glycolipid, to determine the linkage site of the two sialic acid residues.

An acid catalysed methanolysis time course, monitored by FAB-MS, was carried-out in which molecular ions formed by the cleavage of the molecule would be observed. Hydrolysis of the permethylated material would thus give rise to cleavage products with free hydroxyl groups present on the non-reducing end of a residue, where a glycosidic bond had been hydrolysed, but with a methyl glycoside on the reducing end residue (see Scheme 3.1).




Scheme 3.1

Methanolic-HCl[87] was used in these experiments because

a) The reagent itself is compatible with the permethylated sample.

b) The reagent is compatible with the matrix used in FAB experiments (permethylated samples are dissolved in methanol normally). Therefore no sample work-up would be

required.

c) The reagent provides protons which will enhance the formation of molecular ions, thus increasing the sensitivity of the technique.

The permethylated glycolipid was dissolved in methanolic HCl and heated at 40°C. After 15 min. an aliquot was taken and loaded into the FAB matrix, and a spectrum obtained (Fig. 3.2). Another aliquot was taken after heating at 40° C for a further 15 min. and loaded into the FAB matrix and a spectrum obtained (Fig. 3.3). The data from these two spectra are summarised in TABLE 3.2. These spectra contain several signals, not previously observed in figure 3.1, that confirm the assignments made above and allow the determination of the linkage site of the two sialic acid residues. There were molecular ion signals at m/z 2127 $NeuNAc_2Hex_3HexNAc_1Cer_{16:0}$, 1784 $HO\text{-}NeuNAc_1Hex_3HexNAc_1Cer_{16:0}$, 1752 (1784-methanol), 1576 $HO\text{-}NeuNAc_1Hex_2HexNAc_1Cer_{18:0}$ - methanol, 1548 $HO\text{-}NeuNAc_1Hex_2HexNAc_1Cer_{16:0}$ - methanol, 1422 $NeuNAc_2Hex_2HexNAc_1$, 1377 $HO_2\text{-}Hex_3HexNAc_1Cer_{16:0}$ - methanol, 1173 $Ho_2\text{-}Hex_2HexNAc_1Cer_{16:0}$ - methanol, 1047 $HO\text{-}NeuNAc_1Hex_2HexNAc_1$, 1015 $HO\text{-}NeuNAc_1Hex_2HexNAc_1$ - methanol, 942 $HO\text{-}Hex_2Cer_{16:0}$ - methanol, 766 $HO\text{-}Hex_1Cer_{18:0}$ - methanol, 738 $HO\text{-}Hex_1Cer_{16:0}$ - methanol and 408 NeuNAc. Fragment ions were observed at m/z 450 and 436 consistent with $HO\text{-}(Hex_1HexNAc_1)$ and $HO_2\text{-}(Hex_1HexNAc_1)$ respectively. The signal at m/z 450 $HO\text{-}Hex_1HexNAc_1$ is consistent with being a cleavage product from the monosialylated

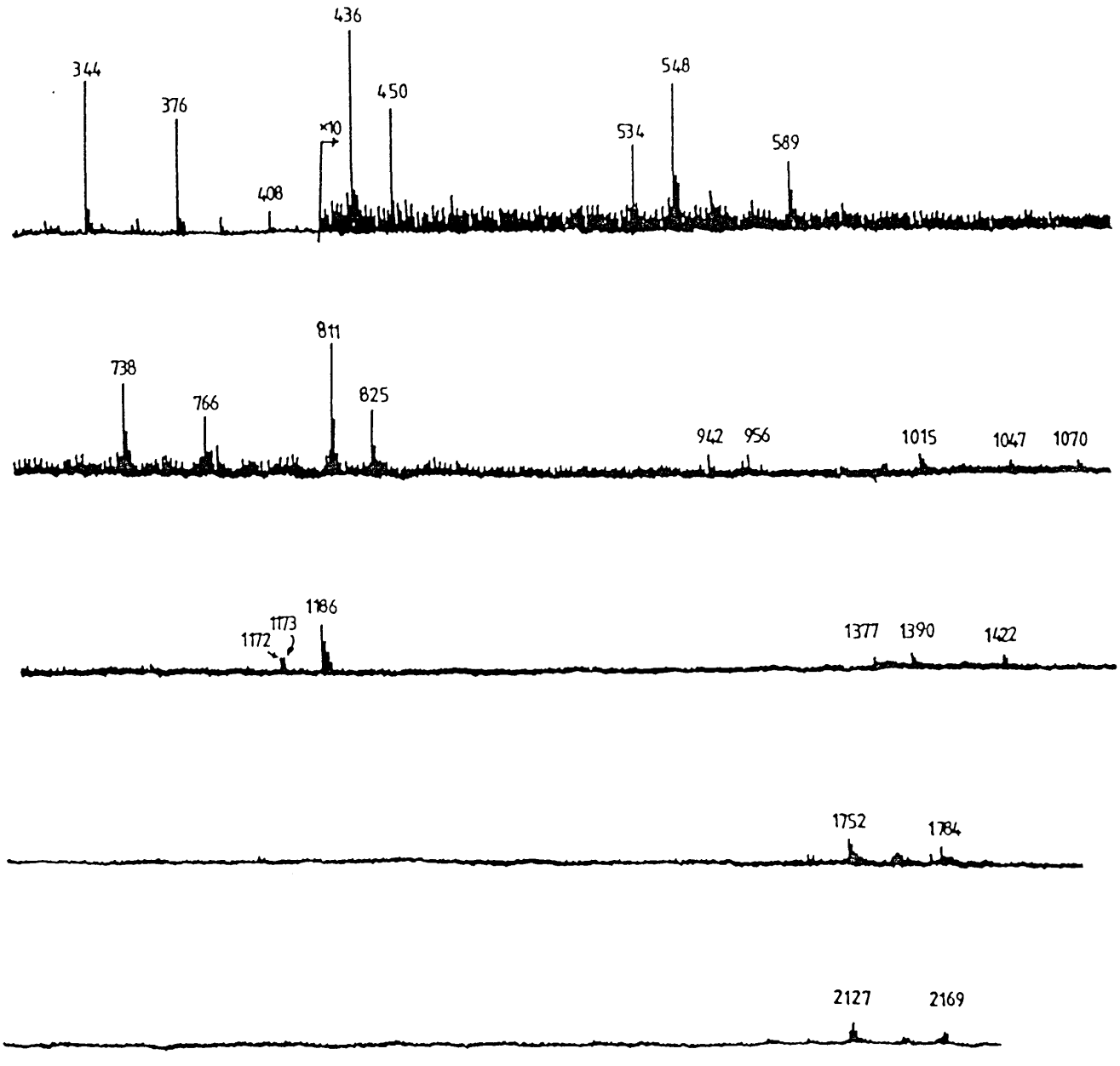



Figure 3.2. Positive ion FAB spectrum of permethylated PA1 glycolipid after 15 mins. methanolysis at 40° C.

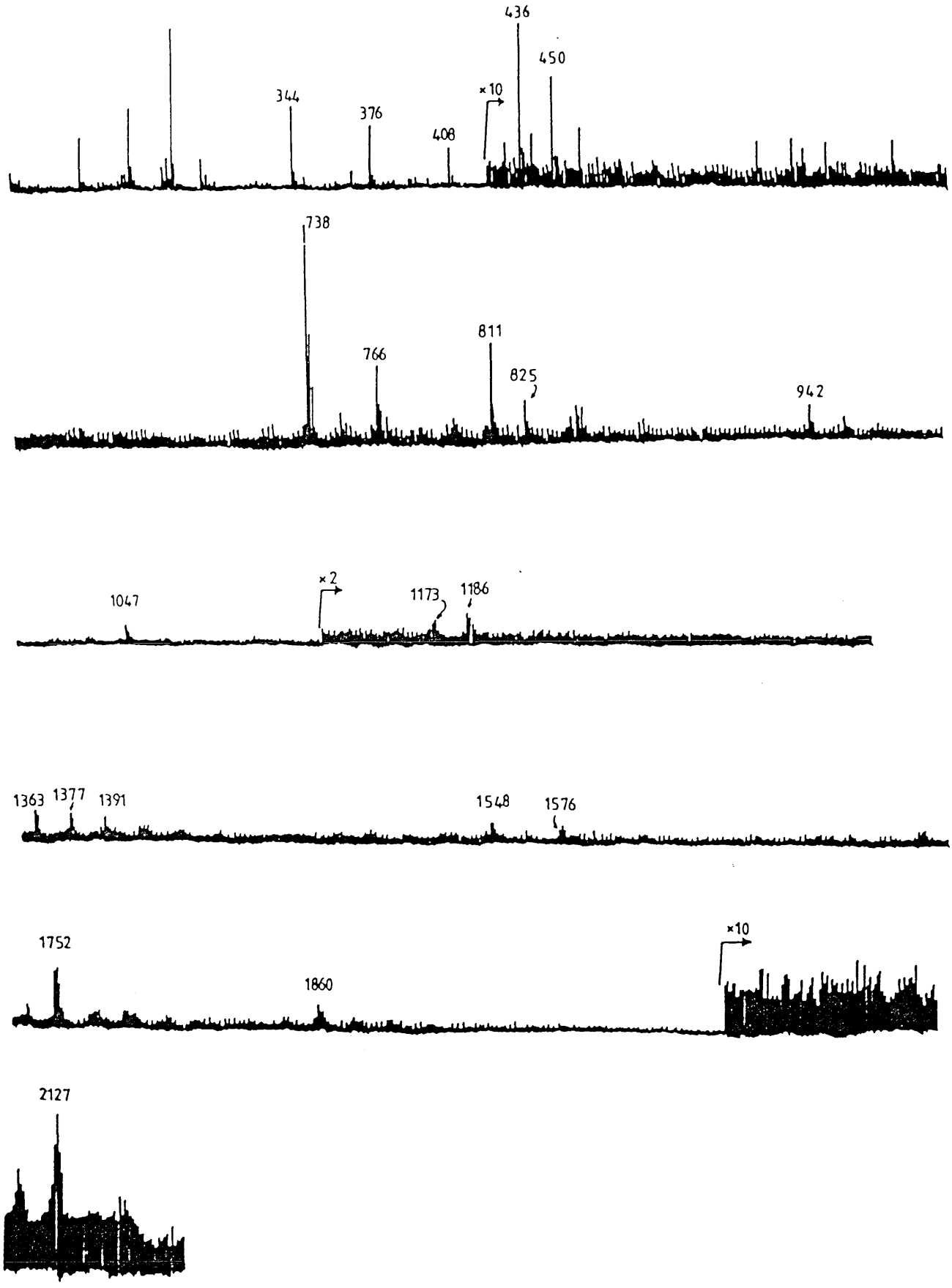
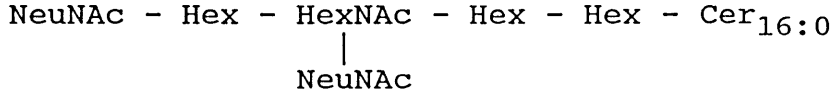



Figure 3.3. Positive ion FAB spectrum of permethylated PA1 glycolipid after 30 mins. methanolysis at 40° C.

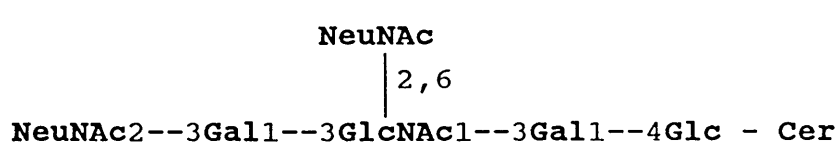
contaminant. The signal at m/z 436 $HO_2$-$Hex_1HexNAc_1$ can be rationalised as being derived from the disialylosyl component.

Many of the observed ions are compatible with one or more of the three proposed structures (see (i), (ii) and (iii) above). But those signals observed at m/z 1173, $Ho_2$-$Hex_2HexNAc_1Cer_{16:0}$ -methanol and 1377 $HO_2$-$Hex_3HexNAc_1Cer_{16:0}$ - methanol are only compatible with structure (iii). The data above are fully consistent with the major component being that in structure (VII).




(VII)

With the sequence and branch information thus defined, the methylation analysis data of the mixture could be used to assign the complete structure of the glycolipid in human embryonal carcinoma cell line PA1 as (VIII).




(VIII)

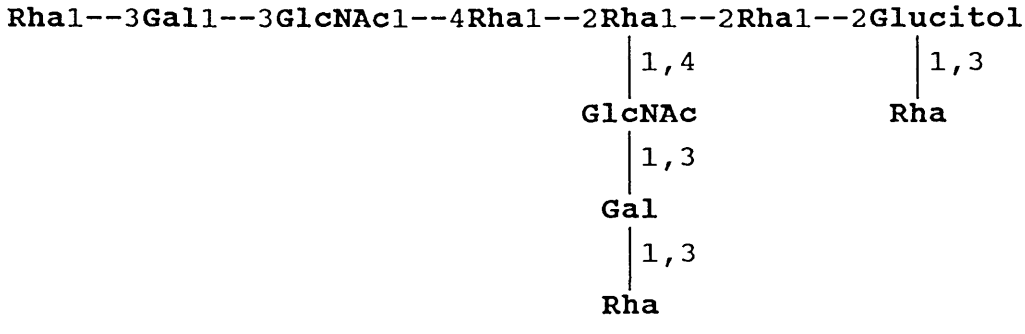
The general applicability and potential sensitivity of the methanolysis/FAB-MS protocol was rigorously assessed using oligosaccharides of bacterial and plant origin. These experiments are described below.

**TABLE 3.2.** Summary of new peaks observed in the spectra of Permethylated PA1 glycolipid, obtained after heating at 40° C for 15 and 30 min. (see figs 3.2 and 3.3).

| MOLECULAR IONS | COMPOSITION |
|---|---|
| 2127 | $NeuNAc_2Hex_3HexNAc_1Cer_{16:0}$ - MeOH |
| 1784 | HO-$NeuNAc_1Hex_3HexNAc_1Cer_{16:0}$ |
| 1752 | HO-$NeuNAc_1Hex_3HexNAc_1Cer_{16:0}$ - MeOH |
| 1576 | HO-$NeuNAc_1Hex_2HexNAc_1Cer_{18:0}$ - MeOH |
| 1548 | HO-$NeuNAc_1Hex_2HexNAc_1Cer_{16:0}$ - MeOH |
| 1422 | $NeuNAc_2Hex_2HexNAc_1$ |
| 1377 | $HO_2$-$Hex_3HexNAc_1Cer_{16:0}$ - MeOH |
| 1173 | $HO_2$-$Hex_2HexNAc_1Cer_{16:0}$ - MeOH |
| 1047 | HO-$NeuNAc_1Hex_2HexNAc_1$ |
| 1015 | HO-$NeuNAc_1Hex_2HexNAc_1$ - MeOH |
| 942 | HO-$Hex_2Cer_{16:0}$ - MeOH |
| 766 | HO-$Hex_1Cer_{18:0}$ - MeOH |
| 738 | HO-$Hex_1Cer_{16:0}$ - MeOH |
| 408 | $NeuNAc_1$ |
| FRAGMENT IONS | COMPOSITIONS |
| 450 | HO-$Hex_1HexNAc_1$ |
| 436 | $HO_2$-$Hex_1HexNAc_1$ |

3:2.2. Optimisation of the experimental conditions for Methanolysis/FAB-MS.

Detailed experiments were carried-out on an oligosaccharide derived from the group-specific antigen of a group B Streptoccocci. This molecule had been previously examined and the structure determined[88] (structure IX).



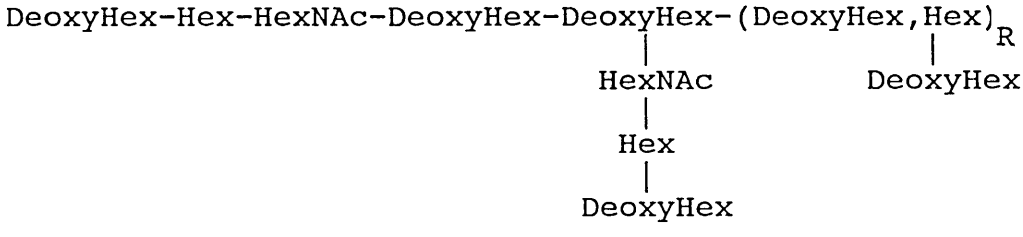

(IX)

A time course methanolysis was carried-out with aliquots taken after 2, 5, 10, 15, 20, 30, 40 and 60 minutes heating at 40° C. It was observed that spectra of several of the aliquots taken, exhibited little change from those previously obtained.

In the next series of experiments the approach taken was to increment the interval between aliquots by the time elapsed since the start of the experiment. Thus aliquots were taken after 2, 5, 10, 20, 40 and 80 minutes had elapsed. It was observed that less duplication of data ensued as a result, though the 2, 5 and 10 minute aliquots were essentially identical.

To determine whether further degradation of the molecule would occur the sample that had been previously heated at 40° C for 80 minutes was heated at 60° C and

aliquots taken after 5, 10 ,20 and 40 minutes. The signals observed in the spectra obtained throughout the course of these experiments are listed in TABLE 3.3. with their compositions. In TABLE 3.4 the possible structures giving rise to each signal observed in the spectra are summarised. All ions assigned have either one or more possible structures that are compatible with the molecule used for these model studies. From the methanolysis-FAB data described above it is possible to determine the structure of this sample to be (X).




(X)

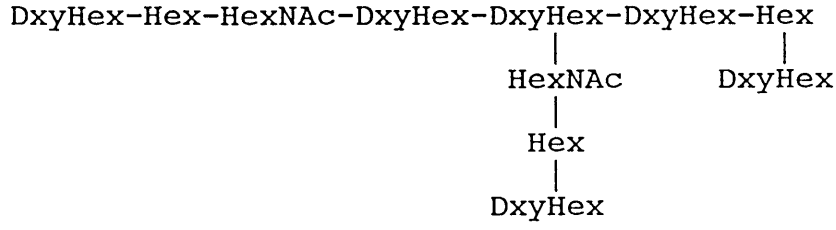
It has beenpossible to determine the branch position as well as the sequence, apart from the order of the two reducing terminal residues in brackets. TABLE 3.5 lists the signals observed according to time course aliquots in which they are present. From TABLE 3.5 it is possible to see a trend in which, as the time course progressed, the mass of the highest mass signal present in the spectrum of an aliquot decreases. TABLE 3.6 is a list of the highest mass ion present in each aliquot. This trend seems to indicate that, as was hoped, the molecule is being steadily degraded throughout the course of the experiment. It is also apparent from TABLE 3.5 that several species

**TABLE 3.3.** Summary of signals observed in the spectra of ermethylated Streptoccoccus group B antigen from aliquots taken after 2, 5, 10, 20, 40 and 80 minutes heating at 40°C and a further 5, 10, 20 and 40 minutes at 60°C in methanolic HCl.

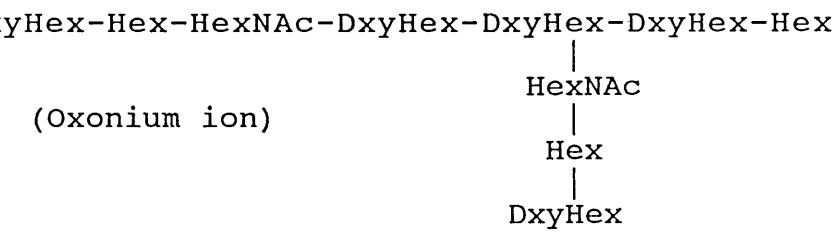
| MOLECULAR IONS | COMPOSITION |
|---|---|
| 2209 | $DeoxyHex_6Hex_3HexNac_{2R}$ |
| 2021 | $HO\text{-}DeoxyHex_5Hex_3HexNAc_{2R}$ |
| 1817 | $HO\text{-}DeoxyHex_5Hex_2HexNAc_{2R}$ |
| 1572 | $HO\text{-}DeoxyHex_5Hex_2HexNAc_{1R}$ |
| 1425 | $HO_2\text{-}DeoxyHex_4Hex_1HexNAc_{2R}$ |
| 1398 | $HO\text{-}DeoxyHex_4Hex_2HexNAc_{1R}$ |
| 1384 | $HO_2\text{-}DeoxyHex_4Hex_2HexNAc_{1R}$ |
| 1237 | $HO_3\text{-}DeoxyHex_3Hex_1HexNAc_{2R}$ |
| 1210 | $HO_2\text{-}DeoxyHex_3Hex_2HexNAc_{1R}$ |
| 1194 | $HO\text{-}DeoxyHex_4Hex_1HexNAc_{1R}$ |
| 1180 | $HO_2\text{-}DeoxyHex_4Hex_1HexNAc_{1R}$ |
| 1006 | $HO_2\text{-}DeoxyHex_3Hex_1HexNAc_{1R}$ |
| 992 | $HO_3\text{-}DeoxyHex_3Hex_1HexNAc_{1R}$ |
| 818 | $HO_3\text{-}DeoxyHex_2Hex_1HexNAc_{1R}$ |
| 747 | $HO_3\text{-}DeoxyHex_3Hex_{1R}$ |
| 670 | $DeoxyHex_1Hex_1HexNAc_1$ |
| **FRAGMENT IONS** | **COMPOSITIONS** |
| 2035 | $DeoxyHex_5Hex_3HexNAc_{2R}$ |
| 1162 | $HO\text{-}DeoxyHex_4Hex_1HexNAc_{1R}$ |
| 638 | $DeoxyHex_1Hex_1HexNAc_1$ |

**TABLE 3.4** Summary of the possible structures each of the signals, observed in the spectra obtained throughout the course of the time course methanolysis, represent.

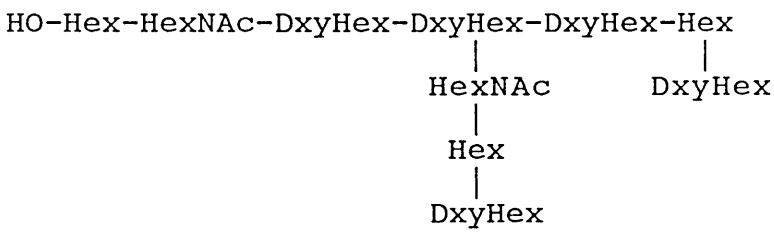
2209

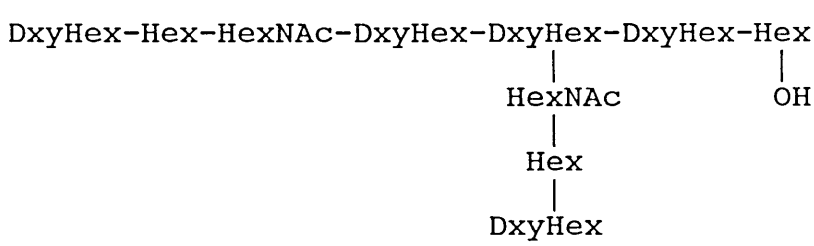


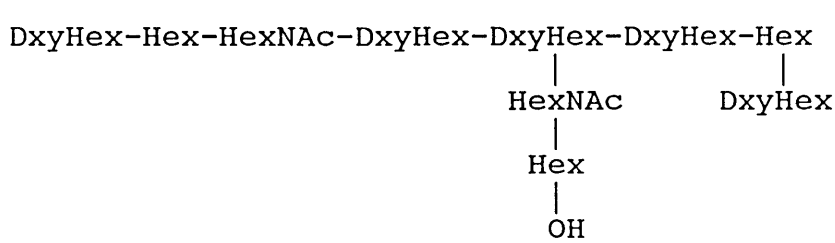

2035



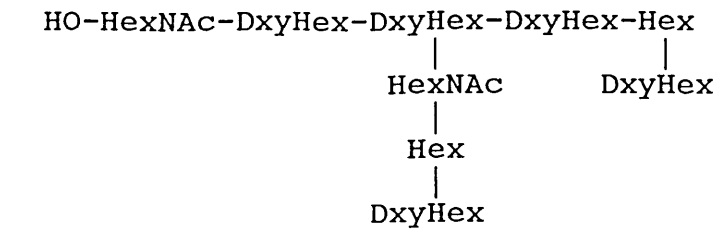

2021

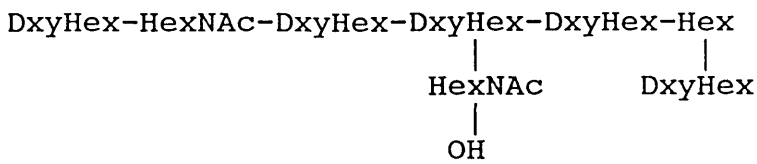


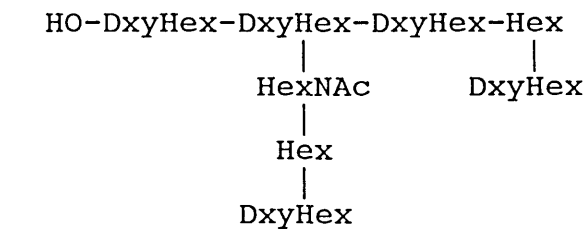



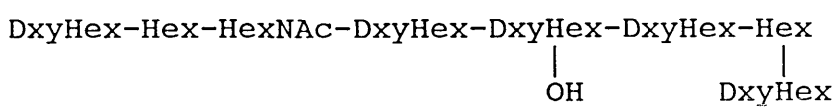
1817



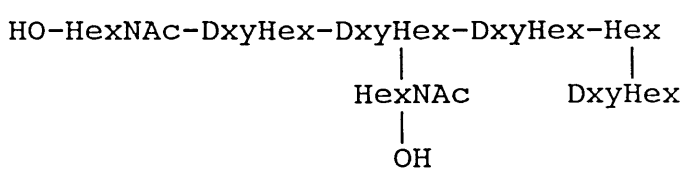




1572

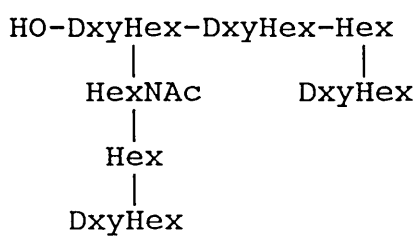


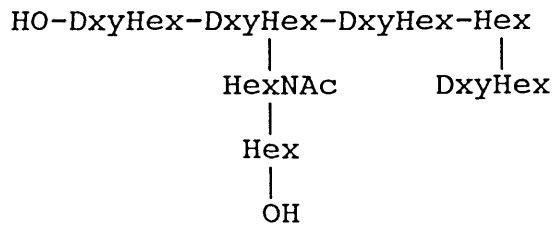

1425

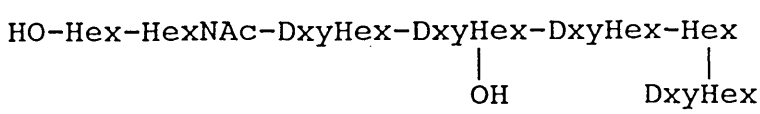


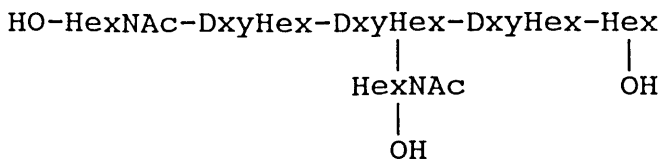

1398

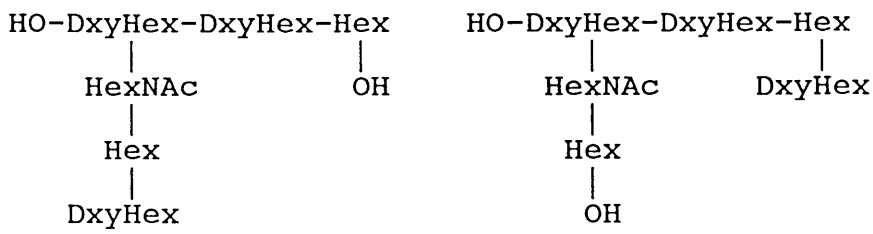


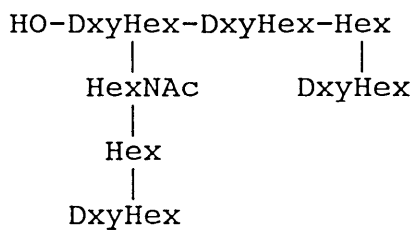

1384

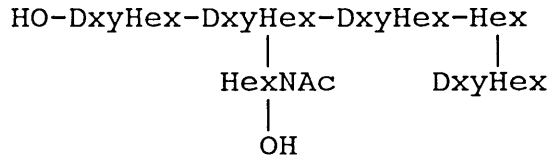


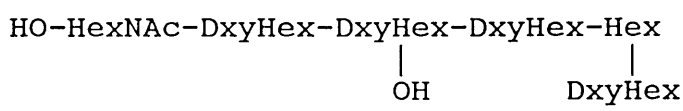



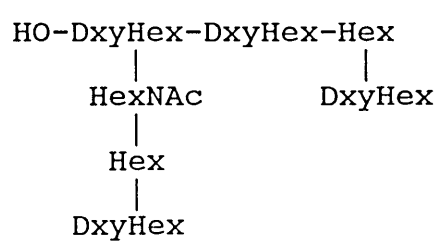
1237 


1210 

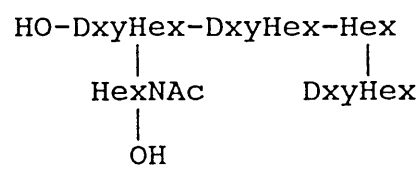

1194 

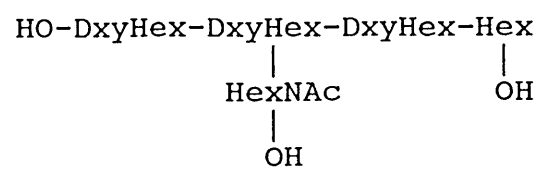

1180 

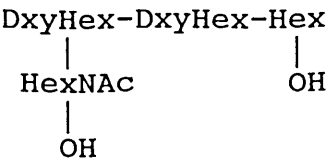



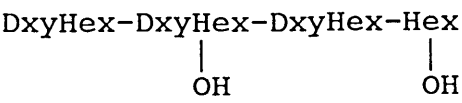

1162 

(Oxonium ion of 1194)

1006 


992 

818 


747 


670 DxyHex-Hex-HexNAc

638 DxyHex-Hex-HexNAc (Oxonium ion of 670)

**TABLE 3.5** Summary of aliquots in which signals were observed.

| | ALIQUOT | | | | | |
|---|---|---|---|---|---|---|
| | 40° C | | | 60° C | | |
| ION | 10 | 20 | 40 | 5 | 10 | 20 |
| 2209 | + | - | - | - | - | - |
| 2035 | + | - | - | - | - | - |
| 2021 | + | - | - | - | - | - |
| 1817 | + | - | - | - | - | - |
| 1572 | + | + | - | - | - | - |
| 1425 | - | - | + | - | - | - |
| 1398 | + | + | - | - | - | - |
| 1384 | + | + | + | - | - | - |
| 1237 | - | - | + | + | + | - |
| 1210 | + | + | - | - | - | - |
| 1194 | + | + | - | - | - | - |
| 1180 | + | + | + | + | - | - |
| 1162 | + | + | - | - | - | - |
| 1134 | - | - | + | + | + | - |
| 1006 | - | - | + | - | - | - |
| 992 | - | - | + | + | + | + |
| 829 | - | - | - | - | + | - |
| 818 | - | - | - | - | + | - |
| 747 | - | - | + | + | + | + |
| 670 | + | + | + | + | + | - |
| 638 | + | + | + | + | + | - |

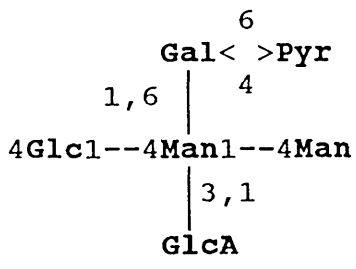
**TABLE 3.6** Summary of the highest mass ion present in each of the methanolysis time course aliuots.

| ALIQUOT | | HIGHEST MASS SIGNAL |
|---|---|---|
| 40° C | 10 | 2209 |
| | 20 | 1572 |
| | 40 | 1425 |
| 60°C | 5 | 1237 |
| | 10 | 1237 |
| | 20 | 992 |

are present in only 1 of the aliquots, namely the signals at m/z 1425, 1006  829 and 818. (The high mass signals at m/z 2209, 2035, 2021 and 1817 were observed in the spectra of the aliquots taken after heating at 40° C for 2, 5 and 10 minutes). The fact that some species are present in only 1 time course aliquot indicated that the interval between each aliquot should not be increased any further. Decreasing the interval between aliquots was discounted since this protocol was being developed to enable analysis of samples where the amount of material available may be limited.

3:2.3. Further Assessment of Methanolysis/FAB-MS.

To further assess the application of this new protocol experiments were carried-out on the Klebsiella K69 capsular polyssacharide P1 repeat, which had been previously examined utilising the deuterioacetylation methodology (Chapter 2, section 2:5.2.). The structure of this molecule is given below.(XI)




(XI)

The methanolysis/FAB-MS strategy was applied to the K69 P1 repeat, heating at 40° C and spectra were obtained of aliquots taken after 2, 5, 10, 20 and 40 minutes. None

of these spectra evidinced methanolysis derived signals. Therefore the second stage of the protocol was carried-out and the sample was heated at 60°C, taking aliquots after 5, 10 and 20 minutes. The aliquot taken after 5 minutes heating at 60 C afforded the spectrum shown in figure 3.4. The ions observed at m/z 1154 and 1122 are the $[M+NH_4]^+$ and oxonium molecular ions for the intact permethylated material, of composition $Hex_4HexA_1Pyr_1$. The remaining signals in the spectrum are $[M+NH_4]^+$ and $[M+H]^+$ molecular ions for methanolysis cleavage products. The pairs of signals at m/z 950/933, 936/919, 922/905, 732/715 and 718/701 correspond to the compositions $Hex_3HexA_1Pyr_1$, HO-$Hex_3HexA_1Pyr_1$, HO-$Hex_4Pyr_1$, HO-$Hex_2HexA_1Pyr_1$ and HO-$Hex_3Pyr_1$. The signals observed at m/z 950/933 correspond to the composition $Hex_3HexA_1Pyr_1$ and are the result of a methanolytic cleavage. The cleavage represented by these two signals has resulted in the formation of the methyl glycoside on the glycosidic oxygen that formerly took part in the 1-4 bond between the two mannose residues (see structure XI).

The spectrum (Fig. 3.5) obtained from the 10 minutes aliquot, afforded signals at m/z 701 and 715, corresponding to $[M+H]^+$ molecular ions of composition HO-$Hex_3Pyr_1$ and HO-$Hex_2HexA_1Pyr_1$ repectively. The final aliquot, taken after 20 minutes heating at 60°C afforded a spectrum in which no signals were observed above the background. The data obtained from these spectra are summarised in TABLE 3.7. TABLE 3.8 lists the structures each of the ions, observed may represent.

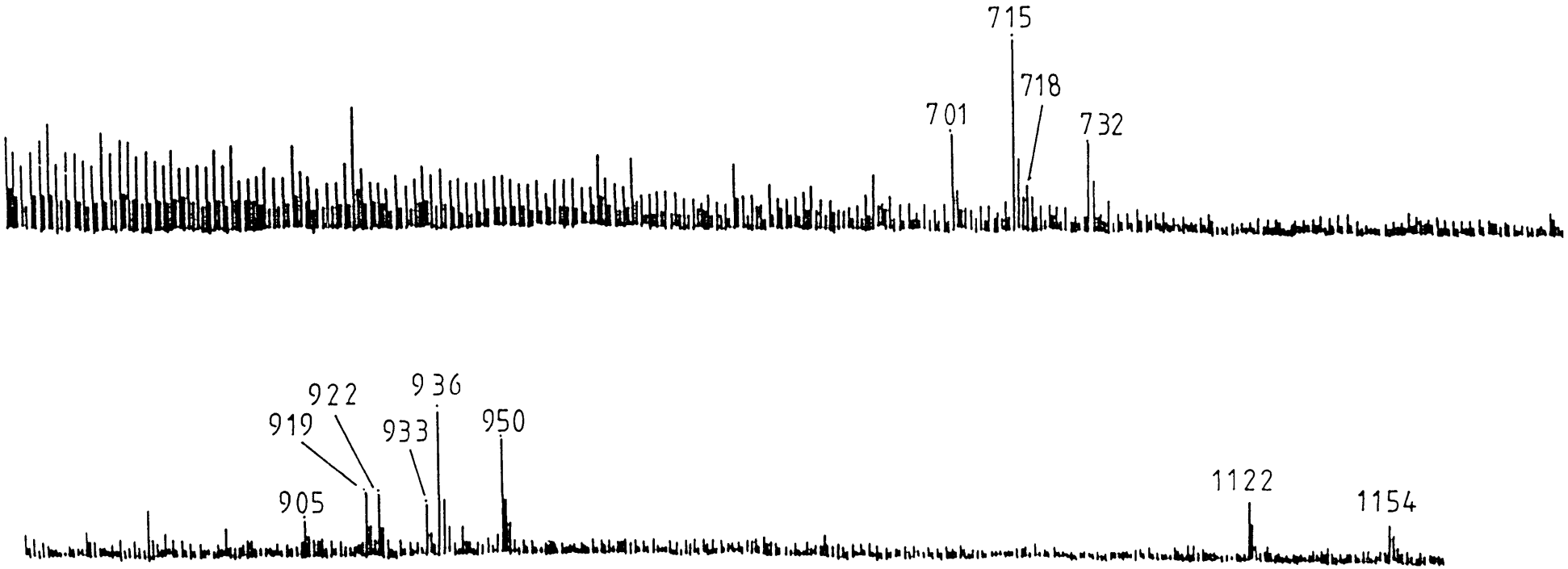



Figure 3.4. Positive ion FAB spectrum of permethylated K 69 P1 repeat after 5 mins. methanolysis at 60° C.

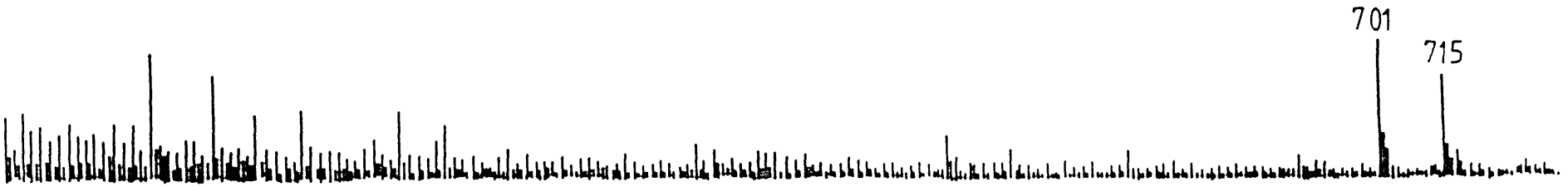


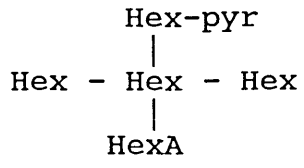

Figure 3.5. Positive ion FAB spectrum of permethylated K 69 P1 repeat after 10 mins. methanolysis at 60°C.

**TABLE 3.7** Summary of ions observed after methanolysis for 120 minutes at 40° C and for a further 10 minutes at 60° C. (see Figs. 3.4 and 3.5).

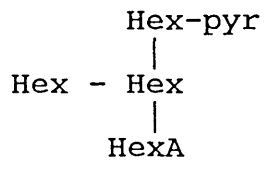
| ION | | COMPOSITION |
|---|---|---|
| 1154 | $[M+NH_4]^+$ | $Hex_4HexA_1Pyr_1$ |
| 1122 | Oxonium | " |
| 950 | $[M+NH_4]^+$ | $Hex_3HexA_1Pyr_1$ |
| 936 | $[M+NH_4]^+$ | $HO\text{-}Hex_3HexA_1Pyr_1$ |
| 933 | $[M+H]^+$ | $Hex_3HexA_1Pyr_1$ |
| 922 | $[M+NH_4]^+$ | $HO\text{-}Hex_4Pyr_1$ |
| 919 | $[M+H]^+$ | $HO\text{-}Hex_3HexA_1Pyr_1$ |
| 905 | $[M+H]^+$ | $HO\text{-}Hex_4Pyr_1$ |
| 732 | $[M+NH_4]^+$ | $HO\text{-}Hex_2HexA_1Pyr_1$ |
| 718 | $[M+NH_4]^+$ | $HO\text{-}Hex_3Pyr_1$ |
| 715 | $[M+H]^+$ | $HO\text{-}Hex_2HexA_1Pyr_1$ |
| 701 | $[M+H]^+$ | $HO\text{-}Hex_3Pyr_1$ |

**TABLE 3.8** Summary of the possible structures each of the signals, observed in Figures 3.4 and 3.5, may represent.

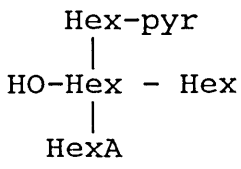
1154 / 1122



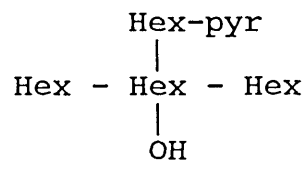

950 / 933



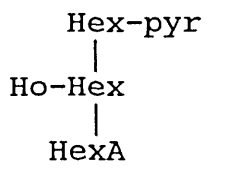

936 / 919



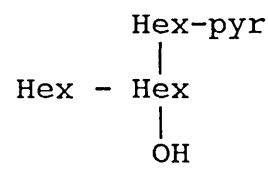

922 / 905



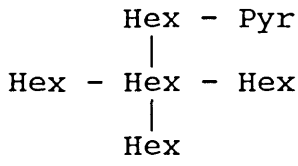

732 / 715




718 / 701



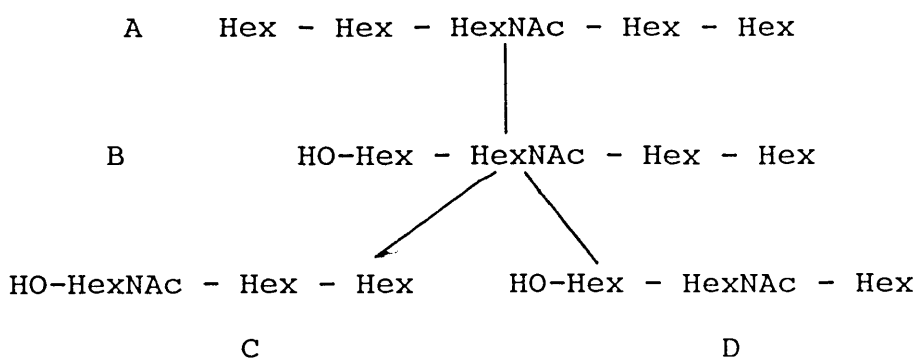
The data obtained from this methanolysis/FAB-MS experiment allow the following structure (XII) to be determined.




(XII)

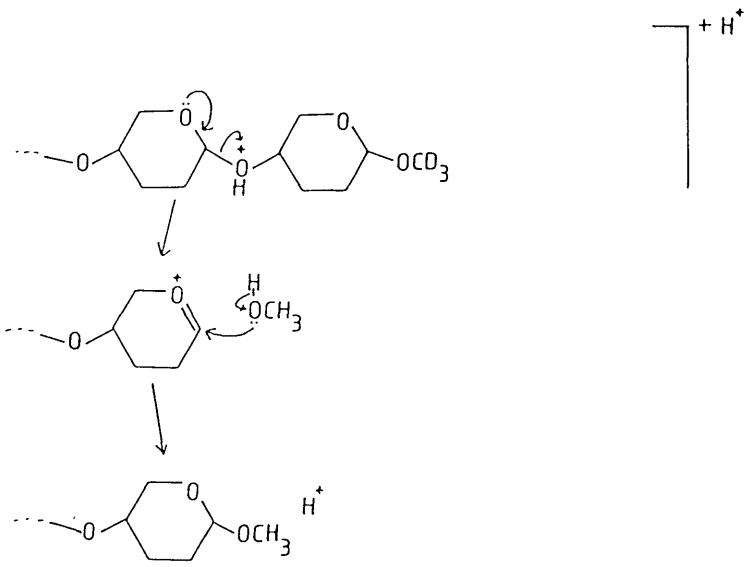
This structural assignment is in complete agreement with that obtained previously[84].

At this point a modification to the methanolysis/FAB-MS protocol was considered prudent. From the data above, in particular the signals at m/z 950 and 933 observed in Fig. 3.4, it was possible to foresee a situation when it would be impossible to determine whether a methanolytic cleavage resulted in a fragment originating from the reducing or non-reducing end of the original material. For example, taking the molecule A, after one non-reducing end methanolytic cleavage, giving B, it would be impossible to differentiate between an additional non-reducing end or a reducing end methanolytic cleavage, giving rise to C or D respectively (see Scheme 3.2).




Scheme 3.2.

This is because the methanolytic cleavage results in the reducing end of the product terminating with a methyl glycoside (see Scheme 3.1). Since the uncleaved molecule also has a methyl glycoside on the reducing end, it is not possible to determine when a cleavage has occurred at the reducing end of the molecule. To avoid this possible ambiguity the final modification made was the use of deuteriomethyl iodide in the permethylation step, but to continue using non-deuterated methanol in the methanolic HCl reagent. This would mean that when a reducing end methanolytic cleavage occurred, the resultant product would afford an ion 3 a.m.u. lower than if it was a fully perdeuteriomethylated species (see Scheme 3.3).

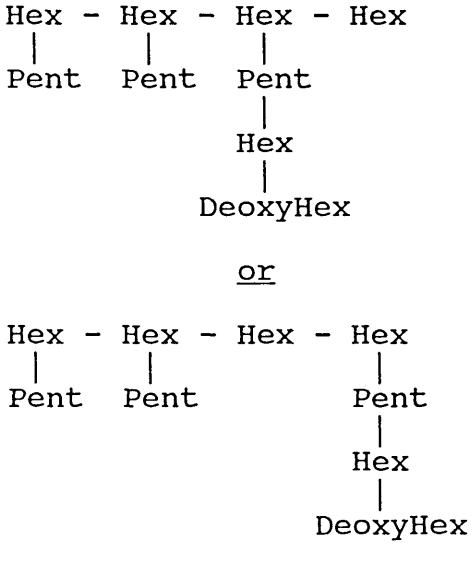



Scheme 3.3

It would therefore be possible to differentiate a methanolytic cleavage that occurred at the reducing end of the molecule from one that occurred at the non-reducing end, due to a mass shift of 3 a.m.u. that would be observed in the mass spctrum.

3:3. Application of Methanolysis/FAB-MS to Xyloglucan.

The structure of the nonasaccharide derived from Sycamore extracellular polysaccharide, previously examined by deuterioacetylation (see Chapter 2:5.3.), had not been fully resolved. The data obtained from the deuterioacetylation study enabled the following structures to be determined (XV).




(XV)

The methanolysis/FAB-MS procedure was applied to complete the sequence and branch data on this molecule, with aliquots taken after 5, 10, 20 and 40 minutes heating at 40° C and 5, 10, 20 and 60 minutes further heating at 60° C.

The 5, 10 and 20 minute aliquots taken while heating at 40° C afforded spectra with minimal evidence for methanolytic cleavage. The 40 minute aliquot afforded the spectrum reproduced in Figure 3.6. The pairs of signals observed at m/z 1813/1796, 1616/1599, 1433/1416, 1403/1386

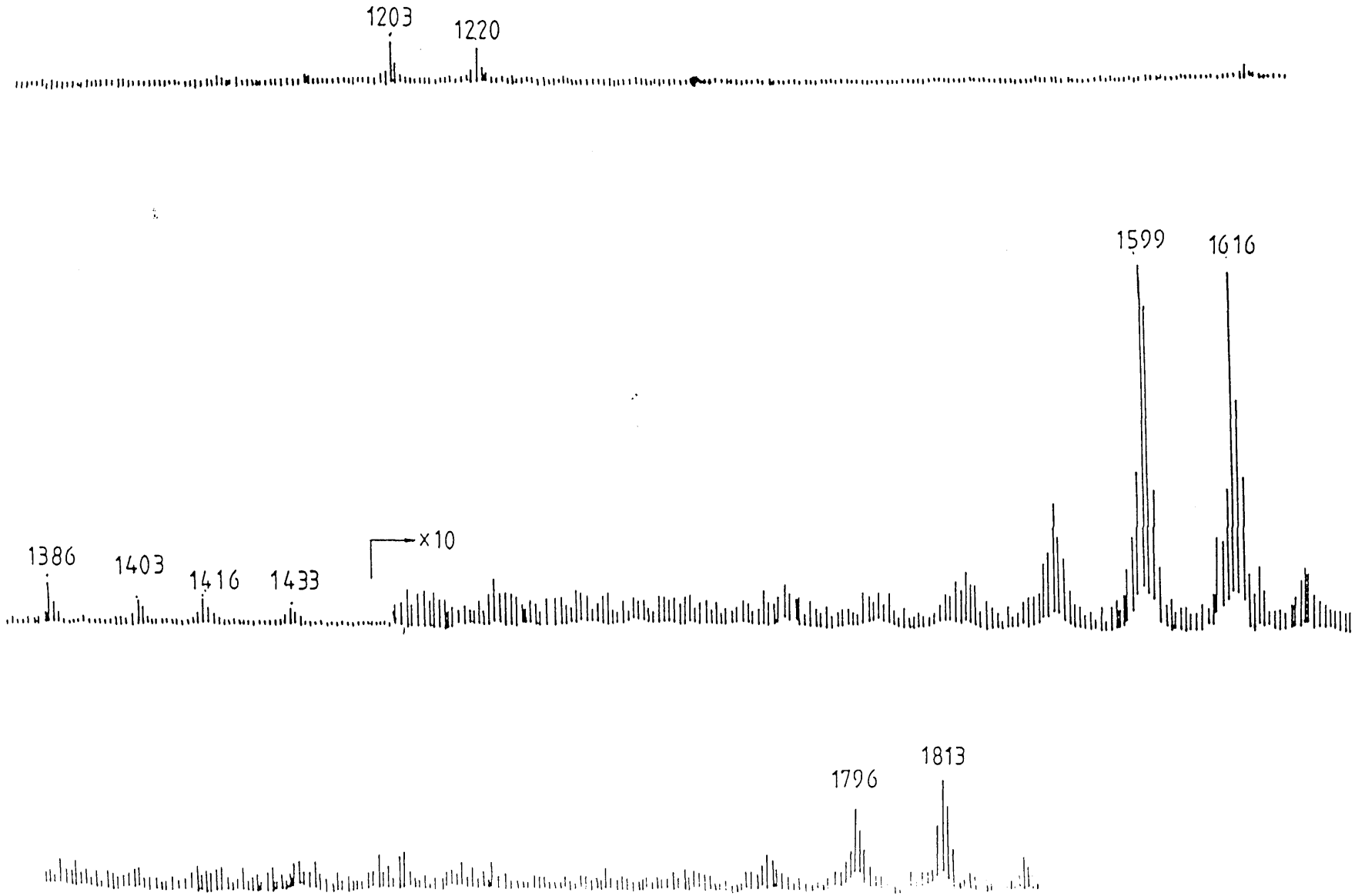



Figure 3.6. Positive ion FAB spectra of deuteriomethyl derivative of Xyloglucan after methanolysis for 40 mins. at 40°C.

and 1220/1203 are $[M+NH_4]^+/[M+H]^+$ molecular ions of composition $DeoxyHex_1Hex_5Pent_3$, $HO\text{-}Hex_5Pent_3$, $HO_2\text{-}Hex_5Pent_2$, $HO\text{-}Hex_4Pent_3$ and $HO_2\text{-}Hex_4Pent_2$.

The 5 minute aliquot taken while heating further at 60° C afforded a spectrum similar to that in Figure 3.6. The aliquot taken after 10 minutes at 60° C is reproduced in Figure 3.7. The ions previously observed in Figure 3.6 at m/z 1616/1599, 1433/1416, 1403/1386 and 1220/1203 were present. In addition 2 new ion pairs were observed at m/z 1037/1020 and 1007/990, consistent with being $[M+NH_4]^+/[M+H]^+$ molecular ions of composition $HO_3\text{-}Hex_4Pent_1$ and $HO_2\text{-}Hex_3Pent_2$ respectively. Another signal was present at m/z 824 consistent with being the $[M+NH_4]^+$ molecular ion of composition $HO_3\text{-}Hex_3Pent_1$.

The 20 minute aliquot afforded a spectrum (Fig. 3.8.) in which the ions previously observed at m/z 1616/1599, 1433/1416, 1403/1386, 1220/1203, 1037/1020, 1007/990 and 824 were present. Additionally ions pairs were observed at m/z 1004/987 and 821/804, consistent with being $[M+NH_4]^+/[M+H]^+$ molecular ions of composition $HO_2\text{-}Hex_3Pent_2$ (reducing end cleavage) and $HO_3\text{-}Hex_3Pent_1$ (reducing end cleavage). The ion observed at m/z 807 is consistent with being the $[M+H]^+$ molecular ion of composition $HO_3\text{-}Hex_3Pent_1$. The ion at m/z 854 is consistent with a $[M+NH_4]^+$ molecular ion of composition $HO_3\text{-}Hex_4$, though it is not accompanied by a $[M+H]^+$ ion. The spectrum of the final aliquot, taken after 60 minutes heating at 60° C, afforded no new signals.

The data obtained from the spectra (Figs. 3.6., 3.7., and 3.8.) are summarised in TABLE 3.9. The ion at

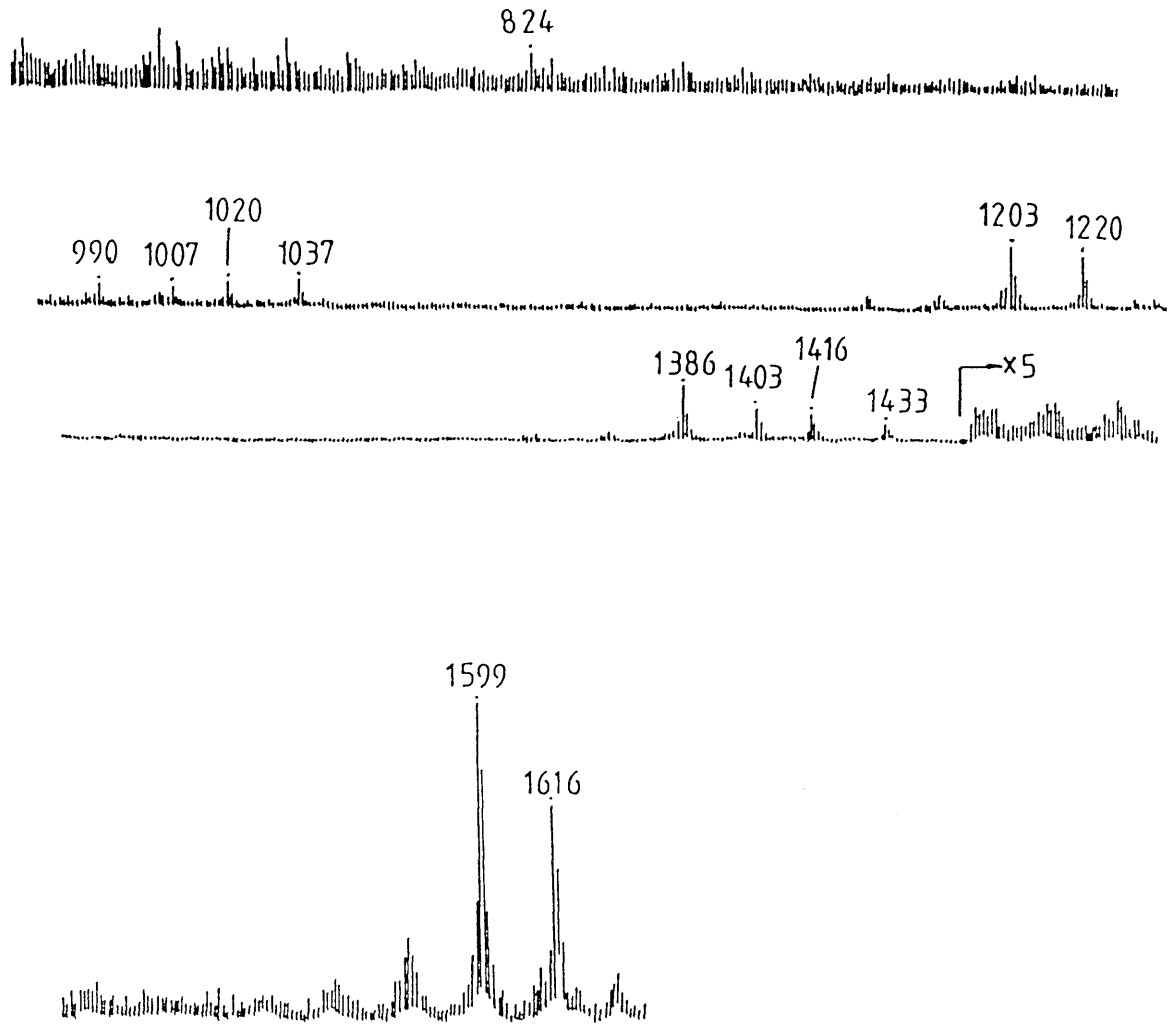



Figure 3.7. Positive ion FAB spectra of deuteriomethyl derivative of Xyloglucan after methanolysis for 10 mins. at 60°C.

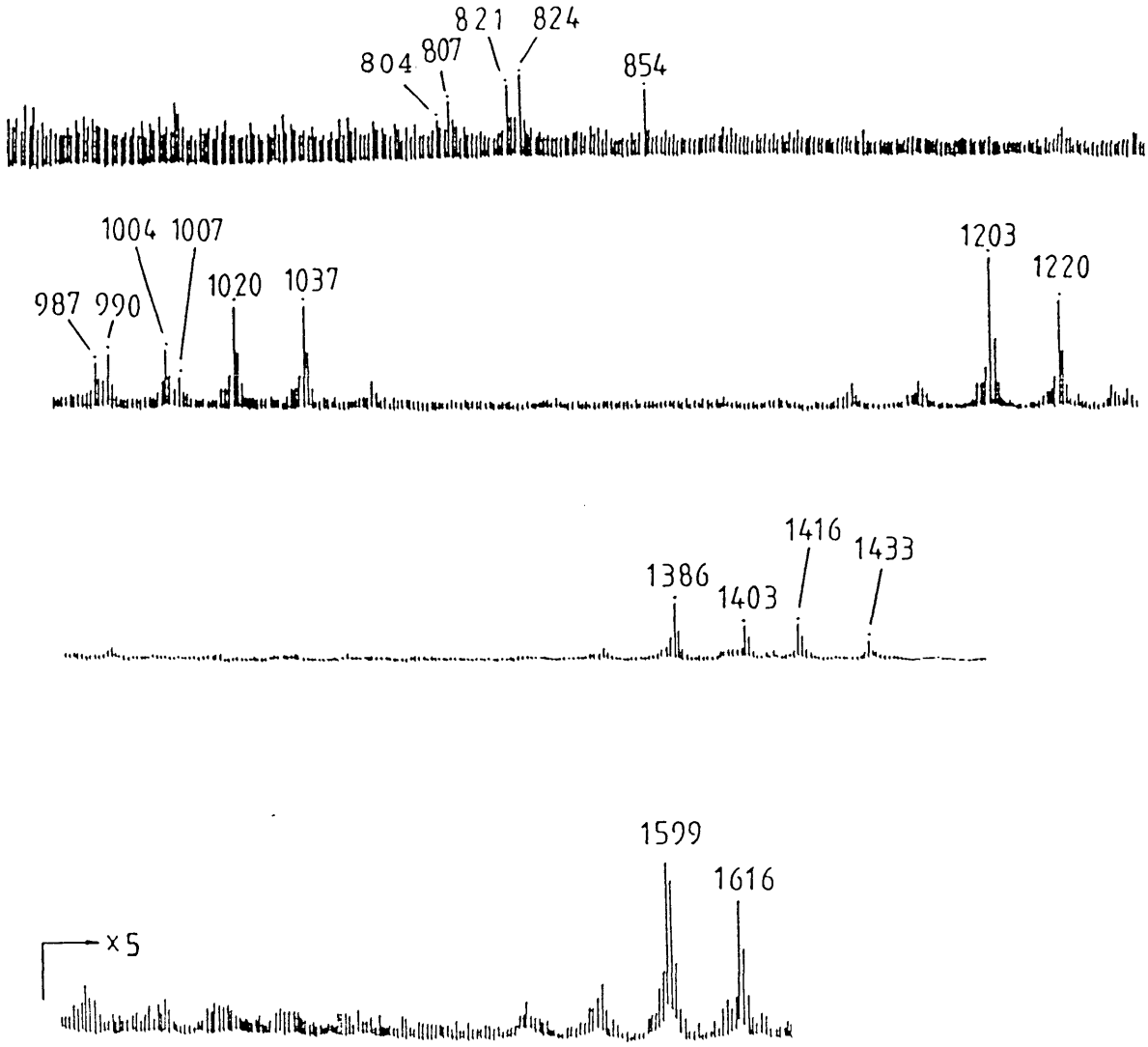
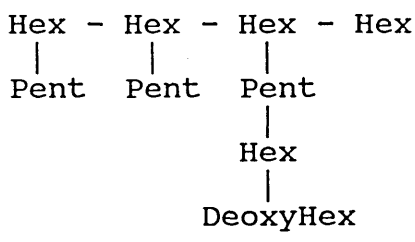



Figure 3.8. Positive ion FAB spectra of deuteriomethyl derivative of Xyloglucan after methanolysis for 20 mins. at 60° C.

m/z 854 stands out as being the only species that does not afford a $[M+H]^+$ molecular ion. It is also the only species with a composition that does not contain a pentose residue. This may indicate that the presence of a pentose residue facilitates the formation of a $[M+H]^+$ molecular ion. The two sets of signals observed at m/z 1004/987 and 821/804 indicate that a reducing end cleavage has occurred. This can be deduced because the mass of these ions is 3 amu. lower than that expected for a fully deuteriomethylated species. This is because a methanolytic cleavage has resulted in the molecule containing 1 non-deuterated methyl group (see Scheme 3.1). This effectively labels the reducing end of the resultant molecule so it is possible to distinguish ions that derive from reducing end cleavages from those derived from non-reducing end cleavages. The possible structures the ions, summarised in TABLE 3.9., may represent are listed in TABLE 3.10.

The 2 sets of ions that contain reducing end cleavages enable the structure of the Xyloglucan derived nonasaccharide to be determined (XVI).




(XVI)

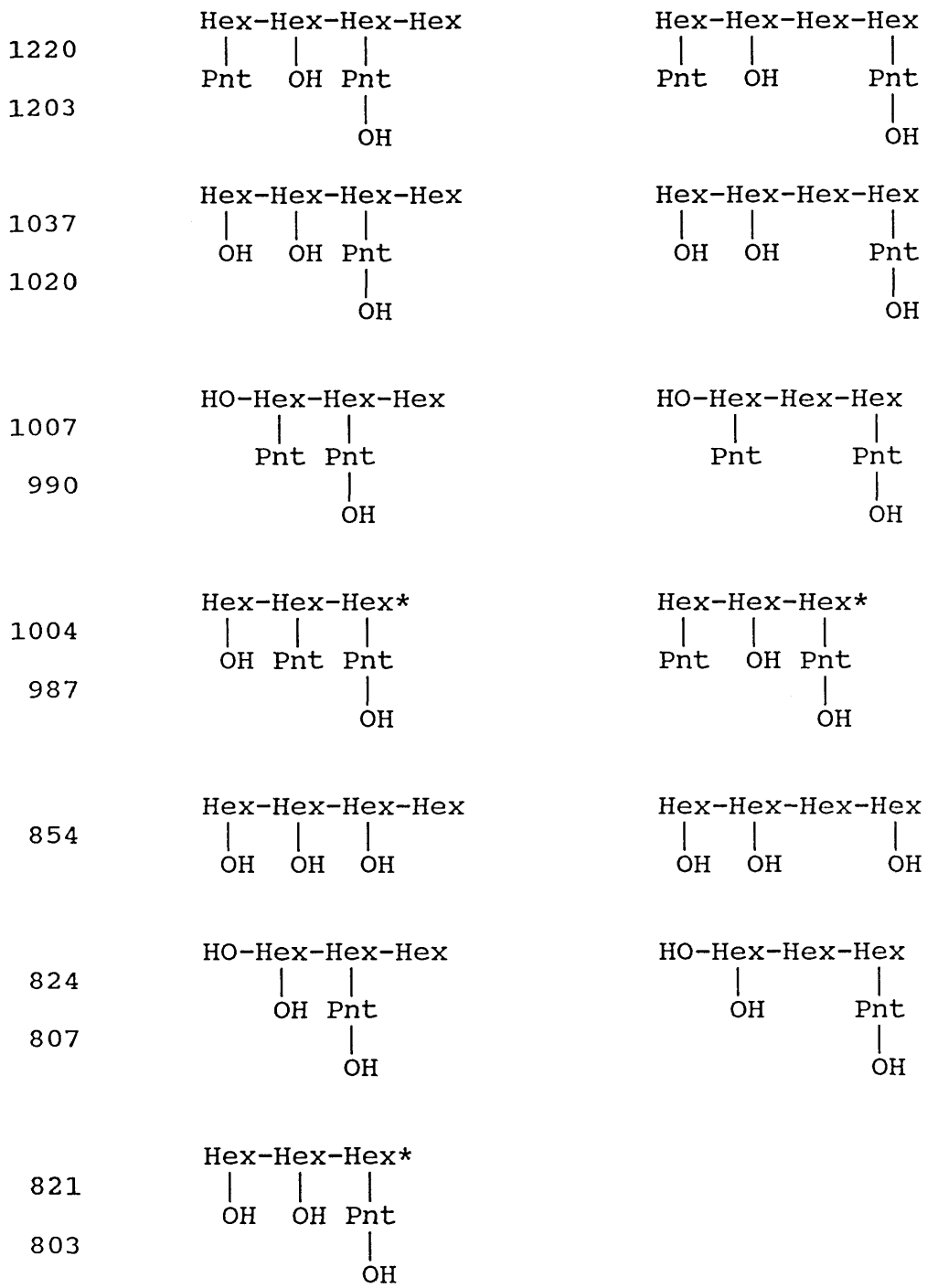
**TABLE 3.9** Summary of ions observed in the methanolysis/FAB-MS study of the Xyloglucan nonasaccharide.

(see Figs. 3.13 - 3.15).

| MOLECULAR IONS | | COMPOSITIONS |
|---|---|---|
| 1813 | $[M+NH_4]^+$ | $DeoxyHex_1Hex_5Pent_3$ |
| 1796 | $[M+H]^+$ | $DeoxyHex_1Hex_5Pent_3$ |
| 1616 | $[M+NH_4]^+$ | $HO\text{-}Hex_5Pent_3$ |
| 1599 | $[M+H]^+$ | $HO\text{-}Hex_5Pent_3$ |
| 1433 | $[M+NH_4]^+$ | $HO_2\text{-}Hex_5Pent_2$ |
| 1416 | $[M+H]^+$ | $HO_2\text{-}Hex_5Pent_2$ |
| 1403 | $[M+NH_4]^+$ | $HO\text{-}Hex_4Pent_3$ |
| 1386 | $[M+H]^+$ | $HO\text{-}Hex_4Pent_3$ |
| 1220 | $[M+NH_4]^+$ | $HO_2\text{-}Hex_4Pent_2$ |
| 1203 | $[M+H]^+$ | $Ho_2\text{-}Hex_4Pent_2$ |
| 1037 | $[M+NH_4]^+$ | $HO_3\text{-}Hex_4Pent_1$ |
| 1020 | $[M+H]^+$ | $HO_3\text{-}Hex_4Pent_1$ |
| 1007 | $[M+NH_4]^+$ | $HO_2\text{-}Hex_3Pent_2$ |
| 990 | $[M+H]^+$ | $HO_2_Hex_3Pent_2$ |
| 1004 | $[M+NH_4]^+$ | $HO_2_Hex_3Pent_2$ (reducing end cleavage) |
| 987 | $[M+H]^+$ | $HO_2_Hex_3Pent_2$ (reducing end cleavage) |
| 854 | $[M+NH_4]^+$ | $Ho_3\text{-}Hex_4$ |
| 824 | $[M+NH_4]^+$ | $HO_3\text{-}Hex_3Pent_1$ |
| 807 | $[M+H]^+$ | $HO_3_Hex_3Pent_1$ |
| 821 | $[M+NH_4]^+$ | $HO_3\text{-}Hex_3Pent_1$ (reducing end cleavage) |
| 804 | $[M+H]^+$ | $HO_3_Hex_3Pent_1$ (reducing end cleavage) |

**TABLE 3.10** Summary of possible structures the ions, observed during methanolysis/FAB-MS of Xyloglucan nonasaccharide, may represent. (see Figs. 3.13 - 3.15).

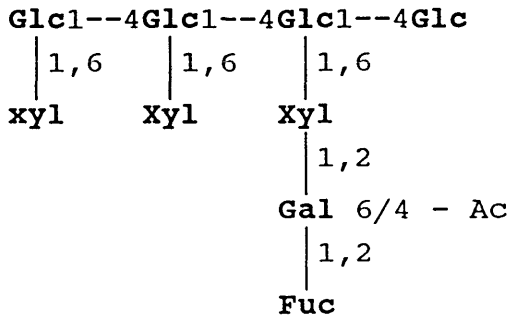
| | | |
|---|---|---|
| 1813 | Hex-Hex-Hex-Hex<br>\| \| \| \|<br>Pnt Pnt Pnt<br>\| | Hex-Hex-Hex-Hex<br>\| \| \|<br>Pnt Pnt Pnt<br>\| |
| 1796 | Hex<br>\|<br>DxyHex | Hex<br>\|<br>DxyHex |
| 1616 | Hex-Hex-Hex-Hex<br>\| \| \| \|<br>Pnt Pnt Pnt<br>\| | Hex-Hex-Hex-Hex<br>\| \| \|<br>Pnt Pnt Pnt<br>\| |
| 1599 | Hex<br>\|<br>OH | Hex<br>\|<br>OH |
| 1433 | Hex-Hex-Hex-Hex<br>\| \| \| \|<br>OH Pnt Pnt<br>\| | Hex-Hex-Hex-Hex<br>\| \| \|<br>OH Pnt Pnt<br>\| |
| 1416 | Hex<br>\|<br>OH | Hex<br>\|<br>OH |
| | Hex-Hex-Hex-Hex<br>\| \| \| \|<br>Pnt OH Pnt<br>\| | Hex-Hex-Hex-Hex<br>\| \| \|<br>Pnt OH Pnt<br>\| |
| | Hex<br>\|<br>OH | Hex<br>\|<br>OH |
| 1403 | Hex-Hex-Hex-Hex<br>\| \| \| \|<br>Pnt Pnt Pnt<br>\| | Hex-Hex-Hex-Hex<br>\| \| \|<br>Pnt Pnt Pnt<br>\| |
| 1386 | OH | OH |
| 1220 | Hex-Hex-Hex-Hex<br>\| \| \| \|<br>OH Pnt Pnt<br>\| | Hex-Hex-Hex-Hex<br>\| \| \|<br>OH Pnt Pnt<br>\| |
| 1203 | OH | OH |




* indicates a reducing end methanolytic cleavage has occurred

Pnt indicates a Pentose residue

The mass spectrometric data discussed above and in chapter 2.3.4. in conjunction with the n.m.r. and composition data obtained by Albersheim and workers[85] enabled the complete structure of this xylogucan fragment to be determined (XVII).




(XVII)

3.4. Discussion of the merits of Methanolysis-FAB-MS.

The aim of the development of the methanolysis-FAB-MS procedure was to facilitate full sequence and branching data. An alternative method to obtain such information, that at first seems appropriate, is tandem mass spectrometry(MS/MS).

Unlike other spectroscopic techniques, in a mass spectrometric experiment the sample moves through the instrument as it is analysed. MS/MS is the coupling of two or more mass analysers and utilising this motion to separate out components and examine them individually. There are various methods of carrying out MS/MS analyses. A reverse geometry double focussing instrument, that is, a mass spectrometer in which the magnet preceeds the electric sector can perform MS/MS analyses. Mass selection is performed by the magnet with dissociation of the selected (parent) ion occurring in the field free region between the magnetic and electric sectors and subsequent analysis of the resultant (daughter) ions achieved by scanning the electric sector[85,89]. Such an experiment is referred to as a daughter ion scan. Tandem quadrapole mass spectrometry is an alternative approach to MS/MS, where two quadrapole mass analysers are linked[90] with a collision chamber between them. The first quadrapole selects the parent ion and the second analyses the collisionally dissociated product ions. Various combination instruments are presently in use with more than two quadrapole filters or more than two sectors. The sector instruments in general afford greater resolution than quadrapoles, while quadrapole systems facilitate much

faster scan times. A favoured combination at present is the hybrid instrument, with a double focussing sector instrument linked to a quadrapole. This system is designed to achieve the "best of both worlds", with high resolution ion selection followed by fast daughter ion analysis.

An MS/MS experiment selects one ion from the many present in the ion beam exiting the source region and is therefore capable of increasing the signal to noise ratio[91]. This can result in an increase in the experimental sensitivity even though the absolute sensitivity may in fact be reduced[92]. The ability to select only one molecular ion and by collisionally activated dissociation obtain fragment ions from the selected parent would, at first, seem to make MS/MS the obvious method for obtaining full fragmentation data. In many cases this has proven to be the case[93,94], though there has been no notable application of MS/MS to carbohydrate polymers. This is due to the problems inherent in the mass spectrometric analysis of oligosaccharides discussed in the introduction to this thesis (Chapter 1.4). It would not be possible to differentiate between fragments derived from the reducing or non-reducing ends of the molecule. So derivatisation would still be neccessary, as is the case in a normal MS experiment.

One inherent benefit of using the methanolysis FAB-MS procedure is that sensitivity is enhanced due to the presence of $H^+$ in the reagent. This means that the hydrolytic cleavages that occur are observed sensitively,

though it may be argued that the improved signal to noise ratio observed in MS/MS experiments affords comparable data. In one respect, the methanolysis procedure described in this chapter is unarguably superior to MS/MS. In an MS/MS experiment dissociations that occur infrequently cannot be observed as the resultant daughter ions are insufficiently abundant to afford signals, and continue to travel through the mass spectrometer. Conversely during a methanolysis-FAB-MS experiment cleavages that occur infrequently can be observed. Because the ions formed due to methanolytic cleavage remain in the reaction vessel they are able to build up to a concentration where a signal is observed in the spectrum. This benefit of methanolysis was clearly demonstrated in the analysis of P1 (section 3.2.3.) where the signals at m/z 704 and 715 were only present at the end of the experiment.

## 3.5. Summary of Methanolysis/FAB-MS protocol.

The experiments discussed above enabled a clear protocol to be defined for use in the examination of unknown samples.

1) obtain the perdeuteromethyl derivative
2) carry-out methanolysis using non-deuterated methanolic HCl
3) obtain aliquots after heating at 40°C for 2, 5, 10, 20 and 40 minutes and after heating at 60°C for an additional 5, 10 and 20 minutes. Further aliquots may be necessary if the molecule under examination is particularly resistant to degredation.
4) obtain FAB spectra of each aliquot

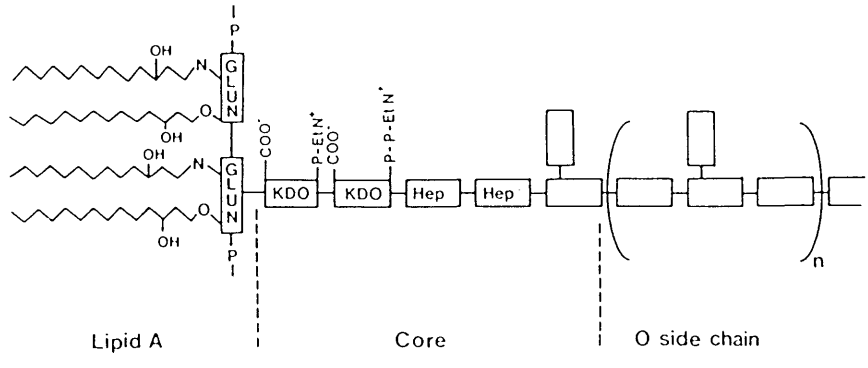
## 3.6. Conclusion

The experiments described above have outlined the development of methanolysis/FAB-MS as a protocol and its application in structural analysis. The method enables a rapid reliable determination of sequence and branch position and is very sensitive, requiring 10 µg of material for a complete time course to be performed.

## Chapter 4 : An Examination of LPS Core Oligosaccharides.

### 4.1. Introduction.

One of the most pronounced differences between Gram negative organisms and other bacteria is that they contain lipopolysaccharide (LPS). The lipopolysaccharide is anchored in the outer membrane and contributes to the antigenic specificity of the organism. The term lipopolysaccharide denotes any molecular species consisting mainly of polysaccharide but possessing a lipid moiety. In bacteriology the term is applied exclusively to the O-antigens from Gram negative bacteria[95]. The classic model for LPS is one where the molecule is divided into three distinct covalently linked regions.

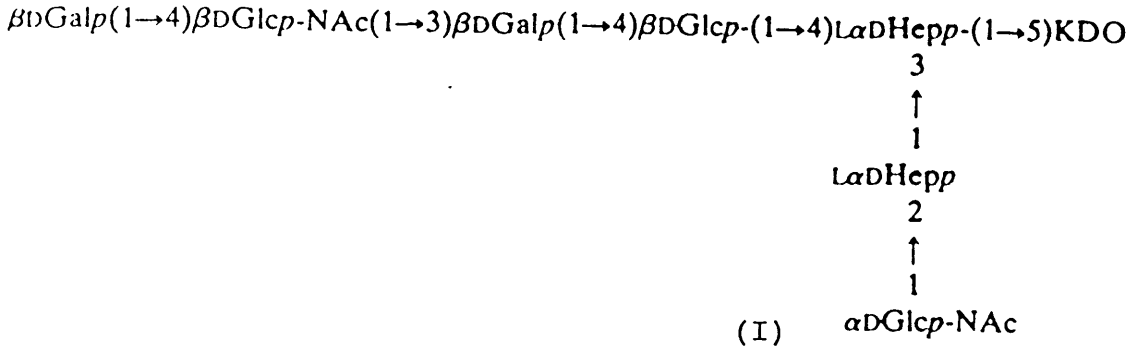



The lipid region consists of fatty acid chains linked to glucosamine, and acts as an anchor in the outer menbrane. It has been found that in most LPS investigated Lipid A has a closely related structure[38]. Extending from the

Lipid A is the core region, consisting of a short carbohydrate chain, which, in the majority of Gram negative species, contains 3-deoxy-D-manno-2-keto-octulosonate (KDO) and heptose residues. Extending from the core region is the O-side chain, a carbohydrate polymer the length of which may vary considerably.

The present interest in LPS structure originates from work by Francis and Tillet in 1930[96], who described the use of pneumococcus capsular polysaccharides to elicit the production of antibodies. Studies on the immunogenicity of polysaccharides from disease causing bacteria have been carried out[97,98] and the use of capsular polysaccharides as human vaccines has been reviewed[88]. A recent study of oligosaccharides from Neisseria gonorrhoeae LPS has determined several partial structures with the aim of producing a vaccine[99].

Polysaccharide antigens of Niesseria meningitidis have been implicated in the immune response to infection[14,13,11]. This has led to structural studies being carried-out on the various serogroups[100,101]. One such study utilised R-type mutants to examine the core oligosaccharide structure of a number of different strains of Niesseria meningitidis. This study[102] found that the core oligosaccharide structure I was common to all the examined strains.




4.2. Structural Studies of The LPS Core.

Oligosaccharides from the lipopolysaccharide core of Niesseria meningitidis, were obtained from R-type mutants by mild acid hydrolysis[102]. These molecules are expected to have a core structure similar to that in (I), but with variations in the elongation pattern and presence and location of non-carbohydrate substituents. Moieties such as acetate, phosphate and phosphoethanolamine have proved, in the past to be difficult to locate. Ten such oligosaccharides were examined using the techniques described in Chapters 2 and 3.

4.2.1. SAMPLE 1 : L3-F-II (4)

The negative ion spectrum of the native material afforded ions at m/z 1700, 1678, 1660, 1658, 1636 and 1618. Those signals observed at m/z 1678 and 1636 are consistent with $[M-H]^-$ molecular ions, while those observed at m/z 1700 and 1658 are consistent with $[M+Na-H]^-$ molecular ions. The signals at m/z 1660 and 1618 are consistent with the species observed at m/z 1678 and 1636 having undergone a dehydration. This may be due to the FAB experiment or due to the KDO forming a 1 - 4 lactone.

The positive ion native spectrum, figure 4.1. afforded two sets of signals at m/z 1702 / 1680 and 1660 / 1638 consistent with $[M+Na]^+$ and $[M+H]^+$ Molecular ions. No signals were observed 18 amu. lower consistent with dehydration occurring. This indicates that the molecule is not forming a lactone as such a species would be expected to be present in the positive ion spectrum if it was observed in the negative ion spectrum.

The negative and positive ion data obtained from native L3-F-II (4) are summarised in TABLE 4.1.

The deuterioacetyl derivative was prepared in order to determine the position and abundance of the O-acetate. A-type fragment ions were observed at m/z 933, 636, 343, 339 and 336 of composition $Hex_2HexNAc$, $Hex_1HexNAc$, Hex, HexNAc and $HexNAc_1Ac_1$. Two signals were observed at m/z 510 and 468. These being 42 amu apart indicate that they

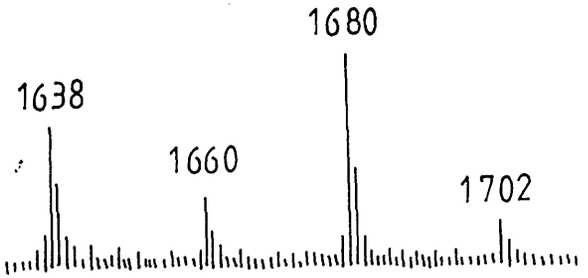



Figure 4.1. Positive ion FAB spectrum of native L3-F-II (4) LPS core oligosaccharide from Neisseria meningitidis.

**TABLE 4.1.** Summary of data obtained from the negative and positive ion spectra of native L3-F-II (4).

| NEGATIVE ION | | |
|---|---|---|
| MOLECULAR IONS | | COMPOSIITON |
| 1700 | $[M+Na-H]^-$ | $Hex_3HexNAc_2Hep_2KDO\text{-}P\text{-}EtNH_2Ac_1$ |
| 1678 | $[M-H]^-$ | $Hex_3HexNAc_2Hep_2KDO\text{-}P\text{-}EtNH_2Ac_1$ |
| 1660 | $[M-H]^-$ | dehydrated m/z 1678 |
| 1658 | $[M+Na-H]^-$ | $Hex_3HexNAc_2Hep_2KDO\text{-}P\text{-}EtNH_2$ |
| 1636 | $[M-H]^-$ | $Hex_3$+$HexNAc_2Hep_2KDO\text{-}P\text{-}EtNH_2$ |
| 1618 | $[M-H]^-$ | dehydrated m/z 1636 |
| POSITIVE ION | | |
| MOLECULAR ION | | COMPOSITION |
| 1702 | $[M+Na]^+$ | $Hex_3HexNAc_2Hep_2KDO\text{-}P\text{-}EtNH_2Ac_1$ |
| 1680 | $[M+H]^+$ | $Hex_3HexNAc_2Hep_2KDO\text{-}P\text{-}EtNH_2Ac_1$ |
| 1660 | $[M+Na]^+$ | $Hex_3HexNAc_2Hep_2KDO\text{-}P\text{-}EtNH_2$ |
| 1638 | $[M+H]^+$ | $Hex_3HexNAc_2Hep_2KDO\text{-}P\text{-}EtNH_2$ |

are not deuterioacetylated and are therefore not sample derived. The ratio of m/z 336 to 339 (1:1) indicates that 50% of molecules carry an O-acetate on the terminal HexNAc residue.

The permethyl derivative, afforded molecular ion signals at m/z 2086, 2072, 2058, 2040, 2026, 1970, 1956, 1810and 1796, figure 4.2. The ion observed at m/z 2072 is consistent with a fully methylated species of the expected composition $Hex_3HexNAc_2Hep_2KDO\text{-}P\text{-}EtNH_2$. All free hydroxyls amides and the carboxylic acid group have been derivatised, and the ion is in the form of a pseudomolecular ion with a proton adduct $[M+H]^+$. At m/z 2086 an ion is observed consistent with one degree of overmethylation, which is thought to be located on the amino moiety of the phosphoethanolamine. The mass of this ion is consistent with a molecular ion in which the charge is generated by the formation of a quaternary ammonium group $[M+CH_3]^+$. A further ion at m/z 2100 was observed that is consistent with the ion at m/z 2086 undergoing a C-methylation. A-type fragment ions were observed at m/z 668, 659, 464, 260 and 219.

The signals observed at m/z 2040 and 2026 are of a composition consistent with the molecules in which the lactonised form of KDO is present (46 amu. lower than the molecular ions). On perdeuteriomethylation, however, ions were still observed at m/z 2139 and 2122 46 amu. lower than the molecular ions. If the signals observed in

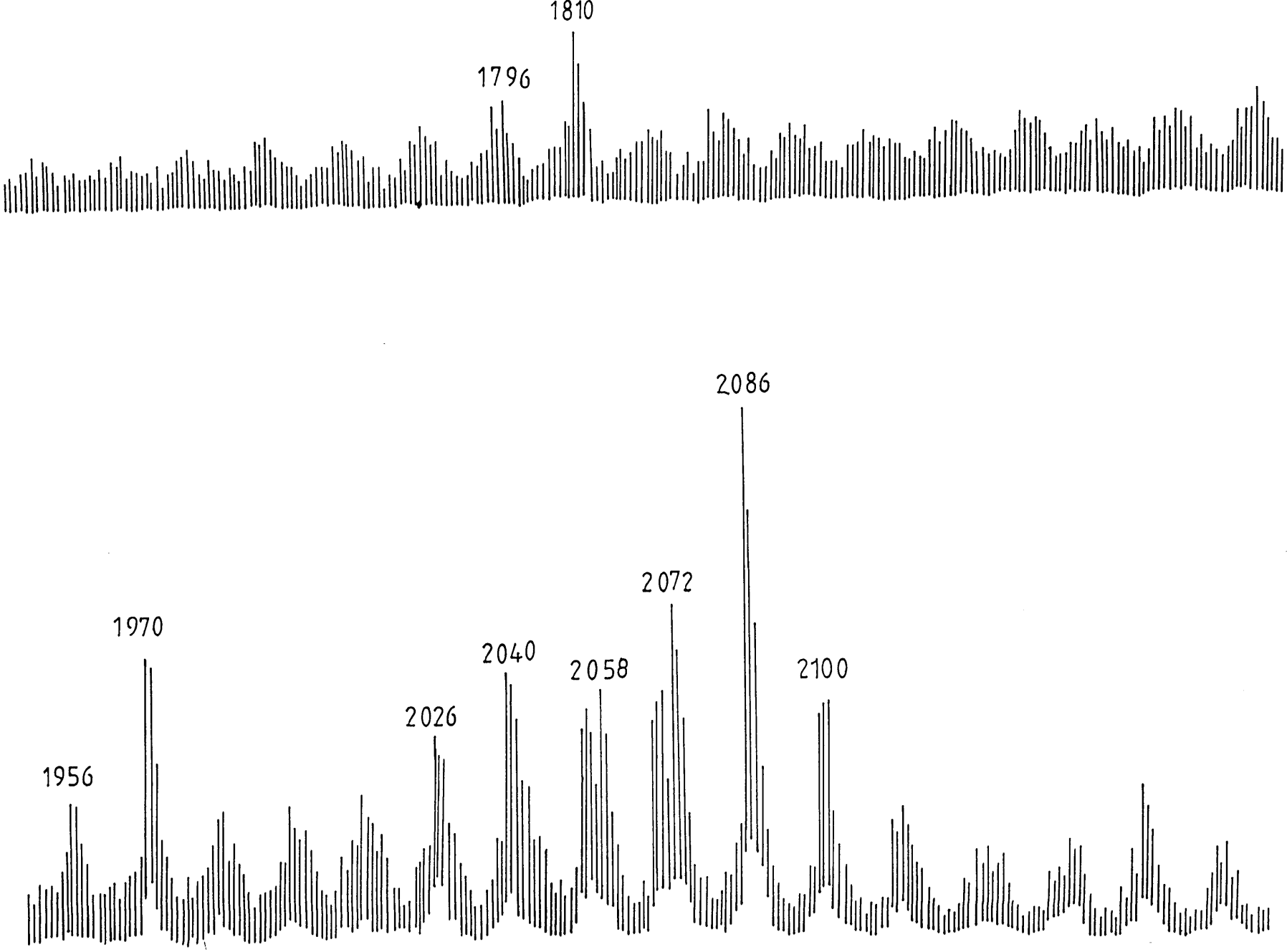
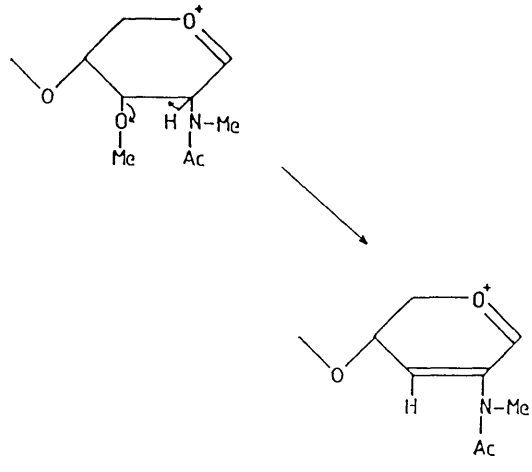



Figure 4.2. Positive ion FAB spectrum of molecular ion region of permethylated L3-F-II (4) LPS core oligosaccharide.

the permethylated spectrum at m/z 2040 and 2026 were due to a 1 - 4 lactone the "minus 46" ions should have been shifted to "minus 52" on deuteriomethylation. The fact that they didn't indicates that these ions are due to an change in the backbone of the KDO residue. The ions observed in the permethyl spectrum at m/z 1970 and 1956 "minus 116" also didn't shift in mass corresponding to a deuteriomethylated equivalent. Therefore it is suggested that the signals at m/z 2040 and 2026 are consistent with a rearrangement reaction within the reducing terminal KDO. The product of this rearrangement appears to undergo a ring cleavage affording ions 116 amu. lower than the molecular ions, at m/z 1970 and 1956. The "minus 46" and "minus 116" pattern seems to be diagnostic for a reducing terminal KDO residue[103]. These data are summarised in Table 4.2. along with the fragment ion data.

An ion was observed at m/z 432, which is commonly associated with m/z 464 as an elimination product (see scheme 4.2).




Scheme 4.2.

This elimination can only occur when the hydroxyl at position 3 in the ring is not a site for branching or substitution and when the group on position 2 is an N-acetyl moiety. The nitrogen at position 2 must play a role in this elimination, as no counterpart of this reaction is observed in non-amino sugars. Therefore since the ion at m/z 432 (the elimination product) is more intense than m/z 464 this indicates that the HexNAc residue is not 3-linked to the terminal Hexose. The Permethyl data are summarised in TABLE 4.2.

The data obtained on this sample so far are consistent with an LPS core saccharide. To obtain the complete structure Methanolysis-FAB-MS was carried out. Aliquots were taken after 2, 20 and 40 minutes heating at 40 C and 5, 30, 60, 120 and 240 minutes further heating at 60 C. The ions observed throughout the time-course are listed with their compositions in TABLE 4.3.

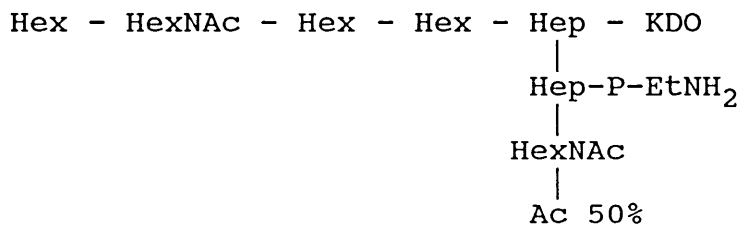
The ions observed at m/z 1115 and 840 are present in the last aliquots taken and are due to aqueous hydrolysis. Their presence indicates that water has entered the reaction vessel while the aliquots were being taken and fresh reagent added. However, though the presence of these hydrolytic ions made the spectrum more complex it was still possible to unambiguously assign compositions to each signal. The possible structures for each of the ions observed in the methanolysis are listed in TABLE 4.4.

Most of the ions observed in the course of the

**TABLE 4.2.** Summary of data obtained from the permethyl spectrum of L3-F-II (4).

| MOLECULAR IONS | | COMPOSIITON |
|---|---|---|
| 2100 | $[M+CH_3]^+$ | C-methylated m/z 2086 |
| 2086 | $[M+CH_3]^+$ | $Hex_3HexNAc_2Hep_2KDO\text{-}P\text{-}EtNH_2$ |
| 2072 | $[M+H]^+$ | $Hex_3HexNAc_2Hep_2KDO\text{-}P\text{-}EtNH_2$ |
| 2058 | $[M+H]^+$ | Undermethylated m/z 2072 |
| 2040 | $[M+CH_3]^+$ | m/z 2086 KDO rearrangement |
| 2026 | $[M+H]^+$ | m/z 2072 KDO rearrangement |
| 1970 | $[M+CH_3]^+$ | m/z 2086 ring cleaved KDO |
| 1956 | $[M+H]^+$ | m/z 2072 ring cleaved KDO |
| 1810 | $[M+CH_3]^+$ | $Hex_3HexNAc_2Hep_2\text{-}P\text{-}EtNH_2$ |
| 1796 | $[M+H]^+$ | undermethylated m/z 1810 |
| FRAGMENT IONS | | COMPOSITION |
| 668 | | $Hex_2HexNAc$ |
| 659 | | $HexNAc_1Hep_1\text{-}P\text{-}EtNH_2$ |
| 464 | | $Hex_1HexNAc$ |
| 260 | | HexNAc |
| 219 | | Hex |

methanolysis time-course served to corroborate data prevously obtained, but the ions at m/z 1405, 1129 and 925 were vital to the full sequence determination of the molecule. These data are completely consistent with structure (I).




(I)

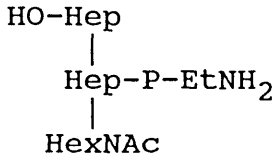
**TABLE 4.3.** Summary of ions observed during the methanolysis time-course of L3-F-II (4).

| ION | | COMPOSITION |
|---|---|---|
| 1854 | $[M+H]^+$ | $HO\text{-}Hex_2HexNAc_2Hep_2KDO\text{-}P\text{-}EtNH_2$ |
| 1808 | $[M+H]^+$ | m/z 1854 KDO rearrangement |
| 1609 | $[M+H]^+$ | $HO\text{-}Hex_2HexNAc_1Hep_1KDO\text{-}P\text{-}EtNH_2$ |
| 1563 | $[M+H]^+$ | m/z 1609 KDO rearrangement |
| 1419 | $[M+CH_3]^+$ | $HO\text{-}Hex_1HexNAc_1Hep_2KDO\text{-}P\text{-}EtNH_2$ |
| 1405 | $[M+H]^+$ | $HO\text{-}Hex_1HexNAc_1KDO\text{-}P\text{-}EtNH_2$ |
| 1359 | $[M+H]^+$ | m/z 1405 KDO rearrangement |
| 1129 | $[M+H]^+$ | $HO\text{-}Hex_1HexNAc_1Hep_2\text{-}P\text{-}EtNH_2$ |
| 1115 | $[M+H]^+$ | $HO_2\text{-}Hex_1HexNAc_1Hep_2\text{-}P\text{-}EtNH_2$ (aq) |
| 925 | $[M+H]^+$ | $HO\text{-}HexNAc_1Hep_2\text{-}P\text{-}EtNH_2$ |
| 854 | $[M+H]^+$ | $HO\text{-}HexNAc_1Hep_2\text{-}P\text{-}OH$ |
| 840 | $[M+H]^+$ | $HO_2\text{-}HexNAc_1Hep_2\text{-}P\text{-}OH$ (aq) |

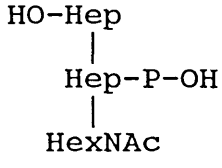
**TABLE 4.4.** Possible structures of ions observed in the methanolysis time course of L3-F-II (4).

| ION | COMPOSITION |
|---|---|
| 1854 | HO-HexNAc-Hex-Hex-Hep-KDO<br>\|<br>Hep-P-EtNH$_2$<br>\|<br>HexNAc |
| 1808 | m/z 1854 KDO rearrangement |
| 1609 | HO-Hex-Hex-Hep-KDO<br>\|<br>Hep-P-EtNH$_2$<br>\|<br>HexNAc |
| 1563 | m/z 1609 KDO rearrangement |
| 1419 | HO-Hex-Hep-KDO<br>\|<br>Hep-P-EtNH$_2^+$<br>\|<br>HexNAc |
| 1405 | HO-Hex-Hep-KDO<br>\|<br>Hep-P-EtNH$_2$<br>\|<br>HexNAc |
| 1359 | m/z 1405 KDO rearrangement |
| 1129 | HO-Hex-Hep<br>\|<br>Hep-P-EtNH$_2$<br>\|<br>HexNAc |
| 1115 | HO-Hex-Hep-OH<br>\|<br>Hep-P-EtNH$_2$<br>\|<br>HexNAc |

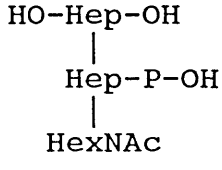
925


HO-Hep
Hep-P-EtNH2
HexNAc

854


HO-Hep
Hep-P-OH
HexNAc

840


HO-Hep-OH
Hep-P-OH
HexNAc

4.2.2. SAMPLE 2 : L4-F-I (6)

This sample gave almost identical data to that observed for sample L3-F-II (4). The negative and positive ion native spectra afforded the same data as did the deuterioacetyl and permethyl spetra. The only differences were the presence of ions in the methanolysis time-course that were not observed in the corresponding data for L3-F-II (4). The same time course profile was followed, taking aliquots after 2, 20 and 40 minutes at 40° C and a further 5, 30, 60, 120 and 240 minutes at 60° C. The ions observed in the methanolysis time-course with their compositions are listed in TABLE 4.5.

There are five ions assigned as resulting from aqueous hydrolisis in this sample m/z 1782, 1564, 1115, 1044 and 840. Only m/z 1115 and 840 were observed in the methanolysis of L3-F-II (4). These other aqueous cleavages may be due to the presence of water in the methanol as well as water entering the reaction vessel during aliquoting. As observed in the case of sample 1 these hydrolytic ions did not affect the interpretation of the data obtained.

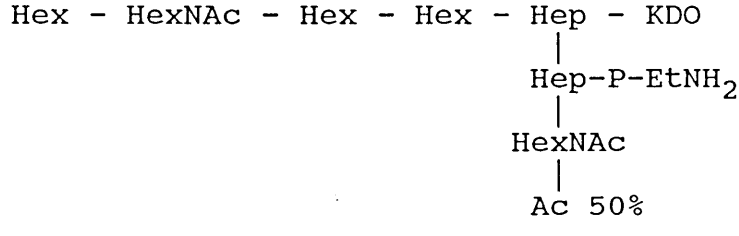
The non-aqueous hydrolysis products observed at m/z 1623, 1201, 1058 and 1044 were not present in the methanolysis spectra of L3-F-II (4). Throughout the time-course fresh reagent is added to replace that which has evaporated and the amount of new reagent added will vary resulting in the reaction conditions being slightly

**TABLE 4.5.** Summary of data obtained during the methanolysis time-course of L4-F-I (6).

| ION | | COMPOSITION |
|---|---|---|
| 1868 | $[M+CH_3]^+$ | HO-$Hex_2HexNAc_2Hep_2$KDO-P-$EtNH_2$ |
| 1854 | $[M+H]^+$ | HO-$Hex_2HexNAc_2Hep_2$KDO-P-$EtNH_2$ |
| 1808 | $[M+H]^+$ | m/z 1854 KDO rearrangement |
| 1782 | $[M+H]^+$ | $Hex_3HexNAc_2Hep_2$-P-$EtNH_2$ (aq) |
| 1623 | $[M+CH_3]^+$ | HO-$Hex_2HexNAc_1Hep_2$KDO-P-$EtNH_2$ |
| 1609 | $[M+H]^+$ | HO-$Hex_2HexNAc_1Hep_1$KDO-P-$EtNH_2$ |
| 1564 | $[M+H]^+$ | HO-$Hex_2HexNAc_2Hep_2$-P-$EtNH_2$ (aq) |
| 1563 | $[M+H]^+$ | m/z 1609 KDO rearrangement |
| 1419 | $[M+CH_3]^+$ | HO-$Hex_1HexNAc_1Hep_2$KDO-P-$EtNH_2$ |
| 1405 | $[M+H]^+$ | HO-$Hex_1HexNAc_1$KDO-P-$EtNH_2$ |
| 1359 | $[M+H]^+$ | m/z 1405 KDO rearrangement |
| 1201 | $[M+H]^+$ | HO-$HexNAc_1Hep_2$KDO-P-$EtNH_2$ |
| 1129 | $[M+H]^+$ | HO-$Hex_1HexNAc_1Hep_2$-P-$EtNH_2$ |
| 1115 | $[M+H]^+$ | $HO_2$-$Hex_1HexNAc_1Hep_2$-P-$EtNH_2$ (aq) |
| 1058 | $[M+H]^+$ | HO-$Hex_1HexNAc_1Hep_2$-P-OH |
| 1044 | $[M+H]^+$ | HO-$Hex_1HexNAc_1Hep_2$-P-OH (aq) |
| 925 | $[M+H]^+$ | HO-$HexNAc_1Hep_2$-P-$EtNH_2$ |
| 854 | $[M+H]^+$ | HO-$HexNAc_1Hep_2$-P-OH |
| 840 | $[M+H]^+$ | $HO_2$-$HexNAc_1Hep_2$-P-OH (aq) |

different each time. Therefore it is thought that sample L4-F-I (6) afforded a greater number of hydrolytic cleavages due to slight differences in the water content of the reagent used throughout the methanolysis, in addition to the ingress of water during aliquoting.

The possible structures of each of the methanolytic ions observed throughout the time-course are listed in TABLE 4.6. Most of the ions observed in the course of the methanolysis time-course served to corroborate data prevously obtained, but the ions at m/z 1405, 1201, 1129 and 925 were essential to the full sequence determination of the molecule. These data are fully compatible with structure (II).

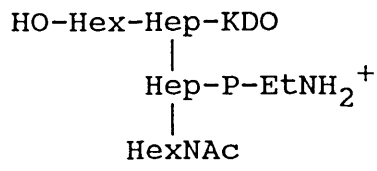



(II)

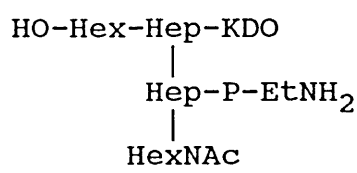
**TABLE 4.6.** Possible structures of ions observed in the methanolysis time course of L4-F-I (6).

| ION | COMPOSITION |
|---|---|
| 1868 | HO-HexNAc-Hex-Hex-Hep-KDO<br>\|<br>Hep-P-$EtNH_2^+$<br>\|<br>HexNAc |
| 1854 | HO-HexNAc-Hex-Hex-Hep-KDO<br>\|<br>Hep-P-$EtNH_2$<br>\|<br>HexNAc |
| 1808 | m/z 1854 KDO rearrangement |
| 1782 | Hex-HexNAc-Hex-Hex-Hep-OH<br>\|<br>Hep-P-$EtNH_2$<br>\|<br>HexNAc |
| 1623 | HO-Hex-Hex-Hep-KDO<br>\|<br>Hep-P-$EtNH_2^+$ |
| 1609 | HO-Hex-Hex-Hep-KDO<br>\|<br>Hep-P-$EtNH_2$<br>\|<br>HexNAc |
| 1564 | HO-HexNAc-Hex-Hex-Hep-OH<br>\|<br>Hep-P-$EtNH_2$<br>\|<br>HexNAc |
| 1563 | m/z 1609 KDO rearrangement |

1419

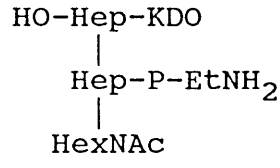



1405

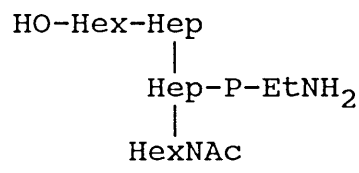



1359 m/z 1405 KDO rearrangement

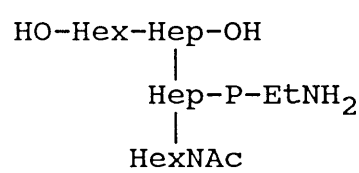
1201



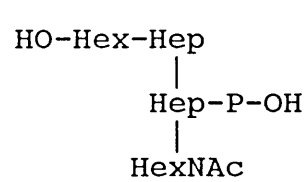

1129



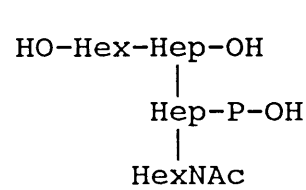

1115



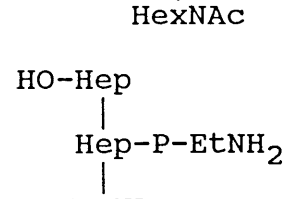

1058



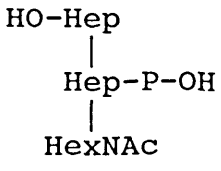

1044



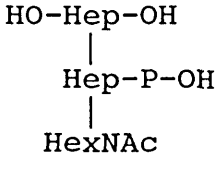

925



854




840



4.2.3. SAMPLE 3 : L5-F-I (5/6)

The negative ion mass spectrum afforded a signal at m/z 1837 consistent with the $[M-H]^-$ Molecular ion of composition $Hex_5HexNAc_2Hep_2KDO$. A further signal observed at m/z 1675 of approximately half the intensity of m/z 1837 is consistent with either the $[M-H]^-$ Molecular ion of composition $Hex_4HexNAc_2Hep_2KDO$ or the product of a $\beta$-cleavage of m/z 1837 with subsequent "loss" of a hexose residue. Additionally signals were observed at m/z 1819 and 1657 consistent with the dehydrated forms of the species observed at m/z 1837 and 1675.

The positive ion native spectrum afforded only two ions at m/z 1861 and 1839 consistent with $[M+H]^+$ and $[M+Na]^+$ Molecular ions of composition $Hex_5HexNAc_2Hep_2KDO$. No ion was present at m/z 1677 therefore confirming that the signal observed in the negative ion spectrum at m/z 1675 is due to a $\beta$-cleavage.

As no acetate groups or other non-carbohydrate moieties are present in this molecule the deuterioacetylation derivative was not prepared.

The permethyl spectrum afforded a $[M+H]^+$ Molecular ion at m/z 2329 consistent with the composition $Hex_5HexNAc_2Hep_2KDO$. No ion was observed at m/z 2125 indicating that there is no $Hex_4HexNAc_2Hep_2KDO$ component present. Providing further confirmation that the ion observed at m/z 1675 in the negative ion native spectrum is due to a $\beta$-cleavage.

A-type fragment ions were observed at m/z 872, 712, 668, 464, 260 and 219 of composition $Hex_3HexNAc$, $Hex_1HexNAc_1Hep$, $Hex_2HexNAc$, $Hex_1HexNAc$, HexNAc and Hex.

The permethylation data indicates the presence of two branches

Hex - HexNAc - Hex - Hex -

and

HexNAc - (Hex, Hep) -

To obtain the complete structure, methanolysis-FAB-MS was carried out with aliquots taken after 2, 20 and 40 minutes heating at 40° C and a further 5, 30, 60 and 120 minutes heating at 60° C. The ions observed in this time course are listed with their compositions in TABLE 4.7.

The progress of the time course carried out on L5-F-I (5/6) was significantly different from those of L3-F-II (4) and L4-F-I (6), samples 1 and 2. No ions were observed with a composition containing KDO and the highest mass ion observed (m/z 1386) is the product of hydrolysis with the resultant "loss" of Hex-HexNAc as well as KDO. This difference in behaviour under the methanolysis conditions may be a result of structural differences.

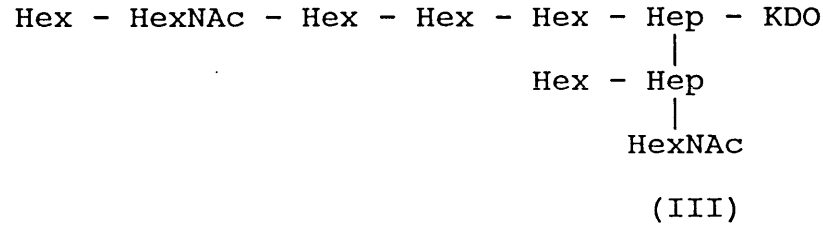
The possible structures of each ion observed in the methanolysis are listed in TABLE 4.8.

The data obtained from the methanolysis experiment served to coroborate that obtained from the native permethyl and deuterioacetyl derivatives. The ions

**TABLE 4.7.** Summary of ions observed during the methanolysis of L5-F-I (5/6).

| ION | | COMPOSITION |
|---|---|---|
| 1386 | $[M+H]^+$ | $HO\text{-}Hex_3HexNAc_1Hep_2$ |
| 1372 | $[M+H]^+$ | $HO_2\text{-}Hex_3HexNAc_1Hep_2$ |
| 1342 | $[M+H]^+$ | $HO\text{-}Hex_4HexNAc_1Hep_1$ |
| 1182 | $[M+H]^+$ | $HO\text{-}Hex_2HexNAc_1Hep_2$ |
| 1168 | $[M+H]^+$ | $HO_2\text{-}Hex_2HexNAc_1Hep_2$ |
| 978 | $[M+H]^+$ | $HO\text{-}Hex_1HexNAc_1Hep_2$ |
| 964 | $[M+H]^+$ | $HO_2\text{-}Hex_1HexNAc_1Hep_2$ |
| 760 | $[M+H]^+$ | $HO_2\text{-}HexNAc_1Hep_2$ |
| 496 | $[M+CH_3]^+$ | $Hex_1HexNAc_1$ |
| 494 | | $HO\text{-}HexNAc_1Hep$ |

observed at m/z 1342 and 760 were important in making final structural conclusions. The data being fully consistent with structure (III).




(III)

**TABLE 4.8.** Summary of possible structures for ions observed during the methanolysis of L5-F-I (5/6).

| ION | STRUCTURE |
|---|---|
| 1386 | HO-Hex-Hex-Hep<br>\|<br>Hex-Hep<br>\|<br>HexNAc |
| 1372 | HO-Hex-Hex-Hex-Hep<br>\|<br>HO-Hep<br>\|<br>HexNAc |
| 1342 | Hex-HexNAc-Hex-Hex-Hex-Hep<br>\|<br>OH |
| 1182 | HO-Hex-Hep<br>\|<br>Hex-Hep<br>\|<br>HexNAc |
| 1168 | HO-Hex-Hex-Hep<br>\|<br>HO-Hep<br>\|<br>HexNAc |
| 978 | HO-Hep<br>\|<br>Hex-Hep<br>\|<br>HexNAc |
| 964 | HO-Hex-Hep<br>\|<br>HO-Hep<br>\|<br>HexNAc |

760 HO-Hep
|
HO-Hep
|
HexNAc

496 Hex-HexNAc

494 HO-Hep (oxonium ion)
|
HexNAc

4.2.4. SAMPLE 4 : L5-F-III (3)

The negative ion spectrum afforded signals at m/z 1352 and 1310 consistent with $[M-H]^-$ Molecular ions. Both these ions had associated signals 18 amu lower at m/z 1334 and 1292 consistent with their dehydrated equivalents. A very minor component afforded signals at m/z 1190 and 1148 consistent with $[M-H]^-$ Molecular ions, with the lactonised equivalents affording signals at m/z 1172 and 1130. Alternativeley these signals could be due to a non-reducing terminal $\beta$-cleavage resulting in the "loss" of a hexose residue.

The positive ion spectrum, figure 4.3. of the native material afforded $[M+H]^+$ and $[M+Na]^+$ molecular ions at m/z 1312, 1354 and 1334, 1376. Ions were observed at m/z 1294 and 1336 consistent with being the 1-4 lactonised KDO form of the species affording the ions at m/z 1312 and 1354 respectively. Since signals are observed in both the negative and positive native spectra 18 amu. lower than the molecular ions and are consistent with being due to a KDO 1 - 4 lactone. The signals observed at m/z 1402, 1424, 1444 and 1466 are rationalised as thioglycerol adducts, which have formed with the lactonised species. Such thioglycerol adducts have been observed in spectra of unsaturated glycolipids. No signals were observed in the positive ion spectrum to indicate the presence of a component of composition $Hex_2HexNAc_1Hep_2KDO$. Indicating that the series of ions observed in the negative ion

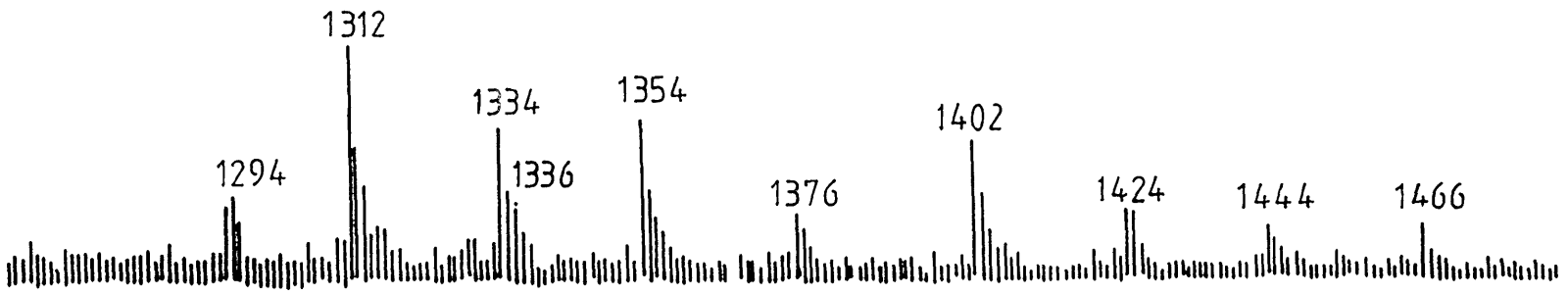



Figure 4.3. Positive ion FAB spectrum of native L5-F-III (3) LPS core oligosaccharide from Neisseria meningitidis.

**TABLE 4.9.** Summary of ions observed in the positive and negative spectra of native L5-F-III (3).

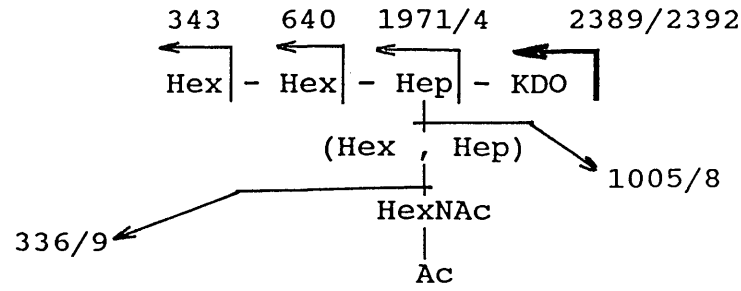
| MOLECULAR IONS | | COMPOSITIONS |
|---|---|---|
| NEGATIVE ION | | |
| 1352 | $[M-H]^-$ | $Hex_3HexNAc_1Hep_2KDO_1Ac_1$ |
| 1334 | $[M-H]^-$ | lactonised m/z 1352 |
| 1310 | $[M-H]^-$ | $Hex_3HexNAc_1Hep_2KDO$ |
| 1292 | $[M-H]^-$ | lactonised m/z 1310 |
| 1190 | $[M-H]^-$ | $Hex_2HexNAc_1Hep_2KDO_1Ac_1$ |
| 1172 | $[M-H]^-$ | Lactonised m/z 1190 |
| 1148 | $[M-H]^-$ | $Hex_2HexNAc_1Hep_2KDO$ |
| 1130 | $[M-H]^-$ | Lactonised m/z 1148 |
| POSITIVE ION | | |
| 1466 | $[M+thio+Na]^+$ | lactonised m/z 1376 |
| 1444 | $[M+thio+H]^+$ | lactonised m/z 1354 |
| 1424 | $[M+thio+Na]^+$ | lactonised m/z 1334 |
| 1402 | $[M+thio+H]^+$ | lactonised m/z 1312 |
| 1376 | $[M+Na]^+$ | $Hex_3HexNAc_1Hep_2KDO_1Ac_1$ |
| 1354 | $[M+H]^+$ | $Hex_3HexNAc_1Hep_2KDO_1Ac_1$ |
| 1336 | $[M+H]^+$ | lactonised m/z 1354 |
| 1334 | $[M+Na]^+$ | $Hex_3HexNAc_1Hep_2KDO_1$ |
| 1312 | $[M+H]^+$ | $Hex_3HexNAc_1Hep_2KDO_1$ |
| 1294 | $[M+H]^+$ | lactonised m/z 1312 |

native spectrum at m/z 1190, 1172, 1148 and 1130 were the result of $\beta$-cleavage ions. The data from the negative and positive ion spectra are summarised in TABLE 4.9.

To afford sequence and acetate location data the perdeuterioacetyl derivative was obtained and a FAB mass spectrum recorded. $[M+H]^+$ molecular ions were observed at 2389 and 2392, additionally oxonium ions of the same composition were observed at m/z 2326 and 2329. There were also ions present at m/z 2281/2284 and 2344/2347 that were rationalised as being due to one degree of under-deuterioacetylation occurring on the oxonium and $[M+H]^+$ molecular ions respectively. A-type fragment ions were observed at m/z 1971/1974 1005/1008 640 , 343 and 336/339 . A signal observed at m/z 1026 is not consistent with any expected fragmentation pathway and remains unassigned. The data afforded by the deuterioacetyl spectrum is summarised in Table 4.10. The doublets of signals observed enable the level of natural O-acetylation and the residue location of the acetate to be determined. The terminal HexNAc residue is the site of O-acetylation with approximately 40% of the sample carrying an acetate.

The data from the native and deuterioacetyl spectra allow the structure (IV) to be determined.

The deuterioacetyl data is insufficient to determine the full structure of the molecule, with the sequence of the bracketed hexose and heptose residues still unknown.




(IV)

The permethyl derivative of L5-F-II (3) was prepared, and a FAB spectrum obtained figure 4.4. $[M+H]^+$ molecular ions were observed at m/z 1676 and 1630 consistent with the compositions $Hex_3HexNAc_1Hep_2KDO_1$ and the lactonised form of $Hex_3HexNAc_1Hep_2KDO_1$ respectively. A further ion was observed at m/z 1690 consistent the ion at m/z 1676 having undergone C-methylation. At m/z 1560 a molecular ion corresponding to the ring cleaved molecular ion at m/z 1676, was also present, corroborating the assignment of a reducing terminal KDO. The other high mass ions observed at m/z 1616, 1662 and 1644 were due to ions resulting from one degree of undermethylation and loss of MeOH respectively. One further $[M+H]^+$ molecular ion was observed at m/z 947, consistent with the composition $Hex_2Hep_1KDO$ which has undergone an elimination of MeOH. This ion would result from a $\beta$-cleavage elimination of the branch terminating in HexNAc. This type of cleavage is not usually as clearly observed in permethylated molecules,

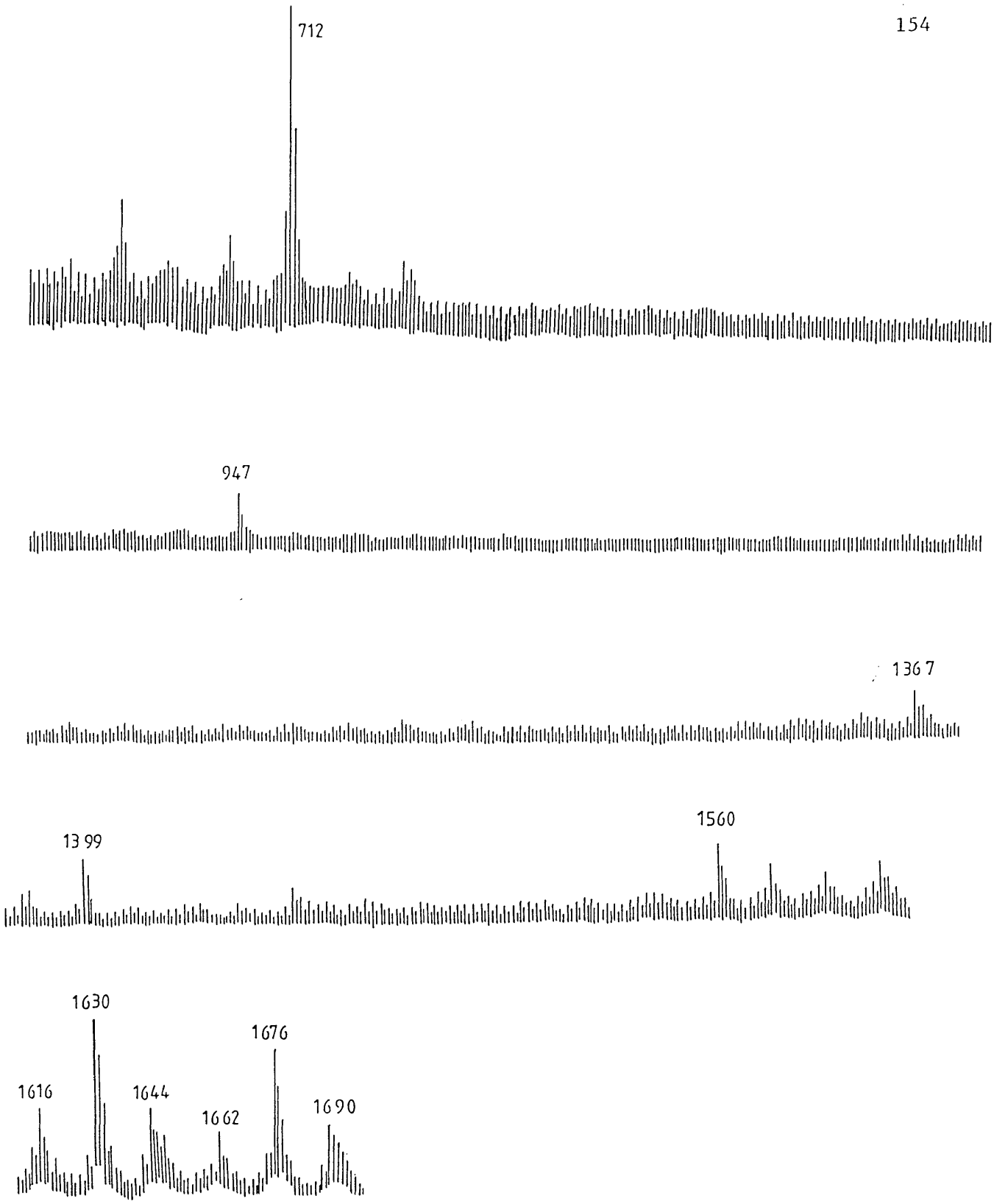



Figure 4.4. Positive ion FAB spectrum of permethylated L5-F-III (3) LPS core oligosaccharide.

**TABLE 4.10.** Summary of ions observed in the spectrum of the deuterioacetyl derivative of L5-F-III (3)

| MOLECULAR IONS | COMPOSITIONS |
|---|---|
| 2389/2392 | $Hex_3HexNAc_1Hep_2KDO_1Ac_{1/0}$ |
| 2344/2347 | 2392/2389 (under-deuterioacetylated) |
| 2326/2329 | $Hex_3HexNAc_1Hep_2KDO_1Ac_{1/0}$ (oxonium ion) |
| 2281/2284 | 2326/2329 (under-deuterioacetylated) |
| **FRAGMENT IONS** | **COMPOSITIONS** |
| 1971/1974 | $Hex_3HexNAc_1Hep_2Ac_{1/0}$ |
| 1005/1008 | $Hex_1HexNAc_1Hep_1Ac_{1/0}$ |
| 640 | $Hex_2$ |
| 343 | $Hex_1$ |
| 336/339 | $HexNAx_1Ac_{1/0}$ |

due to the preferred fragmentation pathways derivatised carbohydrates follow and this
explains why it is a minor signal. The molecular ion observed at m/z 1399 is consistent with the composition $Hex_3HexNAc_1Hep_2Pent$. An A-type fragment ion was observed at m/z 745 ($Hex_1HexNAc_1Hep_1$).

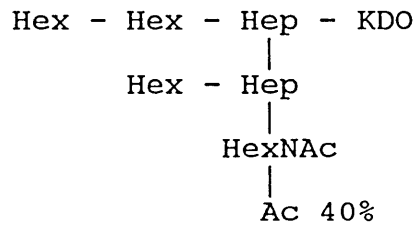
In order to obtain full sequence and branch data a methanolysis/FAB-MS study was carried out on the perdeuteriomethylated material, with aliquots being taken after 5, 10, 20 and 40 minutes heating at 40°C and a further 5, 10, and 40 minutes heating at 60° C. The methanolysis data are summarised in TABLE 4.11. The signals observed at m/z 1233, 1020 and 1003 derive from molecular species that have undergone a reducing end methanolytic cleavage, resulting in the loss of the reducing terminal KDO residue. This can be deduced from the fact that the ions are 3 amu lower than that expected for fully deuteriomethylated species. The signal at m/z 1236 is the result of methanolytic degredation of a molecule in which the reducing terminal KDO residue has been 'cleaved' during derivatisation. Thus the ion at m/z 1236 contains a terminal deuteriomethyl glycoside. The ion observed at m/z 1006 is due to a methanolytic cleavage of the ion observed at m/z 1236, resulting in the 'loss' of a terminal hexose residue. Two other molecular ions are observed at m/z 790 and 547 consistent with the compositions $HO_2$-$HexNAc_1Hep_2$ and HO-$HexNAc_1Hep$. A-type

**TABLE 4.11.** Summary of ions observed in the methanolysis/FAB-MS study of L5-F-III (3).

| MOLECULAR IONS | COMPOSITIONS |
|---|---|
| 1236 | $HO\text{-}Hex_2HexNAc_1Hep_2\text{-}OD_3$ |
| 1233 | $HO\text{-}Hex_2HexNAc_1Hep_2$ |
| 1020 | $HO\text{-}Hex_1HexNAc_1Hep_2$ |
| 1006 | $HO_2Hex_1HexNAc_1Hep_2\text{-}OD_3$ |
| 1003 | $HO_2Hex_1HexNAc_1Hep_2$ |
| 790 | $HO_2\text{-}HexNAc_1Hep_2$ |
| 547 | $HO\text{-}HexNAc_1Hep_1$ |
| **FRAGMENT IONS** | **COMPOSITIONS** |
| 1201 | $HO\text{-}Hex_2HexNAc_1Hep_2$ |
| 988 | $HO\text{-}Hex_1HexNAc_1Hep_2$ |
| 971 | $HO_2\text{-}Hex_1HexNAc_1Hep_2$ |
| 745 | $Hex_1HexNAc_1Hep$ |
| 515 | $HO\text{-}HexNAc_1Hep$ |

fragment ions were observed at m/z 1201, 988, 871, 745 and 515 of composition HO-$Hex_2HexNAc_1Hep_2$, HO-$Hex_1HexNAc_1Hep_2$, $HO_2$-$Hex_2HexNAc_1Hep_2$, $Hex_1HexNAx_1Hep_1$ and HO-$HexNAc_1Hep$. additionally 2 ions were observed at m/z 790 and 515 of composition $HO_2$-$HexNAc_1Hep_2$ and HO-$HexNAc_1Hep_1$ repsectively. An ion observed at m/z 1162 remains unassigned. TABLE 4.12. presents the structures each ion, observed throughout the time course, may represent.

The data from the deuterioacetyl and methanolysis/FAB-MS experiments allow the structure (V) to be determined, the signal observed during the time-course at m/z 547 provided the final information to enable a complete sequence to be deduced.

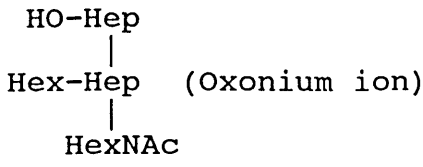



(V)

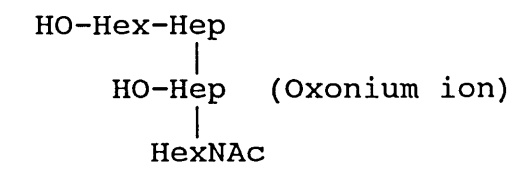
**TABLE 4.12.** Summary of possible structures the ions, observed during methanolysis/FAB-MS of L5-F-III (3).

| ION | STRUCTURE | |
|---|---|---|
| 1236 | HO-Hex-Hep-OD$_3$C<br>\|<br>Hex-Hep<br>\|<br>HexNAc | Hex-Hex-Hep-OD$_3$C<br>\|<br>HO-Hep<br>\|<br>HexNAc |
| 1233 | HO-Hex-Hep<br>\|<br>Hex-Hep<br>\|<br>HexNAc | Hex-Hex-Hep<br>\|<br>HO-Hep<br>\|<br>HexNAc |
| 1201 | HO-Hex-Hep<br>\|<br>Hex-Hep<br>\|<br>HexNAc | (Oxonium ion) |
| | Hex-Hex-Hep<br>\|<br>HO-Hep<br>\|<br>HexNAc | (Oxonium ion) |
| 1020 | HO-Hep<br>\|<br>Hex-Hep<br>\|<br>HexNAc | |
| 1006 | HO-Hex-Hep-OD$_3$C<br>\|<br>HO-Hep<br>\|<br>HexNAc | |
| 1003 | HO-Hex-Hep<br>\|<br>HO-Hep<br>\|<br>HexNAc | |

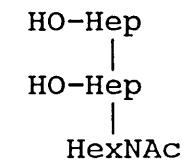
988



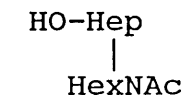

971



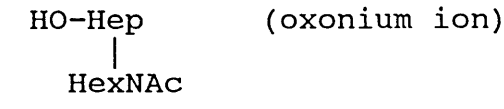

790




547




515



4.2.5. SAMPLE 5 : L5-F-II (3)

The negative ion spectrum of the native material afforded two clusters of ions. The cluster at higher mass afforded $[M-H]^-$ Molecular ions at m/z 1514 and 1472 . Also present were ions 18 amu lower at m/z 1496 and 1454 consistent with the lactonised forms of these two components. Two further signals were observed at m/z 1410 and 1426 which do not correspond to any related saccharide composition. The cluster at lower mass afforded signals approximately twice as intense as those at higher mass. Signals were present at m/z 1352 and 1310 consistent with $[M-H]^-$ Molecular ions both of these signals had associated ions 18 amu lower at m/z 1334 and 1292 consistent with their lactonised forms. Additionally $[M+Na-H]^-$ ions were observed at m/z 1374, 1356, 1332 and 1314 consistent with the sodium adduct of the ions present at m/z 1352, 1334, 1310 and 1292.

A further component afforded ions at m/z 1306 and 1264 consistent with $[M-H]^-$ Molecular ions. There was also an ion observed at m/z 1328 consistent with the $[M+NA-H]^-$ Molecular ion of the same composition, though no signals were present consistent with the lactone form of this component. The data from this spectrum are summarised in TABLE 4.13.

The positive ion native spectrum afforded a complex series of signals in which all ions observed existed as $[M+Na]^+$ or $[M+2Na]^+$ Molecular ions. The signals were in

**TABLE 4.13.** Summary of signals observed in the negative ion spectrum of native L5-F-II (3).

| ION | | COMPOSITION |
|---|---|---|
| 1514 | $[M-H]^-$ | $Hex_4HexNAc_1Hep_2KDO_1Ac_1$ |
| 1496 | $[M-H]^-$ | Lactonised m/z 1514 |
| 1472 | $[M-H]^-$ | $Hex_4HexNAc_1Hep_2KDO$ |
| 1454 | $[M-H]^-$ | Lactonised m/z 1472 |
| 1374 | $[M+Na-H]^-$ | $Hex_3HexNAc_1Hep_2KDO_1Ac_1$ |
| 1356 | $[M+Na-H]^-$ | Lactonised m/z 1352 |
| 1352 | $[M-H]^-$ | $Hex_3HexNAc_1Hep_2KDO_1Ac_1$ |
| 1334 | $[M-H]^-$ | Lactonised m/z 1352 |
| 1332 | $[M+Na-H]^-$ | $Hex_3HexNAc_1Hep_2KDO$ |
| 1328 | $[M+Na-H]^-$ | $Hex_3HexNAc_1Hep_1DeoxyHex_1KDO_1Ac_1$ |
| 1314 | $[M+Na-H]^-$ | Lactonised m/z 1310 |
| 1310 | $[M-H]^-$ | $Hex_3HexNAc_1Hep_2KDO$ |
| 1306 | $[M-H]^-$ | $Hex_3HexNAc_1Hep_1DeoxyHex_1KDO_1Ac_1$ |
| 1292 | $[M-H]^-$ | Lactonised m/z 1310 |
| 1286 | $[M+Na-H]^-$ | $Hex_3HexNAc_1Hep_1DeoxyHex_1KDO$ |
| 1264 | $[M-H]^-$ | $Hex_3HexNAc_1Hep_1DeoxyHex_1KDO$ |

two clusters as observed in the negative ion spectrum. The high mass cluster afforded $[M+Na]^+$ Molecular ions at m/z 1538 and 1496. The signals observed at m/z 1560 and 1518 are $[M+2Na]^+$ Molecular ions of the same composition. All four of the above ions have an associated ion 18 amu lower consistent with the lactonised equivalents at m/z 1542, 1520, 1500 and 1478. There were additionally two signals observed at m/z 1628 and 1586 consistent with thioglycerol adducts of the ions at m/z 1520 and 1478. Such thioglycerol adducts have been observed before in the spectra of unsaturated glycolipids. The low mass cluster afforded ions at m/z 1376 and 1334 consistent with $[M+Na]^+$ Molecular ions. Both of these signals had associated ions 18 amu lower at m/z 1358 and 1316 consistent with the lactonised equivalents. All four of these signals had associated ions 22 amu higher consistent with the $[M+2Na]^+$ Molecular ions of corresponding composition. Two signals were present at m/z 1466 and 1424 consistent with $[M+Na]^+$ thioglycerol adducts of composition $Hex_3HexNAc_1Hep_2KDO_1Ac_1$ and $Hex_3HexNAc_1Hep_2KDO$ respectively.

Two further signals were observed at m/z 1330 and 1288 consistent with $[M+Na]^+$ Molecular ions. The signal at m/z 1310 is consistent with the $[M+2Na]^+$ equivalent of m/z 1288. The signals observed in this specrum are summarised in TABLE 4.14.

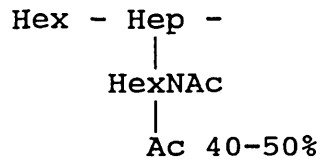
No signals were observed at m/z 1428 and 1412 or 1450 and 1434 for $[M+H]^+$ or $[M+Na]^+$ Molecular ions equivalent

**TABLE 4.14.** Summary of signals observed in the positive ion spectrum of native L5-F-II (3).

| ION | | COMPOSITION |
|---|---|---|
| 1628 | $[M+thio+Na]^+$ | Lactonised m/z 1538 |
| 1586 | $[M+thio+Na]^+$ | Lactonised m/z 1496 |
| 1560 | $[M+2Na]^+$ | $Hex_4HexNAc_1Hep_2KDO_1Ac_1$ |
| 1542 | $[M+2Na]^+$ | Lactonised m/z 1538 |
| 1538 | $[M+Na]^+$ | $Hex_4HexNAc_1Hep_2KDO_1Ac_1$ |
| 1520 | $[M+Na]^+$ | Lactonised m/z 1538 |
| 1518 | $[M+2Na]^+$ | $Hex_4HexNAc_1Hep_2KDO$ |
| 1500 | $[M+2Na]^+$ | Lactonised m/z 1496 |
| 1496 | $[M+Na]^+$ | $Hex_4HexNAc_1Hep_2KDO$ |
| 1478 | $[M+Na]^+$ | Lactonised m/z 1496 |
| 1466 | $[M+thio+Na]^+$ | Lactonised m/z 1376 |
| 1424 | $[M+thio+Na]^+$ | Lactonised m/z 1334 |
| 1398 | $[M+2Na]^+$ | $Hex_3HexNAc_1Hep_2KDO_1Ac_1$ |
| 1376 | $[M+Na]^+$ | $Hex_3HexNAc_1Hep_2KDO_1Ac_1$ |
| 1358 | $[M+Na]^+$ | Lactonised m/z 1376 |
| 1334 | $[M+Na]^+$ | $Hex_3HexNAc_1Hep_2KDO$ |
| 1330 | $[M+Na]^+$ | $Hex_3HexNAc_1Hep_1DeoxyHex_1KDO_1Ac_1$ |
| 1316 | $[M+Na]^+$ | Lactonised m/z 1334 |
| 1310 | $[M+2Na]^+$ | $Hex_3HexNAc_1Hep_1DeoxyHex_1KDO$ |
| 1288 | $[M+Na]^+$ | $Hex_3HexNAc_1Hep_1DeoxyHex_1KDO$ |

to the two signals observed in the negative ion spectrum at m/z 1426 and 1410. This indicates that these two signals (m/z 1426 and 1410) are not sample derived or from a component similar in FAB mass spectrometric behaviour to the sample. No signals were observed at m/z 1312 or 1270 consistent with the lactone form of the component of composition $Hex_3HexNAc_1Hep_1DeoxyHex_1KDO_1Ac_{1/0}$. This may mean that the KDO in this component is linked at position 4 thus preventing formation of the lactone.

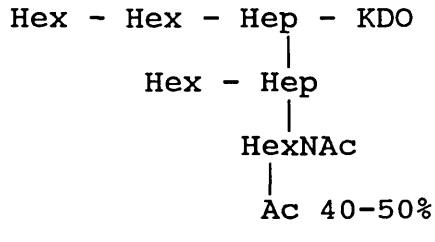
The deuterioacetyl derivative was prepared and a spectrum obtained. $[M+H]^+$ Molecular ion pairs were observed at m/z 2689 / 2686, 2392 / 2389 and 2256 / 2253 of composition $Hex_4HexNAc_1Hep_2KDO_1Ac_{0/1}$, $Hex_3HexNAc_1Hep_2KDO_1Ac_{0/1}$ and $Hex_3HexNAc_1Hep_1DeoxyHex_1KDO_1Ac_{0/1}$ respectively. The intensiites of the signals indicate that 40 - 50% of the molecules are O-acetylated. A-type fragment ions were observed at m/z 1008/1005, 937, 640, 343, 339 and 336, consistent with the compositions $Hex_1HexNAc_1Hep_1Ac_{0/1}$, $Hex_3$, $Hex_2$, Hex, HexNAc and $HexNAc_1Ac_1$. These signals indicated that the O-acetate is sited on the terminal HexNAc exclusively. Additionally since no signals were observed at m/z 636 ($Hex_1HexNAc$), or 711 ($HexNAc_1Hep$), the branch containing the terminal HexNAc must have the following structure (VI).



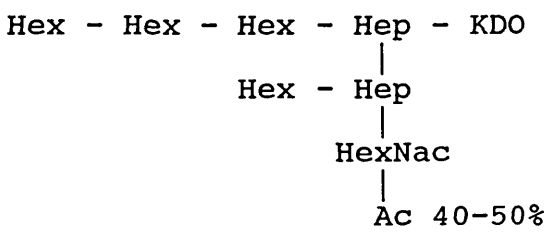

(VI)

The permethyl derivative was prepared and the spectrum obtained. This spectrum afforded signals at m/z 1604 and 1400 consistent with $[M+H]^+$ Molecular ions of composition $Hex_4HexNAc_1Hep_2$ and $Hex_3HexNAc_1Hep_2$. Both of these signals had an associated ion 14 amu lower at m/z 1590 and 1386 consistent with their undermethylated counterparts. No signals were present at m/z 1880 or 1676 of composition $Hex_4HexNAc_1Hep_2$ and $Hex_3HexNAc_1Hep_2$, suggesting that during the course of the permethylation the molecules have undergone degredation with the "loss" of the reducing terminal KDO residue. This process has been previously observed in the permethyl spectra of sample 4 L5 F III (3). A signal was observed at m/z 1588 consistent with the $[M+H]^+$ Molecular ion for undermethylated $Hex_3HexNAc_1Hep_1DeoxyHex_1KDO$. This molecule appears to react very differently under permethylation conditions than the other components. It seems to form the undermethylated species exclusively and retains the KDO residue. No signals were observed at m/z 1556 and 1486 for "minus 46" and "minus 116". In both the positive and negative ion native spectra no signals were observed consistent with the dehydrated form of this component.

These data may indicate that the KDO is not the reducing terminal residue and may also be branched or substituted at position 4. A-type fragment ions were observed at m/z 712, 260 and 219 of composition $Hex_1HexNAc_1Hep$, HexNAc and Hex. No ion was observed at m/z 508 ($HexNAc_1Hep$), thus confirming the structure proposed for the HexNAc containing branch (VI). These data are fully consistent with the structures (VII and VIII).




(VII)




(VIII)

4.2.6. SAMPLE 6 : L2-F-II (1)

The native negative ion spectrum afforded $[M-H]^-$ molecular ions at m/z 1840 and 1798. Both these ions were accompanied by signals 22 amu higher at m/z 1862 and 1820 consistent with $[M+Na-H]^-$ molecular ions of the same composition. Additionally two further ions were observed 18 amu lower at m/z 1822 & 1780 consistent with dehydrated forms of the species observed at m/z 1862 and 1820.

The positive ion spectrum of the native material afforded only two ions, at m/z 1842 and 1800 consistent with $[M+H]^+$ molecular ions. The positive and negative ion data of the native material are summarised in TABLE 4.15.

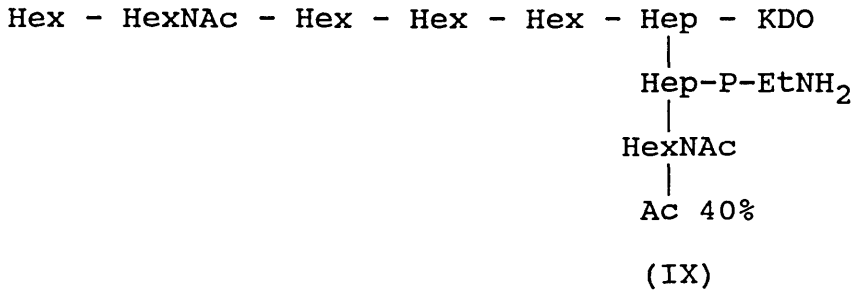
The deuterioacetyl derivative was prepared in order to facilitate sequencing and to locate the O-acetate group. A-type fragment ions were present at m/z 933, 636, 343, 339 and 336. The relative intensities of m/z 336 and 339 indicate that an O-acetate is carried on the non-reducing terminal HexNAc in 40% of molecules.

To obtain further sequence data the permethyl derivative was obtained. The spectrum afforded $[M+H]^+$ molecular ions at m/z 2276 and at m/z 2244 consistent with the elimination of methanol . A-type fragment ions were observed at m/z 863, 668, 659, 464, 260 and 219. The presence of the ions at m/z 863 and 659 indicate that the sample L2-F II (1) is a mixture of two components, one of which carries a Hexose residue on the branch Heptose. The deuterioacetyl and permethyl data are summarised in

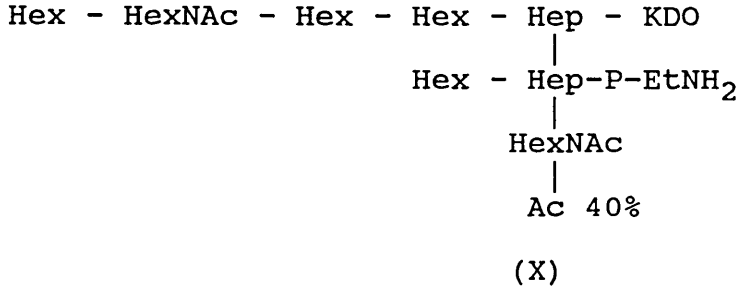
**TABLE 4.15.** Summary of signals observed in the posit negative ion spectra of native L2-F II (1).

| NEGATIVE ION | | |
|---|---|---|
| MOLECULAR IONS | | COMPOSITION |
| 1862 | $[M+Na-H]^-$ | $Hex_4HexNAc_2Hep_2KDO\text{-}P\text{-}EtNH_2Ac_1$ |
| 1840 | $[M-H]^-$ | $Hex_4HexNAc_2Hep_2KDO\text{-}P\text{-}EtNH_2Ac_1$ |
| 1822 | $[M-H]^-$ | dehydrated m/z 1840 |
| 1820 | $[M+Na-H]^-$ | $Hex_4HexNAc_2Hep_2KDO\text{-}P\text{-}EtNH_2$ |
| 1798 | $[M-H]^-$ | $Hex_4HexNAc_2Hep_2KDO\text{-}P\text{-}EtNH_2$ |
| 1780 | $[M-H]^-$ | dehydrated m/z 1798 |
| POSITIVE ION | | |
| MOLECULAR ION | | COMPOSITION |
| 1842 | $[M+H]^+$ | $Hex_4HexNAc_2Hep_2KDO\text{-}P\text{-}EtNH_2Ac_1$ |
| 1800 | $[M+H]^+$ | $Hex_4HexNAc_2Hep_2KDO\text{-}P\text{-}EtNH_2$ |

TABLE 4.16. These data are consistent with the two structures (IX) and (X).




(IX)




(X)

**TABLE 4.16.** Summary of signals observed in the Deuterioacetyl and Permethyl spectra of L2-F II (1).

| DEUTERIOACETYL FRAGMENTS OBSERVED | |
|---|---|
| FRAGMENT ION | COMPOSITION |
| 933 | $Hex_2HexNAc$ |
| 636 | $Hex_1HexNAc$ |
| 343 | Hex |
| 339 | HexNAc |
| 336 | $HexNAc_1Ac_1$ |
| PERMETHYL DATA | |
| MOLECULAR ION | COMPOSITION |
| 2276 $[M+H]^+$ | $Hex_4HexNAc_2Hep_2KDO\text{-}P\text{-}EtNH_2$ |
| 2244 $[M+H]^+$ | m/z 2276- MeOH |
| FRAGMENT IONS | COMPOSITION |
| 863 | $Hex_1HexNAc_1Hep_1\text{-}P\text{-}EtNH_2$ |
| 668 | $Hex_2HexNAc$ |
| 659 | $HexNAc_1Hep_1\text{-}P\text{-}EtNH_2$ |
| 464 | $Hex_1HexNAc$ |
| 260 | HexNAc |
| 219 | Hex |

4.2.7. SAMPLE 7 : L7-F-II (1).

The negative ion native spectrum afforded $[M-H]^-$ Molecular ions at m/z 1516 and 1474. Both of these signals had associated ions 18 amu lower at m/z 1498 and 1456 consistent with the lactonised equivalent.

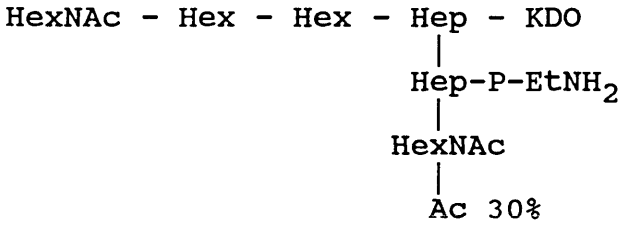
The positive ion spectrum afforded $[M+H]^+$ Molecular ions at m/z 1518 and 1476. The lactonised forms of these two species afforded signals at m/z 1500 and 1458. The $[M+Na]^+$ Molecular ions equivalent to the signals at m/z 1518 and 1476 were observed at m/z 1540 and 1498 respectively. The negative and positive ion native data are summarised in TABLE 4.17.

The deuterioacetyl derivative was prepared and a spectrum obtained. A-type fragment ions were observed at m/z 933, 636, 339 and 336 of composition $Hex_2HexNAc$, $Hex_1HexNAc$, HexNAc and $HexNAc_1Ac_1$ respectively. No signal was observed at m/z 340 indicating that there is no terminal Hexose in the molecule. Since no ions were observed at m/z 930 or 633 for $Hex_2HexNAc_1Ac_1$ and $Hex_1HexNAc_1Ac_1$ the O-acetate is not located on the terminal HexNAc in the hexose branch, but on the non-Hexose linked terminal HexNAc. The relative intensities of the ions at m/z 336 and 339 (0.5 : 1) indicate that 30% of molecules carry an O-acetate. The permethyl spectrum afforded a $[M]^+$ Molecular ion at m/z 1882 of composition $Hex_2HexNAc_2Hep_2KDO\text{-}P\text{-}EtNH_2$, with a signal 32 amu lower at m/z 1850 consistent with the elimination of methanol.

**TABLE 4.17.** Summary of signals observed in the negative and positive ion spectra of L7-F-II (1).

| MOLECULAR IONS | | COMPOSITIONS |
|---|---|---|
| NEGATIVE ION | | |
| 1516 | $[M-H]^-$ | $Hex_2HexNAc_2Hep_2KDO\text{-}P\text{-}EtNH_2Ac_1$ |
| 1498 | $[M-H]^-$ | lactonised m/z 1516 |
| 1474 | $[M-H]^-$ | $Hex_2HexNAc_2Hep_2KDO\text{-}P\text{-}EtNH_2$ |
| 1456 | $[M-H]^-$ | Lactonised m/z 1474 |
| POSITIVE ION | | |
| 1540 | $[M+Na]^+$ | $Hex_2HexNAc_2Hep_2KDO\text{-}P\text{-}EtNH_2Ac_1$ |
| 1518 | $[M+H]^+$ | $Hex_2HexNAc_2Hep_2KDO\text{-}P\text{-}EtNH_2Ac_1$ |
| 1500 | $[M+H]^+$ | lactonised m/z 1518 |
| 1498 | $[M+Na]^+$ | $Hex_2HexNAc_2Hep_2KDO\text{-}P\text{-}EtNH_2$ |
| 1476 | $[M+H]^+$ | $Hex_2HexNAc_2Hep_2KDO\text{-}P\text{-}EtNH_2$ |
| 1458 | $[M+H]^+$ | Lactonised m/z 1476 |

These data are consistent with structure (XI).




(XI)

4.2.8. SAMPLE 8 : L9-F-I (1).

The negative ion spectrum afforded $[M-H]^-$ Molecular ions at m/z 1801 and 1759, consistent with the compositions $Hex_3HexNAc_2Hep_2KDO-(P-EtNH_2)_2Ac_1$ and $Hex_3HexNAc_2Hep_2KDO-(P-EtNH_2)_2$ respectively.

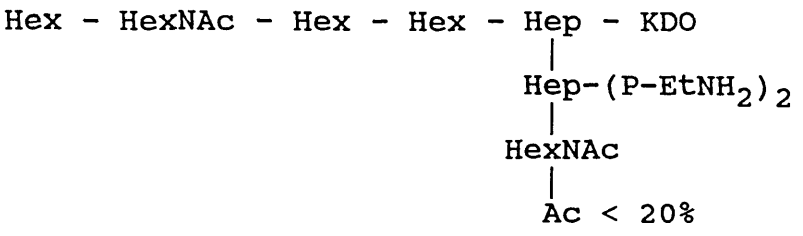
The positive ion native spectrum afforded $[M+H]^+$ Molecular ions at m/z 1803 and 1761 and $[M+Na]^+$ Molecular ions at 1825 and 1783. Additionally signals consistent with $[M+H]^+$ Molecular ions for the dehydrated equivalents were observed at m/z 1785 and 1743. These signals may be due to the formation of a KDO 1 - 4 lactone. The negative and positive ion data are summarised in TABLE 4.18.

The deuterioacetyl derivative afforded A-type ions at m/z 636, 343, 339 and 336 of composition $Hex_1HexNAc$, Hex, HexNAc and $HexNAc_1Ac_1$ respectively. The signal at m/z 336 is not very intense with a significant part of it's intensity due to the matrix signals present at this mass range (see 2.5.2.) Since the intensity of m/z 336 is 25% of that of m/z 339 it is possible only to state that the level of acetylation is less than 20%.

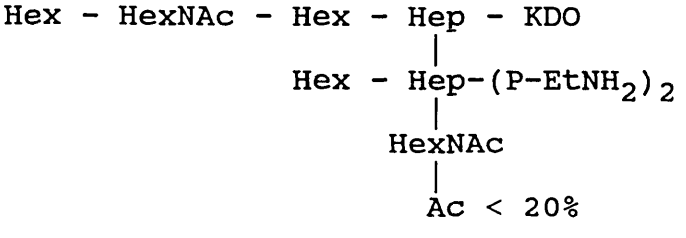
These data define the composition as being $Hex_3HexNAc_2Hep_2KDO-(P-EtNH_2)_2$ with less than 20% of molecules carrying an O-acetate, with the O-acetate located on the terminal HexNAc. The data obtained is consistent with either of two structures (XII) and (XIII).

**TABLE 4.18.** Summary of signals observed in the negative and positive ion spectra of L9-F-I (1).

| MOLECULAR IONS | | COMPOSITIONS |
|---|---|---|
| NEGATIVE ION | | |
| 1801 | $[M-H]^-$ | $Hex_3HexNAc_2Hep_2KDO-(P-EtNH_2)_2Ac_1$ |
| 1759 | $[M-H]^-$ | $Hex_3HexNAc_2Hep_2KDO-(P-EtNH_2)_2$ |
| POSITIVE ION | | |
| 1825 | $[M+Na]^+$ | $Hex_3HexNAc_2Hep_2KDO-(P-EtNH_2)_2Ac_1$ |
| 1803 | $[M+H]^+$ | $Hex_3HexNAc_2Hep_2KDO-(P-EtNH_2)_2Ac_1$ |
| 1785 | $[M+H]^+$ | dehydrated m/z 1803 |
| 1783 | $[M+Na]^+$ | $Hex_3HexNAc_2Hep_2KDO-(P-EtNH_2)_2$ |
| 1761 | $[M+H]^+$ | $Hex_3HexNAc_2Hep_2KDO-(P-EtNH_2)_2$ |
| 1743 | $[M+H]^+$ | dehydrated m/z 1761 |


Hex - HexNAc - Hex - Hex - Hep - KDO
Hep-(P-EtNH2)2
HexNAc
Ac < 20%

(XII)


Hex - HexNAc - Hex - Hep - KDO
Hex - Hep-(P-EtNH2)2
HexNAc
Ac < 20%

(XIII)

4.2.9. SAMPLE 9 : L3-F-I (4)

The negative ion native spectrum afforded $[M-H]^-$ Molecular ions at m/z 1678 and 1636. Both these ions have an associated signal 18 amu lower at m/z 1660 and 1618 consistent with their lactonised forms.

The positive ion spectrum of the native material afforded two signals at m/z 1680 and 1638 consistent with $[M+H]^+$ Molecular ions. Additionally signals were observed at m/z 1660 and 1620 consistent with the $[M+Na]^+$ Molecular ion and the lactonised form of the component affording the ion at m/z 1638. The negative and positive ion data obtained on the native material are summarised in TABLE 4.19.

The deuterioacetyl derivative was prepared to locate the O-acetate. The spectrum obtained afforded A-type fragment iona at m/z 933, 636, 343, 339 and 336 of composition $Hex_2HexNAc$, $Hex_1HexNAc$, Hex, HexNAc and $HexNAc_1Ac_1$ respectively. The ratio of the signals observed at m/z 336 to 339 (0.2 : 1) indicates that 15% of the terminal HexNAc carry an O-acetate.

The permethyl derivative was prepared and Molecular ion signals were observed at m/z 2072 and 2086 consistent with the $[M+H]^+$ ion and the $[M]^+$ mono-overmethylated ion. Another signal was present at m/z 2058 consistent with undermethylation of the species observed at m/z 2072. The signals at m/z 2040 and 2026 are consistent with the rearranged KDO forms of m/z 2086 and 2072 respectively,

**TABLE 4.19.** Summary of data obtained from the negative and positive ion spectra of native L3-F-I (4).

| NEGATIVE ION | | |
|---|---|---|
| MOLECULAR IONS | | COMPOSIITON |
| 1678 | $[M-H]^-$ | $Hex_3HexNAc_2Hep_2KDO\text{-}P\text{-}EtNH_2Ac_1$ |
| 1660 | $[M-H]^-$ | Lactonised m/z 1678 |
| 1658 | $[M+Na-H]^-$ | $Hex_3HexNAc_2Hep_2KDO\text{-}P\text{-}EtNH_2$ |
| 1636 | $[M-H]^-$ | $Hex_3+HexNAc_2Hep_2KDO\text{-}P\text{-}EtNH_2$ |
| 1618 | $[M-H]^-$ | Lactonised m/z 1636 |
| POSITIVE ION | | |
| MOLECULAR ION | | COMPOSITION |
| 1680 | $[M+H]^+$ | $Hex_3HexNAc_2Hep_2KDO\text{-}P\text{-}EtNH_2Ac_1$ |
| 1660 | $[M+Na]^+$ | $Hex_3HexNAc_2Hep_2KDO\text{-}P\text{-}EtNH_2$ |
| 1638 | $[M+H]^+$ | $Hex_3HexNAc_2Hep_2KDO\text{-}P\text{-}EtNH_2$ |
| 1620 | $[M+H]^+$ | Lactonised m/z 1638 |

While the ions observed at m/z 1970 and 1756 are consistent with the $[M]^+$ and $[M+H]^+$ Molecular ion of composition $Hex_3HexNAc_2Hep_2$-P-$EtNH_2$ where the KDO has undergone a ring cleavage. One further ion was observed at m/z 1810 consistent with the $[M]^+$ Molecular ion of composition $Hex_3HexNAc_2Hep_2$-P-$EtNH_2$. A-type fragment ions were observed at m/z 464, 260 and 219 of composition $Hex_1HexNAc$, HexNAc and Hex respectively.

The data obtained from the permethyl spectrum are summarised in Table 4.4. and are consistent with the structure (XIV).



**TABLE 4.20.** Summary of data obtained from the permethyl spectrum of L3-F-I (4).

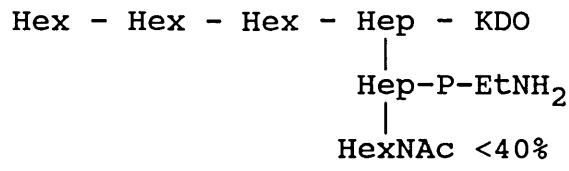
| MOLECULAR IONS | | COMPOSIITON |
|---|---|---|
| 2086 | $[M+CH_3]^+$ | $Hex_3HexNAc_2Hep_2KDO\text{-}P\text{-}EtNH_2$ |
| 2072 | $[M+H]^+$ | $Hex_3HexNAc_2Hep_2KDO\text{-}P\text{-}EtNH_2$ |
| 2058 | $[M+H]^+$ | Undermethylated m/z 2072 |
| 2040 | $[M+H]^+$ | m/z 2086 KDO rearrangement |
| 2026 | $[M+H]^+$ | m/z 2072 KDO rearrangement |
| 1970 | $[M+H]^+$ | ring cleaved m/z 2086 |
| 1956 | $[M+H]^+$ | ring cleaved m/z 2072 |
| 1810 | $[M+CH_3]^+$ | $Hex_3HexNAc_2Hep_2\text{-}P\text{-}EtNH_2$ |
| FRAGMENT IONS | | COMPOSITION |
| 464 | | $Hex_1HexNAc$ |
| 260 | | HexNAc |
| 219 | | Hex |

4.2.10. SAMPLE 10 : L10-F-II (2).

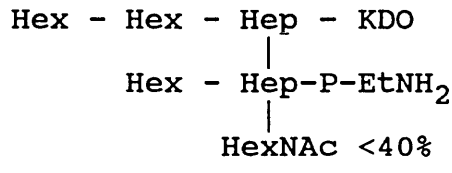
The negative ion spectrum of the native material afforded $[M-H]^-$ Molecular ions at m/z 1475 and 1433 of composition $Hex_3HexNAc_1Hep_2KDO\text{-}P\text{-}EtNH_2Ac_1$ and $Hex_3HexNAc_1Hep_2KDO\text{-}P\text{-}EtNH_2$. signals consistent with the lactonised equivalents were observed at m/z 1457 and 1415 respectively. The relative intensities of the signals at m/z 1475 and 1433 (0.6 : 1) are not a reliable indication of the level of O-acetylation. It is known that the presence of O-acyl groups in carbohydrates enhances the abundance of that component in a FAB spectrum. Therefore it is only possible to conclude that the acetate is present in less than 40% of molecules.

The positive ion mass spectrum afforded $[M+H]^+$ Molecular ions at m/z 1477 and 1435 and $[M+Na]^+$ Molecular ions at m/z 1499 and 1457 of composition $Hex_3HexNAc_1Hep_2KDO\text{-}P\text{-}EtNH_2Ac_1$ and $Hex_3HexNAc_1Hep_2KDO\text{-}P\text{-}EtNH_2$ respectively.The lactonised form of these two components afforded signals at m/z 1459 and 1417.

The permethyl spectrum afforded a $[M+H]^+$ ion at 1841 of composition $Hex_3HexNAc_1Hep_2KDO\text{-}P\text{-}EtNH_2$, with A-type fragment ions at m/z 260 and 219 of composition HexNAc and Hex. These data are consistent with either of the two structures (XV) and (XVI).




(XV)




(XVI)

The acetate that is present in this molecule is probably present on the terminal HexNAc residue as has been observed in all other members of this series of molecules.

## 4.3. Discussion of the results obtained in the examination of LPS core oligosaccharides.

When comparing the data obtained from samples 1 and 2 with that obtained from 3 and 4 a marked difference in behaviour under methanolytic conditions is apparent. In both of the samples that did not contain the phosphoethanolamine moiety (3 and 4) the reducing terminal KDO residue is immediately cleaved so that none of the ions observed in the course of the experiment contain a KDO residue. This suggests that the presence of the phosphoethanolamine moity enhances the stability of the molecule. It is possible that, in the case of samples 1 and 2, the positive charge is sited on the amino group and thus "protects" the KDO residue from degradation. In the methanolysis time course of samples 3 and 4 the degree of degradation is greater, with ions observed at m/z 494 and 496 (sample 3) and 515 and 547 (sample 4). In both samples 1 and 2 the lowest mass ion observed is at m/z 840. this may further indicate that the phosphoethanolamine moiety acts in such a manner as to enhance resistance to methanolysis.

In sample 4 and 5 signals were observed that are consistent with components not normally associated with LPS core oligosaccharides.

The signal at m/z 1399 in permethylated L5 F III (3) (sample 4) seems to be consistent with the composition $Hex_3HexNAc_1Hep_2Pent$ , though there is no evidence for such

a component in either the positive ion or negative ion native spectra or the deuterioacetyl spectrum. The fact that an ion of such a composition is present in only one of the spectra obtained may indicate that it is not due to the sample but is an unrelated component that gives rise to a signal that unfortunately can be assigned a carbohydrate composition. Since Pentose residues have not been found to be present in LPS core structures or their O-antigen polysaccharides the above possible explanation for the signal at m/z 1399 is given credence.

Sample 5 contains a component of composition $Hex_3HexNAc_1Hep_1DeoxyHex_1KDO_1Ac_{1/0}$ which is present in both the negative and positive ion native spectra, the deuterioacetyl and the permethyl spectra. DeoxyHexose residues are found as components of some O-specific side chains in Gram negative bacteria[12], though no report has yet proposed their presence in inner core structures. This may be a novel inner core oligosaccharide, unfortunately further mass spectrometric analysis, such as methanolysis, was not possible due to the presence of the other two components in the sample.

Because sample 5 contained 2 components this precluded the use of methanolysis to further study the structures, as the data obtained would be ambiguous.

TABLE 4.21. lists the structures found to be present in each sample. The classical di-heptose inner core

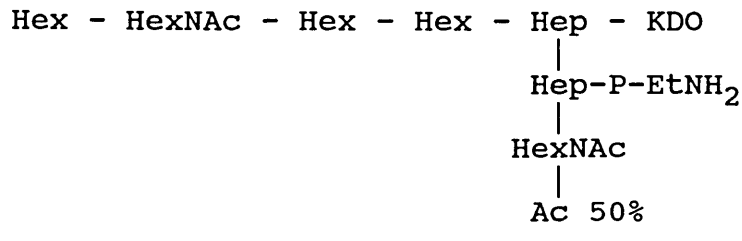
structure is observed in each of the molecules with the site of O-acylation in all cases being the terminal HexNAc residue on the branch.

**TABLE 4.21.** Summary of structures that may be present in the ten LPS oligosaccharides from Neisseria meningitidis.

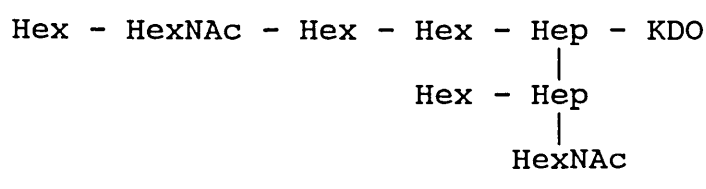
SAMPLE 1



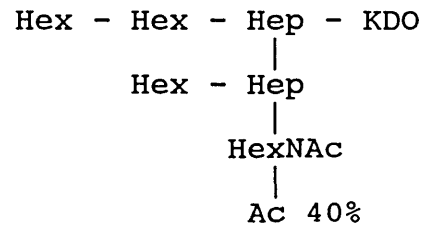

SAMPLE 2



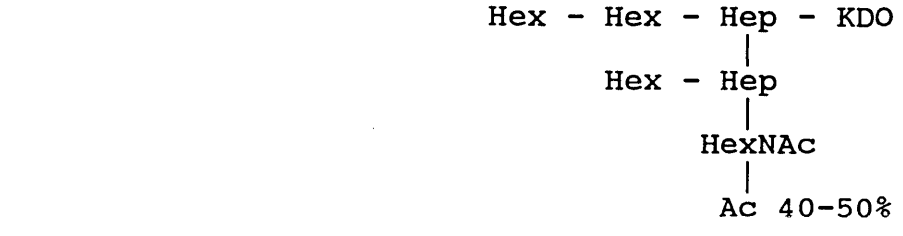

SAMPLE 3

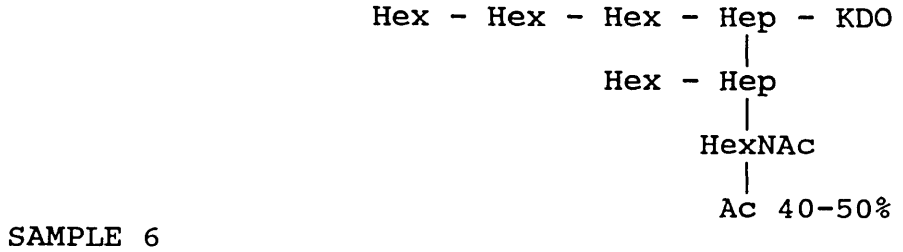



SAMPLE 4

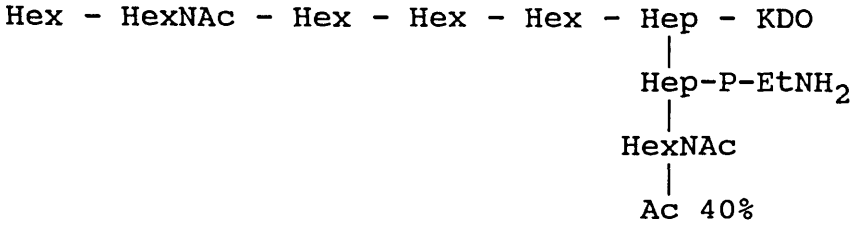


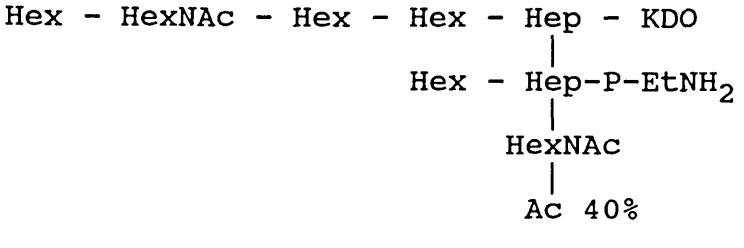
SAMPLE 5



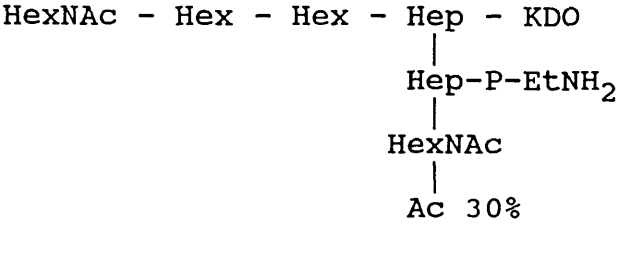




SAMPLE 6

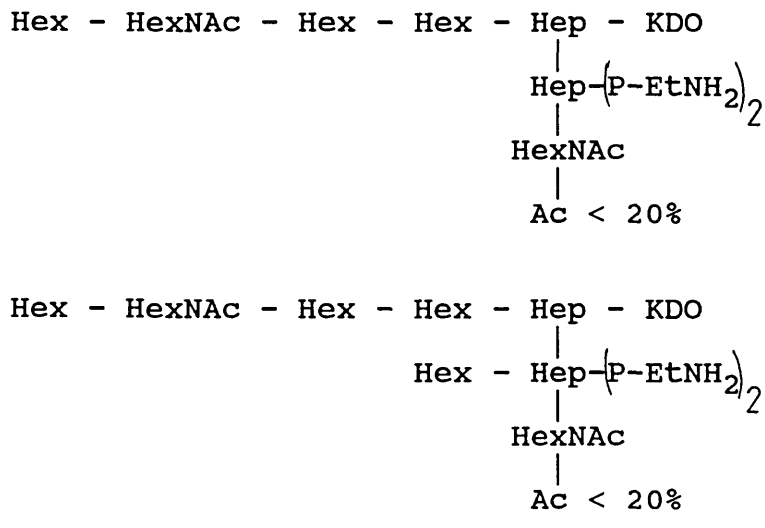


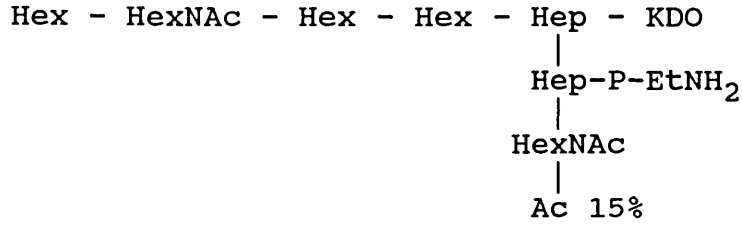

SAMPLE 7



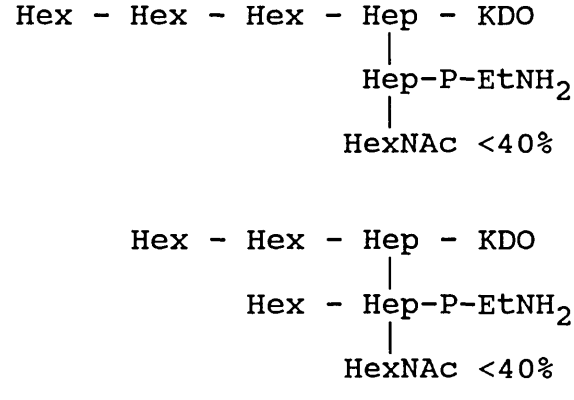
SAMPLE 8




SAMPLE 9




SAMPLE 10



## 4.4. Conclusion.

This series of experiments has examined ten oligosaccharides from Neisseria meningitidis LPS in order to determine the sequence and branch positions within the molecules. The structural assignments reached are fully compatible with all the data obtained and are also consistent with being a series of related molecules. The facility with which these assignments have been made demonstrates the applicability of the new FAB-MS protocols presented in chapters 2 and 3.

## Chapter 5 : Conclusion.

The work presented herein was to develop methods for the elucidation of carbohydrate structure to complement those presently available. To this end two novel protocols were developed based upon the combination of simple wet chemistry and mass-spectrometric analysis.

The first protocol was developed with the aim of enabling sensitive rapid location of the residue within the sequence of an oligosaccharide that carries an O-acyl group or groups. Previously both classical chemical methods and n.m.r. spectroscopy have been utilised to obtain this information with much success, though both of these approaches can lead to unambiguous data. The new protocol makes use of a deuterated derivative that leaves all O-acyl groups intact, enabling their residue location to be determined by mass shifts in the spectra obtained. This procedure has been applied in the analysis of several oligosaccharides, facilitating the analysis of the type and location of O-acyl groups present. This method is sensitive requiring 0.5 - 10 μg of sample to enable the location of the acyl group to be made, compared with 100 - 200 μg or more which is required in the case of n.m.r. and classical chemical methods.

The second protocol was developed to afford complete data relating to the sequence and branch positions within an oligosaccharide, at high sensitivity. Classical chemical methods involving a combination of Smith degradation, partial hydrolysis and methylation analysis requires several chemical manipulations and several 100's of microgrammes of material. This procedure, which

requires 10 - 20 ug of sample, involves a methanolysis time course carried out on a methylated sample which is monitored by FAB-MS. The design of this protocol is such that no sample work up is required prior to the mass spectrometric analysis, with the reagents used actually enhancing the sensitivity of the FAB experiment. A recent report of structural work carried-out on R-type LPS core oligosaccharides from Neisseria gonorrhoeae[99] afforded similar compositions to those obtained in the analysis of the LPS core from N. meningitidis. However, the sequence of these structures were very different, with both heptose residues being part of the LPS "backbone" whereas in the work presented above one of the two heptose residues initiates the major branch. Additionally N. gonorrhoeae LPS appears not to contain an O-acyl group. The structural work on N. gonorrhoeae used methylation analysis to determine composition followed by native, permethyl and perdeuteromethyl spectra to afford sequence data. Tandem mass spectrometry was then applied to locate the residue that is substituted with the phosphoethanolamine moiety. The N. gonorrhoeae LPS core oligosaccharides appear to fragment more readily, affording sequence data from "simple" mass spectrometric analyses. This may be due to the position of the two heptose residues in the LPS "backbone". The incomplete fragmentation data in the spectra obtained from N. meningitidis LPS core oligosaccharides may additionally be due to both the main backbone and the major branch containing HexNAc, thus directing fragmentation and reducing the

abundance of other cleavage ions.

These two procedures have been applied in the analysis of oligosaccharides derived from polysaccharides of plant and bacterial origin, but are equally applicable to oligosaccharides of animal origin. The only requirement for these two methodologies is that the carbohydrate under analysis is amenable to derivatisation. The new protocols described above enable rapid and sensitive analysis of important aspects of carbohydrate structure. Though no information is obtained as to the linkages between residues the data afforded has proven of great value in guiding subsequent n.m.r. analysis and in the interpretion of methylation analysis data. Therefore, in combination with the methods already available to the carbohydrate analyst, these two procedures will enhance the speed and completeness of data obtained in structural studies.

The future development of carbohydrate mass spectrometry is likely to be in two main areas, instrumental and chemical techniques. An approach that is in the last stages of development and is likely to have an impact on the mass spectrometric analysis of carbohydrates is focal plane detection. This involves recording simultaneously a section of the mass range of the instrument, enabling an increase in the sensitivity of ion detection. The development of new derivatives will continue to widen the ability of mass spectrometry to elucidate carbohydrate structure. For example the incorporation of a charged moiety to enhance molecular ion formation, particularly in the case of large molecules.

The combination of chemical methods and mass spectrometry is likely to provide opportunities for further additions to the armoury of analytical methods available for carbohydrate structure elucidation.

# CHAPTER 6 : METHODS AND MATERIALS.

## 5.1. METHODS.

### 5.1.1. Per-O-acetylation.

Per-O-acetylation was carried out using a modification of the method of Bourne et al [104]. The sample was dissolved in trifluoroacetic anhydride and glacial acetic acid (2 : 1), and left to stand at room temperature for 10 min. The reagents were then blown off under a stream of nitrogen and the product taken up in chloroform (1 ml). The sample \ chloroform mixture was then washed with water (2 ml) three times, to remove aqueous soluble contaminants. The washed chloroform was then removed under a stream of nitrogen.

### 5.1.2. Deuterioacetylation.

Deuterioacetylation was carried out using the same method as for per-O-acetylation, except that the glacial acetic acid was replaced with deuterioacetic acid. All other procedures were identical to those used to per-O-acetylate (see above).

### 5.1.3. Permethylation

Permethylation was carried out using a modification of the Hakomori method[25]. The permethylation base was prepared by heating a mixture of sodium hydride (100 $\mu$g) and dry dimethyl sulphoxide (0.5 ml) at 90°C for 10 min. This was allowed to cool and centrifuged for 10 min. at 2,000 rpm. The sample to be permethylated was dissolved in

dry dimethyl sulphoxide (50 µl) in a stoppered tube and 250 µl of base added. After 5 min. methyl iodide (50 µl) was added and the reaction left to stand at room temperature for 20 min. Then a further 1 ml of was base added and after 5 min. 1 ml of methyl iodide added. After a further 20 min. the reaction was quenched with water (1-2 ml) and chloroform (2 ml) was added to extract the reaction products. The chloroform was then washed three times with water (1-2 ml) and dried under a stream of nitrogen.

5.1.4. Perdeuteriomethylation

Perdeuteriomethylation was carried out using the same method as for permethylation, with one exception the methyl iodide was replaced with deuteriomethyl iodide. All other procedures were identical (see 5.1.3.).

5.1.5. Sep-Pak Purification.

The products of the permethylation reaction were purified further using a modification of the procedure of Waeghe et al [105]. A $C_{18}$-reverse phase sep-pak was primed using water (5 ml), acetonitrile (5 ml), ethanol 5(ml) and water (10 ml). The dry product from the permethylation reaction was dissolved in methanol (200 µl) and loaded onto the primed sep-pak. The sep-pak was then washed with water (2 ml), 15% acetonitrile (1 ml), 50% acetonitrile (1 ml), 75% acetonitrile (1 ml) and acetonitrile (1 ml). Each of these fractions were collected in separate glass tubes and dried under vacum. The permethylated product was recovered in either the 50% or 75% acetonitrile wash.

5.1.6. Diazomethylation.

Diazomethylation was carried out using freshly prepared diazomethane. The sample was dissolved in 100 µl of methanol and an excess of diazomethane solution was added dropwise untill the solutiion remained yellow in colour. The mixture was allowd to stand at room temperature for 10 minutes and then dried under a stream of nitrogen.

5.1.7. Methanolysis FAB-MS.

Methanolysis FAB-MS was carried out on permethylated or deuteriopermethylated samples. The sample was dissolved in mehanol and transfered to a reacti-vial, which was then heated at 40°C to drive off the methanol. The dried sample in the reacti-vial was then taken up in methanolic HCl (20 µl) which had been previously prepared by bubbling annhydrous HCl through methanol (10 ml) to obtain a 1 M solution. The reacti-vial was then heated at 40° C and aliquots (1 µl) taken at intervals and FAB mass spectra obtained of these aliquots. The interval between aliquotes was determined according to how fast the hydrolysis was taking place, as observed in the FAB spectra recorded. If complete hydrolysis had not occurred by heating at 40°C, the reacti-vial was heated at 60°C and the same procedure as for the 40°C hydrolysis followed, untill no further hydrolysis was observed.

5.1.8. Fast Atom Bombardment Mass Spectrometry.

All mass spectrometric experiments were carried out using a VG Analytical High Field ZAB 1F mass spectrometer. The instrument was operated at an accelerating voltage of 8KV, giving a mass range of 3,300 dalton. FAB experiments were performed using an M-Scan ion gun operated at 9.5 - 10 KV, with Xenon as the bombarding gas affording a primary beam that due to charge transfer reactions consisted of 70% atoms and 30% ions.

Samples were taken up in an appropriate amount of 5% acetic acid (underivatised) or methanol (derivatised) and a 1 ul aliquot taken for each experiment. The stainless steel target of the FAB probe was prepared by smearing onto it 1 µl of glycerol and adding a further 1 µl of monothioglycerol. Excess matrix was removed until an even layer of matrix was obtained. The 1 µl aliqot of sample was loaded into the matrix using a micropippette, which required blowing the sample gently out of the capillary. The act of blowing clear the micropippette sometimes resulted in air bubbles forming in the matrix which were removed by carefully mixing the matrix/sample mixture. When the sample was taken up in methanol the FAB probe with the sample/matrix mixture was inserted into the vacuum lock of the mass spectrometer, allowed to reach vacuum then removed from the lock. A further 1 µl of monothioglycerol was added to the matrix to replenish that which had been driven off by the evapouration of the methanol. This step was essential to prevent the matrix from being completely utilised during an experiment and thus maintain a good ion

current.

The magnet was scanned from high mass to low mass using an exponential scan function and a scan speed of 300 s per decade. Mass spectra were recorded on UV sensitive paper using an EMI SE 6150 Mk II UV Oscillograph operating at a chart speed of 10 mm/s. This afforded spectra in which the signals were evenly spaced throughout the spectrum and UV sensitive chart paper was used to record the spectra obtained. The glycerol/thioglycerol matrix typically affords a signal at m/z 201 which was used as a reference point to manually count the spectra obtained.

## 5.2. MATERIALS.

Unless otherwise stated all reagents were of ANALAR grade and obtained from BDH. Iodomethane, Triphenyl methane 97%, Sodium Hydride 97%, Methanol 99.9% Gold Label, Acetic Acid 99.7% Gold Label, Triflouroacetic Annhydride 99+ % Gold Label, Acetic Acid 99.5 atom % D Gold Label and Iodomethane 99+ atom % D Gold Label were obtained from Aldrich. Maltotriose, Stachyose, n-butyric acid 99% and monothioglycerol 98% were obtained from Sigma. UV sensitive Oscilloscript recording paper was obatined from Agfa-Gevaert.

Glycolipid (I) was supplied by C.E. Ballou (Berkeley Ca), gellan gum from Pseudomonas elodea was supplied by A. Mort (Oklahoma State), Klebsiella K44 oligosaccharide was supplied by G.G.S. Dutton (British Columbia), Klebsiella K69 oligosaccharide was supplied by H. Parolis (Rhodes S.A.), Xyloglucan nonamer from sycamore extracellular polysaccharide was supplied by P. Albersheim (Complex Carbohydrate research Centre, Athens Ga.), the glycolipid from human embryonal carcinoma cell line PA1 was supplied by M. Fukuda (La Jolla Cancer Research Centre Ca.), the Bacillus streptococci group specific antigen derived oligosaccharide and the Neisseria meningitidis LPS core oligosaccharides were supplied by H.J. Jennings (N.R.C. Canada).

REFERENCES


1. Kanfer J.N. and Hakomori S-I. "Handbook of Lipid Research 3 Sphingolipid Biochemistry", Plenum Press (1983).

2. Obata K., Oide M. and Handa S., Nature, (1979), 266, 369-371.

3. Koscielak J., Zdebska E., Wilczynska z., Miller-Podraza H. and Dzierzkowa-Borodej W., Eur. J. Biochem., (1979), 96, 331-337.

4. Fukuda M. and Fukuda M.N., Journal of Supramolecular Strucutre and Cellular Biochemistry, (1981), 17, 313-324.

5. Fukuda M.N. Dell A., Oates J.E. and Fukuda M.N., J. Biol. Chem., (1985), 260, 6623-6631.

6. Fukuda M., Bothner B., Ramasamooj P., Dell A., Tiller P.R., Varki A. and Klock J.C., J. Biol. Chem. (1985), 260, 12957-12967.

7. Hahn M.G., Darvill A.G. and Albersheim P., Plant Physiol., (1981), 68, 1161-1169.

8. Albersheim P., Darvill A.G., McNeil M., Valent B.S., Hahn M.G., Lyon G., Sharp J.K., Desjardins A.E., Spellman M.W., Ross C.M., Robertsen B.H., Aman P. and Franzen L.E., Pure and Applied Chem., (1981), 53, 79-88.

9. Hindsgaul O., Norberg T., Le Pendu J. and Lemieux R.U., Carbohydr. Res., (1982), 109, 109-142.

10. Kuo M-S., Mort A.J. and Dell A., Carbohydr. Res., (1986), 156, 173-187.

11. I. Goldenschneider, E.C. Gotschlich and M.S. Artenstein, J. Exp. Med., (1969), 129, 1327-1348.

12. "The bacterial Cell Surface", Hammond S.M. Lambert P.A. and Ryecroft A.N., Croom Helm, (1984).

13. Zollinger W.O., Boslego J.E., Frasch C.E. and Froholm L.O., Lancet, (1984), July 21st, p 166.

14. Wall R.A., Hassan-King M., Thomas H. and Greenwood, B.M., Lancet, (1986) Sept 13th, p 624.

14a. Avery, O.T. and Goebel, W.F., J. Exp. Med., (1933), 58, pp. 731-755.

15. Sutherland, I.W., Biochem. J., (1969), 115, 935-945.

16. Hara, C., Kiho, T. and Vkai. S., Carbohydr. Res., (1982), 111, 143-150.

17. Noggle G.R., "The Carbohydrates" Ed. Pigman W. (1957) 602-640.

18. Dubois M., Gilles K.A., Hamilton J.K., Rebers P.A. and Smith F., Anal. Chem., (1956) 28 350-356.

19. Morris D.L., Science, (1948) 107 254

20. Wilson C.M., Anal. Chem., (1959) 31 1199-1201.

21. McInnes A.G., Ball D.H., Cooper F.P. and Bishop C.T., J. Chromatogr., (1958) 1 556-000.

22. Dutton, G.G.S., adv. Carb. Che., (1972) 28, 11-101.

23. Sweeley C.C., Bentley R., Makita M. and Wells W.W., J. Amer. Chem. Soc., (1963) 85 2497-2507.

24. Dische, Z., J. Biol. Chem., (1947), 167, 189-198.

25. Hakomori S., J. Biochem., (Tokyo),(1964) 55 205

26. Sandford P.A. and Conrad H.E., Biochemistry, (1966) 5 1508-1517.

27. Larm O., Lindberg B. and Svensson S., Carbohyd. Res., (1971) 20 39-48.

28. Stellner, K., Saito, H. and Hakomori, S-I., Arch. Biochem. Biophys. (1973) 155 464-472.

29. Haverkamp, J., Kamerling, J.P. and Vliegenthart, J.F.G., Febbs Lett. (1977) 73 215-219.

30. Lindberg B. and Lonngren J., Methods in Enzymology, (1900), 50 3-33.

31. Akher M.A., Cadotte J.E., Montgomery R., Smith F., Van Cleve J.W. and Lewis B.A., Nature.,(1953), 71,474-475.

32. De Belder, A.N. and Norrman, B., Carbohydr. Res., (1968), 8 1-6.

33. Dubos R. and Avery O.T., J. Exp. Med., (1931)54 51-71.

34. Sutherland I.W., Biochem. J., (1967) 104 278-285.

35. Adams E.S. and Park B.H., Virology, (1956) 2 719-736.

36. Eklund C. and Wyss O., J. Bact., (1962) 18 1209-1215.

37. Dutton G.G.S., Di Fabio J.L., Leek D.M., Merrifield E.H., Nunn J.R. and Stephen A.M., Carbohyd. Res., (1981), 97, 127-138.

38. Kenne L. and Lindberg B., The Polysaccharides, Aspinall, G.O. Ed., (1983) 2, 287-363.

39. Jennings, H.J., Johnson, K.O. and Kenne, L., Carbohydr. Res. (1983) 121 233-241.

40. Blanchard, D., Cartron, J-P., Fournet, B., Montreuil, J., Van Halbeek, H. and Vliegenthart, J.F.G., J. Biol. Chem, (1983), 258, 7691-7695.

41. Van Halbeek, H., Dorland, L., Vliegenthart, J.F.G., Hull, W.E., Lamblin, G., Lhermitte, M,. Boersma, A. and Roussel, P., Eur. J. Biochem., (1982), 127, 7-20.

42. Dutton G.G.S. and Karunaratne D.N., Carbohyd. Res., (1985), 138 277-291.

43. Kochetkov, N.K. and Chizov, O.S., Adv. Carb. Chem. (1966), 21, 39-93.

44. Dutton, G.G.S., Adv. Carb. Che., (1974) 30, 19-53.

45. Lonngren, J. and Svensson, S., Adv. Carb. Chem. (1973), 29, 41-106.

46. Morris, H.R., Dell, A., Banner, A.E., Evans, S., McDowell, R. and Hazelby, D., proc 25th Ann, Conf. on Mass Spectrom. and Allied Topics, (1977), pp 73-75.

47. Morris, H.R., Dell, A. and McDowell, R.A., Biomed. Mass Spectrom., (1981) 8, 463-473.

48. Falk, K-E., Karlsson, K-A., Larson, G., Thurin, J., Blaszczyk, M., Steplewski, Z. and Koprowski, H., Biochem. Biophys. Res. Commun., (1983), 110 383-391.

49. Briemer, M.E., Hansson, G.C., Karlsson, A-K., Leffler, H., Pimlott, W. and Samuelsson, B.E., FEBS lett., (1981), 124, 299-303.

50. Egge, H., Michalski, J.C. and Strecker, G., Arch. Biochem. Biophys., (1982), 213, 318-326.

51. Linscheid, M., D'Angona, J., Burlingame, A.L., Dell, A. and Ballou, C.E., Proc. Natl. Acad. Sci. USA, (1981), 78, 1471-1475.

52. Barber, M., Bordoli, R.S., Sedgwick, R.D. and Tyler, A.N., J.C.S. Chem. Commun., (1981), 325-327.

53. Dell, A., Adv. Carb. Chem. Biochem., 45 in press.

54. Forsberg, L.S., Dell, A., Walton, D.J. and Ballou, C.E., J. Biol. Chem., (1982), 257, 3555-3563.

55. Dell, A., Dutton, G.G.S., Jansson, P-E., Lindberg, B., Lindquist, U. and Sutherland, I.W., Carbohydr. Res., (1983), 122, 340-343.

56. McNeil, M., Darvill, J., Darvill, A.G., Albersheim, P., Van Veen, R., Hooykaas, P., Schilperoot, R. and Dell, A., Carbohydr. Res., (1986), 146, 307-326.

57. Jones, C., Mulloy, B., Wilson, A., Dell, A. and Oates, J.E., J. Chem. Soc. Perkin Trans 1, (1985), 1665-1673.

58. Jansson, P-E., Lonngren, J., Widmalm, G., Leontein, K., Slettengren, K., Svenson, S.B., Wrangsell, G., Dell, A. and Tiller, P.R., Carbohydr. Res., (1985), 145, 59-66.

59. Dell, A. and Ballou, C.E., Carbohydr. Res., (1983), 120, 95-111.

60. Altman E. and Dutton G.G.S., Carbohyd. Res., (1985), 138, 293-303.

61. Dell, A., Oates, J., Lugowski, C., Romanowska, E., Kenne, L. and Lindberg, B., Carbohydr. Res. (1984) 133 95-104.

62. Sloneker, J.H. and Orentas, D.G., Nature, (1962) 194, 478-479.

63. Kuo, M-S. and Mort, A.J., Carbohydr. Res., (1985), 145, 247-265.

64. Stoddart, R.W. "The biosythesis of polysaccharides" (1984) Croom Helm.

65. Jann, K. and Jann, B. in "Surface carbohydrates of the prokaryote cell" Sutherland, I. (Ed) (1977), Academic Press pp. 247-287.

66. Davison, I.W., Sutherland, I.W. and Lawson, C.J., J. Gen. Micro., (1977), 98 603-606.

67. Skyak-Braek, G., Larsen, B. and Grasdalen, H., Carbohydr, Res., (1985), 145, 169-174.

68. O'Neill, M.A., Morris, V.J., Selvendran, R.R., Sutherland, I.W. and Taylor, I.T., Carbohydr. Res., (9186), 148, 63-69.

69. Michon, F., Brisson, J.R., Roy, R., Ashton, F.E. and Jennings, H.J., Biochemistry, (1985), 24, 5592-5598.

70. Hestrin, S., J. Biol. Chem., (1949), 180, 249-261.

71. Lindberg, B., Lonngren, J. and Nimmich, W., Carbohydr. Res., (1972), 23, 47-55.

72. Lindberg, B., Lonngren, J., Ruden, U. and Nimmich, W., Carbohydr. Res. (1975), 42,83-93.

73. Bebault, G.M. and Dutton, G.G.S., Carbohydr. Res., (1978), 64, 199-213.

74. Dutton, G.G.S., Proc. 3rd. European Symp. Carbohydr., (1985), Grenoble, pp. 4.

75. Karunaratne, D.N. and Dutton G.G.S., Proc. 12th Internat. Carbohydr. Symp., (1984), Utrecht, pp 370.

76. Tsui, F-P., Boykins, R.A. and Egan, W., Carbohydr. Res. (1982) 102 263-271.

77. Dell, A. and Tiller, P.R., Carbohydr. Res., (1986), 135, 1126-1134.

78. Dell, A., Advances Carbohydr. Chem. Biochem., (1987) 45, 19-72.

79. Egge, H., Dell, A. and Von Nicolai, H., Arch. Biochem. Biophys., 224, 235-253.

80. Lemieux, R.U., Advan. Carbohydr. Chem., (1954), 9, 1-57.

81. Sutherland, I.W., Adv. Microb. Phys., (1972), 8, 143-213.

82. Kuo, M-S., Mort, A.J. and Dell, A., Carbohydr. Res., (1986), 156, 173-187.

83. Dutton G.G.S., Parolis H., Joseleau J-P. and Marais M-F, Carbohyd. Res., (1986), 149, 411-423.

84. Hackland, P.L., Parolis, H., Dell, A. and Tiller, P.R., Carbohydr. Res., (1988), 181, 153-162.

85. York, W.S., Oates, J.E., Van Halbeek, H., Darvill, A.G., Albershiem, P., Tiller, P.R. and Dell, A., Carbohydr. Res., (1988) 173 113-132.

86. Fukuda, M.N., Bothner, B., Lloyd, K.O., Rettig, W.j., Tiller, P.R. and Dell, a., J. Biol. Chem. (1986) 261 5145-5153.

87. Tiller, P.R. and Dell, A., Abstracts R.S.C. Carbohydrate Group Meeting, 29th March - 1st April 1987, pp 24

88. H.J. Jennings, Advances in Carbohydrate Chem. & Biochem., (1983) 41, 155-208.

89. T.L. Kruger, J.F. Litton, R.W. Kondrat and R.G. Cotts, Anal. Chem, (1976), 48, 2113.

90. R.A. Yost and C.G. Enke, J. Amm. Chem. Soc. (1978), 100, 2274.

91. F.W. McLafferty Tandem Mass Spectrometry John Wiley and Sons 1983.

92. Personnal communication with V.G. Analytical Ltd.

93. D. Zakett, J.D. Ciupek and R.G. Cooks, Anal. Chem., (1981), 53, 723-726.

94. B. Shushan and R.K. Boyd, Anal. Chem., (1981), 53, 421-427.

95. The Bacterial Cell Surface, S.M. Hammond, P.A. Lambert and A.N. Ryecroft, Croom Helm (1984).

96. T. Francis jnr. and W.S. Tillet, J. Exp. Med. (1930), 52, 573-585.

97. R.E. Schifferle, H.J. Jennings, M.R. Wessels, E. Katzenellenbogen, R. Roy and D.L. Kasper, J. Immunol., (1985), 135, 4164-4170.

98. H.J. Jennings, R. Roy and A. Gamian, J. Immunol., (1986), 137, 1708-1713.

99. Gibson B.W., Webb J.E., Yamasaki R., Fisher S., Burlingame A.L., Mandrell R.E., Schneider H. and McLeod Griffiss J., Proc. Natl. Acad. Sci. U.S.A., (1989), 86, 17-21.

100. H.J. Jennings, C.W. Lugowski, F.E. Ashton and J.A. Ryan, Carbohydr. Res. (1983), 112, 105-111.

101. F. Michon, R. Roy, H.J. Jennings and F.E. Ashton, Can. J. Chem., (1984), 62, 1519-1524.

102. H.J. Jennings, K.G. Johnson and L. Kenne, Carbohydr. Res., (1983), 121, 233-241.

103. Dell A., Azadi P., Tiller P.R., Thomas-Oates J.E. and Jennings H.J., Carbohydr. Res. (1989) in press.

104. E.J. Bourne, M. Stacey, J.C. Tatlow, J. Chem. Soc. (1949), 2976-2979.

105. T.J. Waeghe, A.G. Darvill, M. McNiel and P. Albersheim, Carbohydr. Res., (1983), 123, 281-304.

LIST OF PUBLICATIONS.

(1) FAB-Mapping of permethylated glycoconjugates of molecular weights in excess of 15,000 dalton.
P.R. Tiller, A. Dell and M. Fukuda.
Abstracts 10th International Mass Spectrometry Conference, Swansea (1985).

(2) Structure of sialylated fucosyl polylactosaminoglycans isolated from chronic myelogenous leukemia cells.
M. Fukuda, B. Bothner, P. Ramsamooj, A. Dell, P.R. Tiller, A. Varki and J.C. Klock.
J. Biol. Chem., (1985), 260, 12957-12967.

(3) Structural studies of the O-antigen polysaccharide of Klebsiella O5 and Escherichia O8.
P-E. Jansson, J. Lonngren, G. Widmalm, K. Leontin, K. Slettengren, S-B. Svenson, G. Wrangsell, A. Dell and P.R. Tiller.
Carbohydr. Res., (1985), 145, 59-66.

(4) GM1 gangliosidosis (type 1) in a cat.
C.G. Barker, W.F. Blakemore, A. Dell, A.C. Palmer, P.R. Tiller and B.G. Winchester.
Biochem. J., (1986), 235, 151-158.

(5) Structure of a novel fucosyl lacto-N-nor-hexaosylceramide isolated from chronic myelogenous leukemia cells.
M.N. Fukuda, A. Dell, P.R. Tiller, A. Varki, J.C. Klock and M. Fukuda.
J. Biol. Chem., (1986), 261, 2376-2383.

(6) A novel mass spectrometric procedure to rapidly determine the positiion of O-acylated residues in the sequence of naturally occurring oligosaccharides.
A. Dell and P.R. Tiller.
B.B.R.C., (1986), 135, 1126-1134.

(7) Structures of glycosphingplipids isolated from human embryonal carcinoma cells.
M.N. Fukuda, B. Bothner, K.O. Lloyd, W.J. Rettig P.R. Tiller and A. Dell.
J. Biol. Chem., (1986), 261, 5145-5153.

(8) Applications of FAB-MS in the structure determination of large glycoconjugates.
A. Dell, M. Rogers and P.R. Tiller.
Abstracts 618th mtg. Biochem. Soc., Liverpool (1986)

(9) Novel fast atom bombardment mass spectrometric procedures for glycoprotein analysis.
A. Dell, J. Thomas-Oates, M.E. Rogers and P.R. Tiller.
Biochimie, (1988), 70, 1435-1444.

(10) Location of the O-acetyl substituents on a nonasaccharide repeating unit of sycamore extracellular xyloglucan.
W.S. York, J.E. Oates, H. Van Helbeek, A.G. Darvill, P. Albersheim, P.R. Tiller and A. Dell.
Carbohydr. Res., (1988), 173, 113-132.

(11) Bacteriophage degredation of the capsular polysaccharide from Klebsiella K69. Location of the O-acetyl groups.
P.L. Hackland, H Parolis, A. Dell and P.R. Tiller.
Carbohydr. Res., (1988), 181, 153-162.

(12) Fast atom bombardment mass spectrometric strategies for characterizing carbohydrtae-containing biopolymers.
A. Dell, N.H. Carman, P.R. Tiller and J.E. Thomas-Oates.
B.E.M.S., (1989), 16, 19-24.

(13) Analysis of Oligosaccharides from the core region of meningococcal Lipopolysaccharides by Fast Atom Bombardment Mass Spectrometry.
A. Dell, P. Azadi, P.R. Tiller and J.E. Thomas-Oates.
Carbohydr. Res. (1989) in press.